From the Department of Clinical Science and Education,
Södersjukhuset, Karolinska Institutet, Stockholm, Sweden

Roles of the Transient Receptor Potential Channels and the Intracellular Ca^{2+} Channels in Ca^{2+} Signaling in the β-cells

Amanda Jabin Fågelskiöld

Stockholm 2011

Published by Karolinska Institutet. Printed by Universitetsservice US-AB digitaltryck.

ISBN 987-91-7457-216-2

If we knew what it was we were doing,
it would not be called research, would it?
Albert Einstein

To my beloved family,

Academic dissertation for PhD degree
at Karolinska Institutet
Public defence at Aulan, 6th floor,
Södersjukhuset, Stockholm

Friday, March 25th, 2011 at 09.00

Supervisor: Docent Md Shahidul Islam, shaisl@ki.se, Department of Clinical Sciences and Education, Södersjukhuset, Karolinska Institutet.

Co-supervisor: Professor Håkan Westerblad, Department of Physiology and Pharmacology, Karolinska Institutet

Opponent: Professor Antony Galione, Department of Pharmacology, Oxford University, England, U.K.

Examination board: Docent Carani Sanjeevi, Department of Medicine, Solna, Karolinska Institutet

Docent Robert Bränström, Department of Molecular Medicine and Surgery, Karolinska Institutet

Docent Anna Forsby, Department of Neurochemistry,
Stockholm University

1 Abstract

Previous studies from our group reported that pancreatic β-cells express ryanodine receptors (RyRs) that can mediate Ca^{2+}-induced Ca^{2+} release (CICR). The full consequences of the activation of RyRs on Ca^{2+} signaling in these cells, however, remained unclear. An important open question was whether activation of the RyRs leads to activation of any Ca^{2+} channels in the plasma membrane, and thereby depolarizes membrane potential. One main aim of the thesis was to address this question. As a corollary, we have also looked for the existence of functional TRPV1 channels, and have elucidated the molecular mechanisms that underlie the $[Ca^{2+}]_i$-elevating effect of ADP ribose in these cells.

We used methods such as measurement of the $[Ca^{2+}]_i$ in single cells loaded with fura-2, patch clamp technique, Western blot analysis, immunohistochemistry, a variety of pharmacological tools, and a series of carefully designed protocols. In most experiments, we used S5 cells, derived from the rat insulinoma cell line INS-1E, but we also used primary β-cells from mice, rat, and human.

Activation of the RyRs by 9-methyl 5,7-dibromoeudistomin D (MBED) increased the $[Ca^{2+}]_i$ with an initial peak, followed by a decline to a plateau phase, and regenerative spikes superimposed on the plateau. The initial $[Ca^{2+}]_i$ increase was due to the activation of the RyRs in the ER, since it was abolished by thapsigargin, but was present when extracellular Ca^{2+} was omitted or when Ca^{2+} entry was blocked by SKF 96365. The plateau phase was due to Ca^{2+} entry across the plasma membrane, since it was abolished by omission of extracellular Ca^{2+}, and blocked by SKF 96365. The plateau phase was not solely dependent on the filling state of the ER, since it was not abolished by thapsigargin. Inhibition of the voltage-gated Ca^{2+} channels by nimodipine did not inhibit the plateau phase. Several agents that block TRP channels, e.g. La^{3+}, Gd^{3+}, niflumic acid, and 2-APB, inhibited the plateau phase. It was also inhibited by membrane depolarization. We conclude that the plateau phase was due to activation of some TRP-like channels. Activation of RyRs by MBED also induced membrane depolarization. The spikes required Ca^{2+} entry through the L-type voltage-gated Ca^{2+} channels, as they were abolished by nimodipine. The spikes resulted from CICR, since they were inhibited in a use-dependent way by ryanodine, and abolished after depletion of the ER by thapsigargin. Thus, activation of RyRs activated TRP-like channels, depolarized the plasma membrane, activated L-type voltage-gated Ca^{2+} channels and triggered CICR.

During the course of this thesis we reported that TRPM2 is present in the INS1-E cells and the human β-cells. We studied whether TRPM2 was involved in the Ca^{2+} entry triggered by the activation of RyRs. N-(p-amylcinnamoyl) anthranilic acid (ACA), an inhibitor of TRPM2, did not inhibit the MBED-induced $[Ca^{2+}]_i$ entry. ADP ribose (ADPr), when applied intracellularly, is an agonist of TRPM2. We found that extracellularly applied ADPr increased $[Ca^{2+}]_i$ in the form of an initial peak followed by a plateau that depended on extracellular Ca^{2+}. EC_{50} of ADPr was ~30 μM. NAD^+, cADPr, a phosphonate analogue of ADPr (PADPr), 8-bromo-ADPr or breakdown products of ADPr did not increase $[Ca^{2+}]_i$. Inhibitors of TRPM2, e.g. flufenamic acid, niflumic acid, and ACA did not affect the ADPr-induced $[Ca^{2+}]_i$ increase. Two specific inhibitors of the purinergic receptor P2Y1, e.g. MRS 2179 and MRS 2279 completely blocked the ADPr-induced $[Ca^{2+}]_i$ increase. The $[Ca^{2+}]_i$ increase by ADPr required activation of PI-PLC, since the PI-PLC inhibitor U73122 abolished the $[Ca^{2+}]_i$ increase. The ADPr-induced $[Ca^{2+}]_i$ increase was through the IP_3 receptors, since it was inhibited by 2-APB, an inhibitor of the IP_3 receptors. ADPr increased $[Ca^{2+}]_i$ in the transfected human astrocytoma cells that expressed the P2Y1 receptors, but not in the wild type astrocytoma cells. We conclude that extracellular ADPr is an endogenous and specific agonist of P2Y1 receptors.

Capsaicin and AM404, two specific agonists of TRPV1, increased $[Ca^{2+}]_i$ in the INS-1E cells. Capsazepine, a specific antagonist of TRPV1, completely blocked the capsaicin-induced $[Ca^{2+}]_i$ increase. Capsaicin elicited inward currents that were abolished by capsazepine. TRPV1 protein was detected in the INS-1E cells and human β-cells by Western blot. However, no TRPV1 immunoreactivity was detected in the human islet cells and human insulinoma by immunohistochemistry. Capsaicin did not increase $[Ca^{2+}]_i$ in primary β-cells from rat or human. We conclude that INS-1E cells express functional TRPV1 channels.

In summary, we have shown that (1) RyR activation leads to activation of TRP-like channels in the plasma membrane, membrane depolarization, activation of L-type voltage-gated Ca^{2+} channels and CICR. (2) ADPr is a specific and endogenous low affinity ligand for the P2Y1 receptors. (3) Functional TRPV1 channels are expressed in the INS-1E cells, but not in the primary β-cells.

Keywords: Ca^{2+} signaling, signal transduction, islets of Langerhans, β-cells, ryanodine receptors, Ca^{2+}-induced Ca^{2+} release, TRP-channels, TRPV1, capsaicin, P2Y1 receptors, and ADP ribose.

2 Erratum

Paper IA: page 302, paragraph 2, line 10: -40 mV, not -40 mM.

Paper IB: page 4, line 38: -40 mV, not -40 mM,
page 3, line 4; page 4, line 13; page 13, figure legend 1, line 6: Wistar rat, not Wister rat.

Paper II: fig. 3C: The concentrations are in µM, not mM.

3 List of publications

I. **Jabin Gustafsson, A.**, Ingelman-Sundberg, H., Dzabic, M., Awasum,J., Hoa, N.K., Östenson, C-G., Pierro, C., Tedeschi, P., Woolcott, O.O., Chiounan, S., Lund, P.-E., Larsson, O., and Islam M.S. Ryanodine receptor-operated activation of TRP-like channels can trigger critical Ca^{2+} signaling events in pancreatic β-cells.

A. FASEB Journal express article:
FASEB J. 2005 Feb;19(2):301-3.

B. Full paper:
DOI: 10.1096/fj.04-2621fje
http://tinyurl.com/trp-like
Epub 2004 Nov 30.

II. **Jabin Gustafsson, A.**, Muraro, L., Dahlberg, C., Migaud, M. Chevallier, O., Hoa, N.K., Krishnan, K., Li, N., and Islam, M.S., 2011. ADP ribose is an endogenous ligand of P2Y1 receptor. Mol Cell Endocrinol 333:8-19.

III. **Jabin Fågelskiöld, A.**, Kannisto, K., Boström, A., Hadrovic. B., Farre, C., Eweida, M., Wester, K., and Islam, M.S. Insulin-secreting INS-1E cells express functional TRPV1 channels (submitted).

Other papers published during the PhD period, but not included in the thesis:

Original papers:

Woolcott,O.O., **Gustafsson,A.J.**, Dzabic,M., Pierro,C., Tedeschi,P., Sandgren,J., Bari,M.R., Hoa, N.K., Bianchi,M., Rakonjac,M., Rådmark,O., Östenson,C.G., and Islam,M.S., 2006. Arachidonic acid is a physiological activator of the ryanodine receptor in pancreatic beta-cells. Cell Calcium, 39:529-537.

Bari, M.R., Akbar, S., Eweida, M., Kühn, F.J.P., **Gustafsson, A.J.**, Lückhoff, A., and Islam, M.S., 2009. H_2O_2-induced Ca^{2+} influx and its inhibition by N-(p-amylcinnamoyl) anthranilic acid in the beta-cells: involvement of TRPM2 channels. J Cell Mol Med, 13:3260-3267.

Reviews:

Gustafsson A.J., Islam, M.S., 2005. Cellens kalciumjonsignalering – från grundforskning till patientnytta. (Cellular calcium ion signaling - from basic research to benefits for patients) Läkartidningen, 102:3214-3219.

Book chapter:

Gustafsson A.J., Islam, M.S., 2007. Islets of Langerhans - cellular structure and physiology in Chronic Allograft Failure: Natural History, Pathogenesis, Diagnosis, and Managements. Editor: Ahsan, N., Landes Bioscience.

4 List of abbreviations

ACA	*N*-(p-amylcinnamoyl) anthranilic acid
ADPr	Adenosine diphosphate ribose
AM	Acetoxymethyl ester
AM404	*N*-(4-hydroxyphenyl)-arachidonoylamide
AMP	Adenosine monophosphate
ATP	Adenosine triphosphate
BSA	Bovine serum albumin
cADPr	Cyclic adenosine diphosphate ribose
cAMP	Adenosine 3´5´-cyclic monophosphate
CICR	Ca^{2+}-induced Ca^{2+} release
DAG	Diacylglycerol
DMSO	Dimethyl sulfoxide
EGTA	Ethylene glycol tetraacetic acid
ER	Endoplasmic reticulum
GLP-1	Glucagon-like peptide
HBSS	Hank's balanced salt solution
I_{CRAC}	Ca^{2+} release activated Ca^{2+} current
IP_3	Inositol 1,4,5-trisphosphate
IP_3R	Inositol 1,4,5-trisphosphate receptor
K_{ATP} channel	ATP-sensitive potassium channel
KRBH	Krebs Ringer bicarbonate HEPES buffer
NAADP	Nicotinic acid adenine dinucleotide phosphate
NAD^+	Nicotinamide adenine dinucleotide
$NADP^+$	Nicotinamide adenine dinucleotide phosphate
Orai1	A pore forming subunit of the mammalian CRAC channel
P2Y1	Purinergic receptor type 2Y1
PIP_2	Phosphatidylinositol 4,5-bisphosphate
PKA	cAMP-dependent protein kinase
PKC	Protein kinase C
PI-PLC	Phosphoinositide-specific phospholipase C
PMCA	Plasma membrane Ca^{2+} ATPase
RPM	Revolutions per minute
RPMI	Roswell Park Memorial Institute medium
RyR	Ryanodine receptor
SERCA	Sarco(endo)plasmic reticulum Ca^{2+}-ATPase
SOCE	Store-operated Ca^{2+} entry
STIM1	Stromal interaction molecule 1
TRP	Transient receptor potential
TRPM2	Transient receptor potential melastatin 2
TRPV1	Transient receptor potential vanilloid 1

Contents

5 Introduction and Background

5.1 The islets of Langerhans

The islets of Langerhans, named after the German pathologist Paul Langerhans, is a critical organ unique in that it is split into about a million units hidden in the pancreas. In 1869 Langerhans described small, clearer areas in the pancreas that stained differently from the rest of the pancreas. He thought that these structures were lymphatic tissues. Others thought that these could be embryonic remnants. These were named "islets of Langerhans" by the French histologist Gustave-Edouard Laguesse 24 years later. He suggested that the structures formed the endocrine part of the pancreas with a possibility to produce a hormone with glucose-lowering effect (1).

The islets have an essential role in regulation of the glucose homeostasis. The glucose concentration in the plasma is kept in a narrow interval irrespective of food intake or starving situation, by a fine-tuning system where the plasma glucose-lowering hormone insulin is antagonized by glucagon. The location of the islets is advantageous, since the hormones are secreted into the portal vein enabling direct control of the hepatic function. Impaired function or destruction of the cells in the islets underlies pathogenesis of different forms of diabetes, which is a public health problem throughout the world.

In humans, islets of Langerhans are spherical clusters of cells with a diameter between ~50-250 µm (2). The total number of islets varies depending on age, body mass index, size of the pancreas, and conditions such as pregnancy (3). They are in a higher number in the tail than in the head and body of the pancreas (4). The number of islets increases as the diameter of the islets decreases (5). Most of the islets are of small diameter, i.e. ~50-100 µm. However, medium sized islets with a diameter of ~100-200 µm contribute most to the total islet volume at all ages with the exception of the newborn, where it is the opposite (5). The islets of patients who have diabetes can be very large, up to ~350 µm in diameter, because of oedema and deposition of amyloid (2).

There are three major types of cells in the islets, i.e. the α-, β-, and δ-cells. In addition, there are other minor cell types, e.g. the pancreatic polypeptide-secreting (PP)-cells, the ε-cells, and the dendritic cells. Most of the cells (70-80%) in the adult human islets are insulin-secreting β-cells. Among the remaining are 15-20% glucagon-secreting α-cells, 5-10% δ-cells, 1% ε-cells (6), and 1% PP-cells. δ-cells secrete somatostatin and possibly gastrin. ε-cells secrete ghrelin, which stimulates growth hormone release and apetite (7). In each islet there are 5-20 dendritic cells, which express class II antigen with phagocytotic capacity (8). In addition to insulin, the β-cells secrete islet amyloid polypeptide (IAPP). However, all β-cells do not secrete IAPP since only 54% of β-cells stain for IAPP (2).

The islets coordinate their work even though they are structurally separated. A β-cell communicates with another through paracrine mechanisms or via a local vascular system within the islet. There is electrical synchronization between β-cells through gap junctions. Also, the β-cells communicate with non-β-cells via gap junctions. The gap junctions are made of connexin36, which is important for the oscillation of insulin secretion (9;10).

Today, there are about 285 million people in the world with overt islet failure (11). By the year of 2030, the number is likely to increase to 438 million. A gradual decrease in function of the islets takes place over years, and it is not until as much as 90% of the islets have stopped to function or are destroyed that any decline in health is noticed.

5.2 Insulin secretion

When studying β-cells, it is common to assume that they have a resting state when they do not secret insulin, and a stimulated state when they do. However, under physiological conditions, large insulin secretion occurs even under the fasting state, and secretion increases after food intake. In human, about 75% of the insulin secretion occurs in the form of oscillations with an interpulse interval of about five minutes (12;13). The pulsatile pattern of insulin secretion, which has many physiological advantages, is lost in patients with type 2 diabetes. The insulin secretion is regulated by the amplitude rather than the frequency of insulin oscillation. The synchronization signals for insulin secretion from a large number of islets are unclear, but neural networks are thought to be important in this process.

After a meal, the concentrations of nutrients including glucose, amino acids, and free fatty acids in the plasma increase, and the amplitude of insulin pulses increases. To trigger insulin secretion, glucose needs to be metabolized by glucokinase. Some mutations in the glucokinase gene can cause maturity onset diabetes of the young (MODY) (14). Metabolism of pyruvate and ATP production in the mitochondria are essential for glucose-stimulated insulin secretion. Several other factors generated from the mitochondria also potentiate insulin secretion. Some uncommon forms of diabetes are due to mutations or deletions in mitochondrial DNA.

A $[Ca^{2+}]_i$ increase is an essential trigger for insulin exocytosis. Insulin secretion is also regulated by neurotransmitters, and incretin hormones secreted from the gut. Glucagon like peptide 1 (GLP-1) is one important incretin hormone that augments insulin secretion, somatostatin secretion, and inhibits glucagon secretion. Furthermore, it promotes β-cell survival and proliferation. These actions of GLP-1 are mediated by Ca^{2+} as well as cyclic AMP (cAMP), and other signaling pathways. Thus, the insulin secretion is a highly controlled process that involves multiple nutrients, neurotransmitters, and hormones.

5.3 Ca^{2+} signaling in the β-cells

The calcium of importance for intracellular signaling is the ionized form of calcium, Ca^{2+}, inside the cell. Changes in the cytosolic free Ca^{2+} concentration ($[Ca^{2+}]_i$) induces signals for various cellular processes. Many Ca^{2+}-binding proteins, membranes, channels, pumps, stores, and other organelles are involved in the generation, and shaping of the Ca^{2+} signals. The Ca^{2+} signals in the β-cells control exocytosis of insulin. In a "resting" β-cell in vitro, the $[Ca^{2+}]_i$ is ~ 20-100 nM, and outside the cells the Ca^{2+} concentration is 10 000 times higher.

To avoid toxicity, the $[Ca^{2+}]_i$ must return to a resting level, and this is achieved by the plasma membrane Ca^{2+} ATPases (PMCA) that pumps out Ca^{2+} from the cytoplasm. Also, there are Na^+/Ca^{2+} exchangers for lowering $[Ca^{2+}]_i$. The ATP-driven pumps have high affinity but low capacity, compared to the exchangers that take care of the large Ca^{2+} loads. In Ca^{2+} signaling the $[Ca^{2+}]_i$ increases, and returns to the resting level shortly after. The $[Ca^{2+}]_i$ increase is likened to pressing the on-button, and a decrease in $[Ca^{2+}]_i$ means that the off-button is pressed.

Other molecules that are involved in Ca^{2+} signaling include Ca^{2+} binding proteins, Ca^{2+} channels, Ca^{2+} mobilizing messengers, and Ca^{2+}-sensing molecules. Calmodulin is a Ca^{2+} binding protein present in almost all cells. It contains a single polypeptide chain of 150 amino acids with four Ca^{2+} binding sites. Calmodulin constitutes about 1% of the total protein mass of the β-cells. Besides $[Ca^{2+}]_i$ regulation, calmodulin mediates many Ca^{2+} regulated processes in the cell, and works as a multipurpose intracellular Ca^{2+} receptor. The binding of Ca^{2+} enables calmodulin to bind to various target proteins, and alter their activity. Ca^{2+}/calmodulin binds to, and activates the PMCA that pumps Ca^{2+} out of the cell. Most effects of Ca^{2+}/calmodulin are mediated by the Ca^{2+}/calmodulin-dependent kinases.

In the plasma membrane there are different Ca^{2+} channels: voltage-gated, receptor-activated, and channels belonging to the "transient receptor potential" (TRP) family. Glutamate receptors and purinergic receptors of P2X type are examples of receptor-activated channels that are present in many cells. IP_3 is the most well characterized Ca^{2+} mobilizing intracellular messenger. Others are cADPr and nicotinic acid adenine dinucleotide phosphate (NAADP). Together, all the molecules involved in Ca^{2+} signaling in the β-cells orchestrate the $[Ca^{2+}]_i$ to fine-tune the insulin secretion.

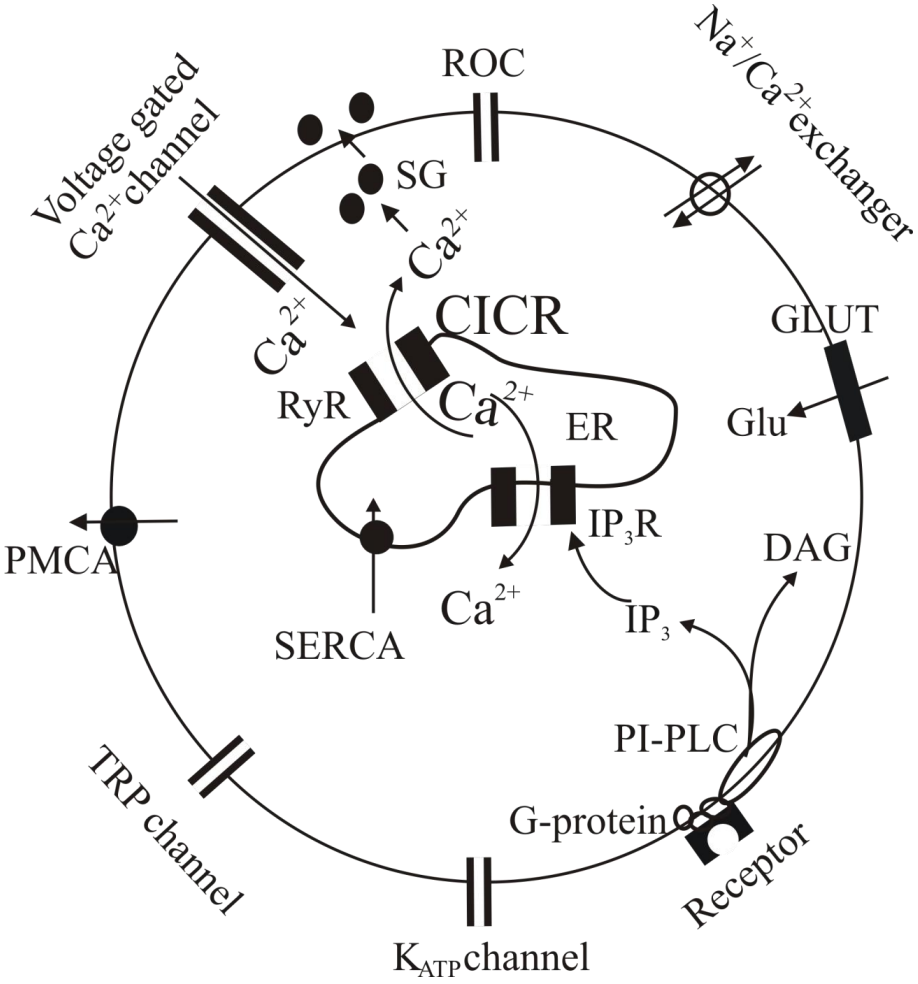

Figure 1. The figure shows some of the molecules involved in Ca^{2+} signaling in the β-cell. The figure also shows a mechanism for Ca^{2+} induced Ca^{2+} release (CICR). DAG = diacylglycerol; ER = endoplasmic reticulum; Glu = glucose; GLUT = glucose transporter; IP_3 = inositol 1,4,5-trisphosphate; IP_3R = inositol 1,4,5-trisphosphate receptor; RyR = ryanodine receptor; SG = secretory granulae; PI-PLC = phosphatidyl inositol specific phospholipase C; PMCA = plasmamembrane Ca^{2+}ATPase; ROC = receptor activated channel; SERCA = sacro(endo)plasmic reticulum Ca^{2+}ATPase.

5.3.1 Ca^{2+} oscillations

The $[Ca^{2+}]_i$ increase often takes place in the form of oscillations. Low concentration of an agonist leads to a low frequency, whereas a higher concentration leads to a higher frequency of the oscillations. The advantage of Ca^{2+} oscillations compared to continuously increased $[Ca^{2+}]_i$ is that the cells are not damaged by Ca^{2+} when the $[Ca^{2+}]_i$ oscillates. There is also a less likelihood of desensitization of the intracellular Ca^{2+} sensors. The β-cells interpret the Ca^{2+} signals by the degree of $[Ca^{2+}]_i$ increase or the frequency of Ca^{2+} oscillations. It has been shown that Ca^{2+} oscillations increase the efficiency, and the information content of Ca^{2+} signals that lead gene expression. In β-cells, at least three different types of Ca^{2+} oscillation have been described (15). The mechanism involved in the formation and decoding of Ca^{2+} oscillations is an active research field. Perturbed oscillations may be a cause for impaired insulin release that is normally pulsatile possibly because of the Ca^{2+} oscillations (16).

5.4 Stimulus-secretion coupling in the β-cells

The main triggers for insulin secretion from the β-cells are nutrient-induced $[Ca^{2+}]_i$ increases. Glucose is transported into the β-cell through a facilitative glucose transporter (GLUT1 and 3 in humans, and GLUT 2 in rodents) (17;18). Glycolysis, and metabolism in the mitochondria increases ATP/ADP ratio (19;20). The cytoplasmic ATP/ADP ratio acts as intracellular messenger that couples nutrient metabolism to electrical activity of β-cells. In this respect, the ATP-sensitive potassium channel (K_{ATP} channel) acts as a sensor of cellular metabolism. K_{ATP} channels of β-cells consist of two subunits, the channel subunit KIR6.2, and the sulfonylurea receptor SUR1. These channels are inhibited by, and are targets for the insulin-lowering sulfonylurea drugs (21). The K_{ATP} channels can be activated by agents such as MgADP and diazoxide, by involvement of the two nucleotide binding folds (NBF) 1, and 2 of SUR1 (22). This leads to hyperpolarization of the plasma membrane. When plasma glucose concentrations are reduced, a decreased ATP/ADP ratio leads to opening of the K_{ATP} channels, and causes repolarization. In this way, insulin secretion, and hypoglycaemia is prevented. Closure of the K_{ATP} channels is an initial signaling event leading to membrane depolarization. It should be emphasized, however, that closure of the K_{ATP} channels alone is not sufficient to depolarize the cell. That needs a co-existing inward depolarizing current. These depolarizing currents through as yet unknown channels depolarize the plasma membrane when the K_{ATP} channels are closed. It has been suggested that some TRP channels may account for these currents.

5.5 Transient receptor potential channels

The TRP channels were discovered in the photoreceptor cells of blind fruit flies (23). The light-induced change of membrane potential in these cells was transient rather than sustained. This was due to a mutation of a channel, thus called the transient receptor potential channel. There are 28 (27 in human) TRP channels, and one or other TRP channels are present in almost all cells. They are diverse when it comes to the regulation and function. The TRP channels are tetrameric ion channels that may form both homo-

and heterotetramers, and this gives possibilities for formation of many different channels. TRP channels mediate many sensory functions. The channels are divided into two groups according to their molecular similarities. Group 1 has five subfamilies. There are seven TRP channels related to the classical or canonical channel (TRPC). These channels are the most related to the original TRP channels. There are six TRP channels related to the vanilloid receptor (TRPV), and eight TRP channels related to the melastatin subfamily (TRPM). There are also TRPA channels, with many ankyrin repeats, and TRPN channels (24).

Group 2 TRP channels consist of two subfamilies: TRPP and TRPML. Mutations in the TRPP channels cause autosomal dominant polycystic kidney disease. Mutation in TRPML causes the neurodegenerative disorder mucolipidosis type IV.

We studied the mechanisms of RyR-activated membrane depolarization. TRP channels are known to mediate membrane depolarization in many cells (25;26). Therefore, we studied whether TRP channels were involved in the RyR-activated membrane depolarization in the β-cells.

5.5.1 TRP channels in the β-cells

At the beginning of this thesis, there was scanty information in the literature about TRP channels in the β-cells. During subsequent years, research from many groups has shown that many TRP channels are present in the β-cells. These are TRPC1-6 (27-29), TRPM2-5 (30-34), and TRPV1, 2, and 4 (35-37). Two of these have been dealt with in this thesis, and these will be discussed further. It is possible that some of the TRP channels mediate the inward depolarizing currents in the β-cells. The depolarization leads to activation of voltage-gated Ca^{2+} channels, and influx of Ca^{2+}.

5.5.1.1 TRPM2 channels

The type 2 melastatin-like transient receptor potential (TRPM2) is a chanzyme, forming a non-selective cation channel permeable to Na^+, K^+, and Ca^{2+} (38). The C-terminal of TRPM2 has an ADPr pyrophosphatase domain (38;39). TRPM2 expression is highest in the brain, but several peripheral cell types also express TRPM2 (40).TRPM2 functions as a cellular redox sensor, and TRPM2 activation leads to apoptosis and cell death (41;42).

TRPM2 is also activated by ADP ribose, NAD^+, nitric oxide, arachidonic acid, temperatures >35 ºC and Ca^{2+}. TRPM2 can be activated by Ca^{2+} released from the intracellular stores (43). *N*-(p-amylcinnamoyl) anthranilic acid (ACA) is an inhibitor of TRPM2, but it is not so specific. Flufenamic acid, the antifungal agents miconazole and clotrimazole are also inhibitors of TRPM2 (44;45). Whether 2-APB inhibits TRPM2 is controversial (46;47) Our group has shown that in the human islets, there are at least two main isoforms of TRPM2 channels: one is the full-length form (TRPM2-L) and the other is a nonfunctional form because of C-terminal truncation (TRPM2-S) (48). TRPM2 is mainly located in the plasma membrane and allows Ca^{2+} entry. However, TRPM2 is also located on the lysosomal membranes Activation of TRPM2 releases Ca^{2+} from the lysosomes (49). We have shown that functional TRPM2 channels are present in the INS-1E cells and the human β-cells (fig. 2) (30).

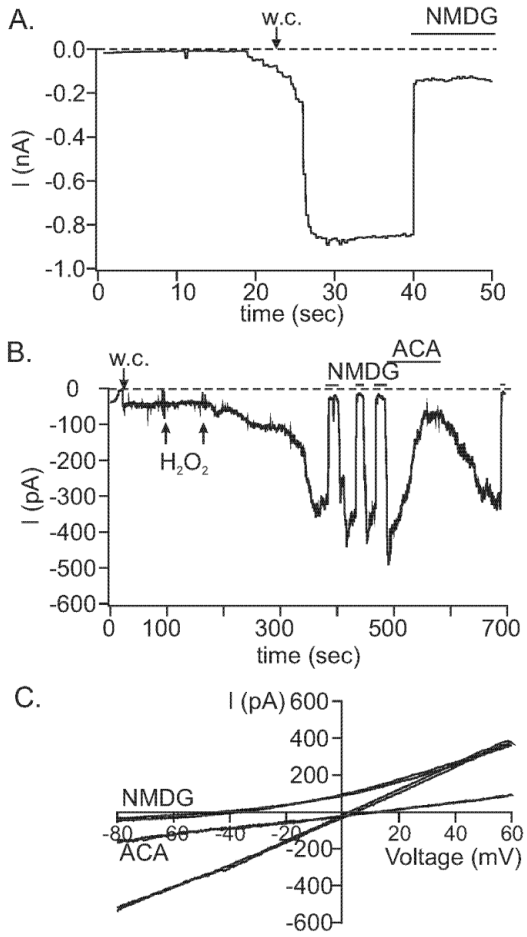

Figure 2. Whole-cell currents induced by ADPr and H_2O_2 in INS-1E cells. The figure is reproduced from Bari *et al* 2009 with permission. The whole-cell configuration was attained at the point indicated with "w.c.". Recordings were performed at room temperature and the holding potential was -60 mV. Bars indicate times where the standard bath solution was changed to a solution containing ACA, a TRPM2 inhibitor, or N-methyl-D-glucamine ($NMDG^+$), which is impermeable to TRPM2. Whole-cell current was recorded in the presence of intracellular ADPr. The pipette solution contained 0.6 mM ADPr and 1μM Ca^{2+} (A). Whole cell currents recorded without ADPr and after application of 1-2 μl 30% H_2O_2 directly into the recording chamber. The estimated final concentration of H_2O_2 in the chamber was ~10 mM. The pipette solution contained 1 μM free Ca^{2+} (B). Current-voltage relationship of H_2O_2-induced currents as derived from (B), recorded during voltage ramps from -90 to +60 mV of 400 ms duration (C).

5.5.1.2 TRPV1 channels

TRPV1 is a non-selective cation channel that mediates peripheral nociception and pain sensation. It is abundant in the trigeminal and the dorsal root ganglia. TRPV1 positive afferent neurons have been claimed to play a critical role in local islet inflammation in autoimmune diabetes pathoetiology (50). One group has reported that TRPV1 protein is expressed in the rat insulinoma cell lines RIN and INS-1 (35). Whether TRPV1 exists in the primary β-cells remains controversial. TRPV1 immunoreactivity has been described in primary β-cells of Sprague-Dawley rats by one group (35), but not in those of Zucker diabetic rats (51) or NOD mice (50). It is not known whether TRPV1 is present in the human β-cells.

Capsaicin, resiniferatoxin, temperature >43 ºC and low pH are some of the activators of TRPV1 (52). Capsaicin is the pungent component of chili pepper. It produces burning pain, desensitisation and degeneration of a specific subset of sensory fibres that are also sensitive to chemical irritants and noxious heat. This explains the burning sensation of chili pepper intake. Due to desensitization of nociceptive terminals, capsaicin also exhibits analgesic properties. Capsaicin is lipophilic and binds to the intracellular part of TRPV1 and thereby activates the TRPV1 channel (53;54).

TRPV1 is expressed in nerve fibres in the islets of Langerhans of rats and mice (50;51). Akiba *et al* have reported that TRPV1 protein is expressed in the rat insulinoma cell lines RIN and INS-1, and that insulin secretion is increased by capsaicin in the RIN cells (35). We have studied whether TRPV1 activation leads to $[Ca^{2+}]_i$ increase or induces currents in the β-cells.

We have used capsaicin and AM404 as agonists of TRPV1. The active metabolite of paracetamol, AM404 activates TRPV1 at analgesic doses of paracetamol (55;56). After ingestion, paracetamol is metabolized into, among others, *p*-aminophenol. AM404 is formed by conjugation of *p*-aminophenol and arachidonic acid. AM404 is formed in the brain by the action of fatty acid amide hydrolase (FAAH) (57). The TRPV1 antagonist capsazepine is a synthetic analogue that competitively inhibits capsaicin binding (58). It also blocks TRPV1 activation induced by low pH (59). We used capsaicin, AM404 and capsazepine as tools for identifying the TRPV1 channel in the β-cells.

It is not fully established whether TRPV1 exists in the primary β-cells. Therefore, we studied the effect of capsaicin on $[Ca^{2+}]_i$ in primary rat and human primary β-cells. Immunohistochemistry was used to study the expression of TRPV1 protein in the human islet cells and the human insulinoma cells.

5.6 The role of the endoplasmic reticulum in Ca^{2+} signaling

Like many other cells,the β-cells have several Ca^{2+} stores. Among these, the endoplasmic reticulum (ER) is the best characterized. The ER is best known for its role in the protein synthesis, but it is also a sophisticated instrument for Ca^{2+} signaling. The Ca^{2+} concentration in the ER of resting β-cells is high, about 250 μM. On the ER membranes,

there are Ca^{2+} channels and Ca^{2+} pumps that regulate the luminal $[Ca^{2+}]_i$. ER is filled with Ca^{2+} by sarcoendoplasmic reticulum Ca^{2+} ATPase (SERCA). There is a large amount of Ca^{2+} binding proteins in the ER. Calsequestrin is one such Ca^{2+} binding protein in the ER lumen. It has a high capacity and low affinity for binding Ca^{2+}. Thus, the ER has many important players that regulate the $[Ca^{2+}]_i$ inside the lumen and release Ca^{2+} in response to various signals.

5.7 Ca^{2+} channels in the ER

5.7.1 Activation of RyRs and IP_3Rs

There are two main families of Ca^{2+} channels in the ER: the inositol 1,4,5-trisphosphate receptors (IP_3Rs), and the RyRs. The latter name is derived from the plant alkaloid ryanodine, which binds to the receptor with nanomolar affinity, and activates the channel. Whereas submicromolar concentrations of ryanodine lock the channel in a long-lived open state, micromolar concentrations inhibit the channel. Insulin secretion is stimulated by low concentrations (~1 nM) of ryanodine (60). While IP_3 activates the IP_3 receptor, the ryanodine receptor is activated by several mechanisms. Fructose 1,6 diphosphate, arachidonic acid, cyclic adenosine diphosphate ribose (cADPr), long chain Acyl CoA, and ATP are some of the activators or positive modulators of RyRs (61-63). Caffeine is a widely used pharmacological activator of RyRs (64). But caffeine has many non-specific effects. Our group has shown that caffeine inhibits the K_{ATP} channels, elevates the cAMP concentration, and inhibits the L-type voltage-gated Ca^{2+} channels (65). Caffeine also inhibits store-operated Ca^{2+} entry (66).

5.7.2 MBED

Instead of caffeine, we have used 9-methyl 5,7-dibromoeudistomin D (MBED) as a RyR activator. MBED is derived from the natural product eudistomin D, isolated from the marine tunicate *Eudistoma olivaceum* (67). MBED has caffeine-like properties, but it is a more specific, and more potent activator of RyRs, and is thus more suitable for mechanistic studies of these channels (68). It has been suggested that MBED binds to a different site than ryanodine on the RyRs, since MBED does not inhibit ryanodine binding to the receptor (68). The effects of MBED on RyRs have been known for about 20 years, and so far no non-specific effect has been reported. We have reported that MBED does not inhibit cAMP-phosphodiesterases, IP_3Rs, voltage-gated Ca^{2+} channels or K_{ATP} channels in the β-cells (69).

5.7.3 Isoforms of RyRs and IP_3Rs

Both IP_3Rs and RyRs are present in many cells, and are regulated by positive feedback, whereby the released Ca^{2+} can bind to the channel, and increase the Ca^{2+} release. There are three isoforms of both channels. The rat insulinoma cell line INS-1 express mRNA for IP_3R1, IP_3R2, and IP_3R3, and IP_3R1 is in abundance (70). mRNA for all the three

isoforms is also found in rat pancreatic islets, rat insulinoma RINm5F cells, and mouse insulinoma βHC9 cells, but in these cells IP_3R1 is in greater abundance (71). RyR1 and RyR2 are mainly expressed in the skeletal muscles and heart, respectively, while the RyR3 is expressed in the brain, the smooth muscles and the epithelial cells (72). All the three isoforms of RyRs, i.e. RyR1, RyR2, and RyR3, are present in human islets (73). RyR2, but not RyR1 has been detected by RT-PCR in INS-1 cells, and rat islets (29). The RyR2 is mainly located on the ER/SR membranes (74). One group has shown that the RyR2 is also expressed on the plasma membrane in the β-cells (75).

5.8 Store-operated Ca^{2+} entry

Store-operated Ca^{2+} entry (SOCE), also called capacitative Ca^{2+} entry, is a process whereby the Ca^{2+} entry across the plasma membrane is closely coordinated with the depletion of ER Ca^{2+} stores (76). It is conserved from lower organisms such as yeast, worms, and flies to human. SOCE has been described in β-cells (77). In β-cells, as in many other cells, an important molecule involved in SOCE is the stromal interaction molecule 1 (STIM1) that acts as the Ca^{2+} sensor in the ER. Mammals also have a related gene that encodes STIM2. STIM2 is also a Ca^{2+} sensor, but with a different sensitivity for the ER Ca^{2+} concentration than STIM1 (78). An intraluminal EF-hand domain of STIM1 senses the Ca^{2+} concentration in the ER lumen. STIM1 is transported to the plasma membrane upon ER Ca^{2+} pool depletion. Orai1, also called CRACM1, is the pore-forming subunit of a store-operated Ca^{2+} channel in the plasma membrane. This channel conducts a highly Ca^{2+}-selective, non voltage-gated, inwardly rectifying current, called Ca^{2+} release activated Ca^{2+} current (I_{CRAC}) (79). According to one report, I_{CRAC} is inhibited when the RyRs are inhibited (80). It is unknown whether STIM1 interacts with Orai1 in the β-cells. Interaction between STIM1, Orai1, and TRPC might be of importance in SOCE (81). One study has shown a connection between the IP_3Rs and some TRP channels in the plasma membrane (82). Thus, multiple mechanisms may underlie different forms of SOCE.

5.9 Voltage-gated Ca^{2+} channels

In β-cells, the most important Ca^{2+} channels are the ones that are activated upon plasma membrane depolarization. Ca^{2+} entry through voltage-gated Ca^{2+} channels triggers exocytosis of insulin (83). There are ten voltage-gated Ca^{2+} channels coded by three gene families: The Ca_v1 family has electrical properties of L-type, i.e. they require high voltage for activation, and are open for a longer period ("Large and Long"). These channels are inhibited by dihydropyridine antagonists. Glucose-induced insulin release is inhibited to 80-100% by dihydropyridine antagonists (84;85). The main form of L-type voltage-gated Ca^{2+} channels in the β-cells is $Ca_v1.3$ (α_{1D}). It is activated at a lower membrane potential (~-55mV) compared to $Ca_v1.2$ (α_{1C}).

The Ca_v2 family mediates currents of N-, P/Q- or R-type. The P/Q-type Ca^{2+} channels are also coupled to insulin secretion, and account for 45% of integrated whole-cell Ca^{2+} current in human β-cells. R-type Ca^{2+} channels are not present in human β-cells (85), but

may be involved in insulin secretion through central neurons or GLP-1-producing L-cells in the gut (86). There is also the Ca_v3 family of ion channels that is activated by low voltage and have electrical properties of T-type, with smaller and shorter lasting currents ("tiny and transient"). The T-type current in human β-cells is mediated by $Ca_v3.2$ (α_{1G}), and is involved in insulin release induced by 6 mM but not by 20 mM glucose (85). Neither Ca_v2 nor Ca_v3 are blocked by dihydropyridine antagonists. We have shown that L-type voltage-gated Ca^{2+} channels are activated by membrane depolarization after RyR activated Ca^{2+} entry.

5.10 Ca^{2+}-induced Ca^{2+} release

Ca^{2+}-induced Ca^{2+} release (CICR) is an intracellular signaling phenomenon, where a $[Ca^{2+}]_i$ increase triggers Ca^{2+} release from the ER. CICR was first described in the heart muscle cells, where a small Ca^{2+} entry trough the L-type voltage-gated Ca^{2+} channels caused a large Ca^{2+} release from the SR. This phenomenon takes place in many excitable cells, e.g. muscle cells, nerve cells, and the β-cells. CICR induces synchronous, transient rises in the $[Ca^{2+}]_i$ that amplifies the Ca^{2+} signals. Both IP_3Rs and RyRs are Ca^{2+}-gated Ca^{2+} channels in the ER (87). In the β-cells, activation of RyRs or IP_3Rs amplifies Ca^{2+}-dependent exocytosis of insulin by CICR (88;89). GLP-1, a blood-glucose-lowering incretin hormone, increase the cAMP in the cytoplasm of the β-cells, and facilitates CICR by cAMP-dependent phosphorylation of the RyRs (90;91). CICR is also stimulated by activation of RyRs by cAMP-regulated guanine nucleotide exchange factors (Epac) in the human β-cells (92).

5.11 Pyridine nucleotide-derived molecules and Ca^{2+} signaling

Several reports have demonstrated that glucose elevation increases cyclic ADPr (cADPr) and NAADP concentration in the β-cells. cADPr is known to stimulate insulin secretion in β-cells by Ca^{2+} release from the intracellular Ca^{2+} stores, and has also been shown to activate the TRPM2 channels (31). NAADP releases Ca^{2+} from acidic Ca^{2+} stores, and from insulin secretory vesicles (74). A group of voltage-gated ion channels called two-pore channels (TPCs) are located on the lysosomal membranes, and are activated by nanomolar concentrations of NAADP, while micromolar concentrations of NAADP inhibit them (93).

ADPr is formed from β-NAD^+, and NAADP is formed from $NADP^+$ by ADP ribosyl cyclases, including CD38 (94). CD38 and its homologues have NADase, ADP-ribosyl cyclase, and cADPr hydrolase activities (95). ADPr constitutes more than 99% of the products produced by the action of CD38 (96-98). ADPr is also produced by hydrolysis of cADPr, and from NAD^+ by NAD glycohydrolases, (95). Furthermore, poly (ADPr) glycohydrolase can produce ADPr from poly (ADPr) (99;100).

Since CD38 is located with its catalytic site oriented extracellularly in the plasma membrane (101;102), ADPr produced by CD38 and related enzymes is likely to be released extracellularly. Extracellular release of ADPr has been shown in cortical

astrocytes (103). Synaptosomes have been reported to have NADase activity, giving rise to speculations that ADPr could be a neurotransmitter (104). ADPr is shown to be released during nerve stimulation (105).

CD38 and related enzymes are also present in the β-cells, and they are thought to play some roles in mediating insulin secretion (106). The role of CD38 in insulin secretion is generally attributed to RyR activation by cADPr and NAADP (107). It remains unclear whether extracellular ADPr can signal by acting on cell surface receptors or whether it must enter into the cell. The entrance of ADPr is thought to be via CD38, but the transport rate is slow, and this mechanism is not universal (108;109). Ecto-nucleotide pyrophosphatases degrade ADPr to AMP (110;111). The conversion of ADPr to AMP can also be catalysed by apyrase, and AMP is further metabolized to adenosine by 5´nucleotidase (112;113). Extracellular ADPr is thus a well-suited nucleotide for signaling by activating cell surface receptors. Our studies show that ADPr increase $[Ca^{2+}]_i$ by activation of purinergic receptors of type P2Y1 in the INS-1E cells as well as in the rat and human β-cells.

5.12 Purinergic receptors

Receptors for purine nucleotides and nucleosides are present in numerous tissues. The purinoceptors are classified into P1, which are more specific for adenosine and AMP than for ADP and ATP. The adenosine/P1 purinoceptors are in turn divided into A1, A2a, A2b, and A3 (114). The A1 and A3 subtypes inhibit adenylate cyclase, while the A2 subtypes activates adenylate cyclase (115;116).

The P2 purinoceptors are, in contrast, more specific for ATP and ADP than for adenosine and AMP. They are divided into P2X and P2Y subtypes, which can be discriminated by their response profiles to different ATP-analogues (117). P2X receptors are intrinsic ion channels (not G-protein coupled) permeable to Na^{2+}, K^{+}, and Ca^{2+} (118). P2X receptors in the β-cells are of subtype P2X1, P2X3, P2X4, P2X6, and P2X7 (119-122).

There are eight human P2Y receptors: P2Y1, P2Y2, P2Y4, P2Y6, P2Y11, P2Y12, P2Y13, and P2Y14 (123-125). The missing numbers in the sequence are receptors that are cloned from non-mammalian vertebrates or receptors under characterization. The P2 receptor subtypes in β-cells are P2Y1, P2Y2, P2Y4, P2Y6, and P2Y12 (126). The P2Y1 receptor has been shown to be involved in insulin secretion, but both stimulation of insulin secretion and inhibition of secretion have been reported (127). Some studies have claimed that P2Y purinoceptors can constitute new targets for antidiabetic drugs (128;129). P2Y receptors are G-protein coupled, and often activate the PI-PLC pathway leading to IP_3 production (130).

5.13 The signaling enzyme PI-PLC

Phosphatidylinositol specific phospholipase C (PI-PLC) constitutes a family of key enzymes in the Ca^{2+} signaling. There are eleven isoforms of PI-PLC, and they are divided into four families: β, γ, δ, and ε. G-protein coupled receptors activate PI-PLCβ, and receptor protein-tyrosine kinases activate PI-PLCγ (131). Thus, there are many growth factors that activate PI-PLCγ. PI-PLCδ is activated by Ca^{2+}, and PI-PLCε is activated by GTP-Ras (132). PI-PLCε is involved in activation of the GLP-1-receptor-induced facilitation of CICR (133).

The PI-PLC enzymes cleave phosphatidyl inositol 4,5-biphosphate (PIP_2) to inositol 1,4,5-trisphosphate (IP_3) and diacylglycerol (DAG). IP_3 is a second messenger that binds to the IP_3 receptor in the ER, and triggers release of Ca^{2+} into the cytoplasm. DAG has two signaling roles: it can be cleaved to release arachidonic acid that either works as a messenger in its own right, or is used in the synthesis of eicosanoids, such as prostaglandins, prostacyclins, tromboxanes, and leukotrienes. DAG activates protein kinase C (PKC), and the activation is usually Ca^{2+} dependent (134;135). When the $[Ca^{2+}]_i$ increases, PKC translocates from the cytosol to the cytoplasmic face of the plasma membrane, where it is activated by Ca^{2+}, DAG, and negatively charged membrane phospholipids such as phosphatidylserine.

6 Aims of the thesis

The aims of this thesis were to study:

1. the consequences of activation of RyRs on $[Ca^{2+}]_i$ in pancreatic β-cells.

2. whether functional Ca^{2+} permeable TRP-like channels operate in the β-cells.

3. whether activation of the RyRs leads to the activation of plasma membrane ion channels, and depolarization of the membrane potential.

4. the molecular mechanisms by which ADPr increases $[Ca^{2+}]_i$ in the insulin-secreting cells.

5. whether functional TRPV1 channels are present in the insulin-secreting cells.

7 Methods

7.1 Cells

In most of the experiments, we used the rat insulinoma cell line INS-1E (subclone S5). INS-1E cells are widely used as a model for β-cells. The S5 cells were derived from INS-1E cells in our laboratory, and they differ from the INS-1E cells in that they are adjusted to grow in 2.5% FBS while they require a higher concentration of β-mercaptoethanol. The advantage of using insulinoma cell lines instead of primary β-cells is that the cell lines consist of pure insulin-secreting cells, whereas cells prepared from islets contain a mixture of cells, which cannot be easily identified under microscope. For the experiments, cells of round shape that looked like differentiated β-cells were chosen. Such cells constitute only about 10-20% of the cells in the microscope field. The handling of the cells is described in the methods section of each paper.

The use of primary β-cells and human islets for experiments was approved by local ethics committee. Primary β-cells were prepared from the Wistar rat islets. Primary β-cells from CD1 mice of 12-16 weeks of age were used for insulin secretion studies. The procedures for isolation of islets and preparation of β-cells are described in the attached papers. Human islets were obtained from islet transplantation programmes, and single cells were prepared as described in the papers. In paper II, we used 1321N1 human astrocytoma cells that stably overexpress human recombinant P2Y1 receptors, and wild type (WT) astrocytoma cells that do not express any P2Y1 receptors.

7.2 Chemical tools used

Compound	**Effects**	**Side effects**	**Used concentration**	**Paper**
ADP	Activates purinergic receptors		30 µM	II
ADP ribose (ADPr)	Activates TRPM2		30 µM	II
2-aminoethoxy-diphenyl borate (2-APB)	Inhibits I_{CRAC} and activates TRPV1-3 Inhibits IP_3R and some TRP channels, including TRPC1,3-6	Inhibits SERCA (136)	30 µM	I
Arachidonic acid	Activates many TRP channels and RyRs		5 µM	III

8-Bromo-ADPr	ADPr antagonist		30 µM	II
cADPr	Activates RyR (?)	Activates TRPM2	30 µM	II
Capsaicin	Activates TRPV1		300 nM	III
Capsazepine	Inhibits TRPV1		10 µM	III
Carbachol (cch)	Muscarinic agonist		10-100 µM	I, II, III
2-chloro N6-methyl-(N)-methanocarba-2-deoxyadenosine-3,5-bisphosphate (MRS 2279)	Inhibits P2Y1 receptor	Not reported	10 µM	II
2´Deoxy-N6-methyladenosine 3,5-bisphosphate (MRS 2179)	Inhibits P2Y1 receptor	Inhibits P2X1 receptor (137)	1-10 µM	II
Diazoxide	Opens K_{ATP} channels		100 µM	I
Gadolinium chloride ($GdCl_3$)	Blocks several TRP channels, including TRPC1,3,6, TRPM3,4, TRPV4, TRPP1, TRPML1	Inhibits voltage-gated Ca^{2+} channels and stretch-activated channels (138;139)	10 µM	I
Lanthanium chloride ($LaCl_3$)	Blocks several TRP channels, including TRPC3-7, TRPV2,4-6, TPRM4,7, TRPP1, TRPML1	Activates TRPC3 and 5 in µM concentrations.	100 µM	I
9-methyl 5,7-dibromoeudistomin D (MBED)	RyR activation	Not reported	50 µM	I
Nimodipine	Blocks L-type voltage-gated Ca^{2+} channels		5 µM	I
NAD^+	Activates TRPM2 through conversion to ADPr		30 µM	II

Niflumic acid	Inhibits TRP channels, including TRPC4,6, TRPM2,3, and TRPV4 (140;141)		50 µM	I
Nimodipine	Blocks L-type voltage-gated Ca^{2+} channels		5 µM	I
N-(4-hydroxyphenyl)-5,8,11,14-eicosatetraenamide (AM404)	Activates TRPV1		5 µM	III
N-(p-amylcinna-moyl) anthranilic acid (ACA)	Inhibits TRPM2	Inhibits TRPM8 and TRPC6 (142)	20 µM	II
N-propargyl-nitrendipene (MRS 1845)	Blocks SOCE		5 µM	I
O-acetyl adenosine diphosphate ribose (OAADPr)	Actylated analogue of ADPr, activates TRPM2 (143)		10 µM	II
PADPr	Stable analogue of ADPr		100 µM	II
p-aminophenol	Metabolite of paracetamol		5 µM	III
Potassium chloride (KCl)	Depolarization of plasma membrane		25 mM	I, II, III
Ruthenium red (RR)	Blocks RyRs and TRP channels, including TRPC3, TRPV1-6, TRPM3,6, and TRPA1	Many nonspecific effects	10 µM	I
Ryanodine	Activates (nM) and inhibits (µM) RyR		50 µM	I
SKF 96365	Inhibits several TRP cannels including TRPC6, 7 and TRPV2.	Inhibits voltage-gated Ca^{2+} channels and SOCE.	10 µM	I

Thapsigargin	Inhibits SERCA		125-500 nM	I, II, III
U73122	Inhibits PI-PLC		10 µM	II

7.3 Measurements of $[Ca^{2+}]_i$ by microfluorometry

It is nowadays common to use fluorescence techniques to measure $[Ca^{2+}]_i$ in single living cells in real time. The measurement is done by use of a variety of fluorescent Ca^{2+} indicators. For measurement of $[Ca^{2+}]$i, fura-2 is the most commonly used indicator. The fluorescence ratio between the free and the Ca^{2+}-bound forms of fura-2 enables one to calculate the $[Ca^{2+}]_i$. Since fura-2 is cell-impermeant, an acetoxymethyl (AM) ester is coupled to the carboxylate groups of fura-2 to enable penetration through the cell membrane. Once inside the cell, the AM-group is hydrolyzed by the intracellular esterases, and fura-2 becomes Ca^{2+}-sensitive.

The fluorescence of fura-2 at 340 nm increases about threefold and at 380 nm decreases about tenfold upon Ca^{2+}-binding. The emission maximum of fura-2 is at 510 nm. $[Ca^{2+}]_i$ is calculated from *F*340/*F*380 according to Grynkiewicz *et al* (144). R_{max} and R_{min} were determined in our studies by using external standards containing fura-2 free acid and sucrose (2 M) (145). The method is described in detail in paper I, II, and III.

7.4 Electrophysiology

Patch clamp-recordings enable measurement of the electrical potential or the electrical current across the cell membrane. It is possible to isolate currents through a specific class of channels by adjustment of the ionic composition of the extracellular and intracellular solutions, application of pharmacological inhibitors etc. There are several modes of patch clamp, depending on whether single channels or a group of channels are going to be studied.

All patch clamp experiments start in the cell-attached patch mode. A tight contact between the recording pipette and the cell is accomplished by light suction to the pipette interior. A high shunt resistance (> 1 gigaohm) is produced. This is called a giga-seal. The cell is still intact. We used the pore-forming agent amphotericin B to perforate the cell membrane. This is called perforated patch whole-cell configuration. Physical contact with the cell interior is thus established. The advantage of the perforated-patch whole cell method is that there is no washout of intracellular compounds, since the pores only allow passage of small monovalent ions but not larger molecules or ions such as Ca^{2+} (146). In this way, it is a more physiological configuration than the standard whole-cell configuration, where the membrane rupture is achieved by a pulse of negative pressure by gentle suction.

For current measurements, we used a fully automated patch clamp workstation (Port-a-patch, Nanion, Munich, Germany) equipped with an HEKA EPC 10 amplifier (HEKA, Lambrecht/Pfalz, Germany). The planar patch clamp glass chip containing a micron sized

aperture was primed by adding 5 µl of internal and external solution to the respective sides of the chip. The PatchControl software (Nanion Technologies, Munich, Germany) applied a suction protocol to automatically capture a cell, obtain a giga-seal between the glass substrate and the cellular membrane, and eventually obtain whole cell voltage clamp configuration. Details are written in the respective papers.

7.5 Measurement of insulin secretion

The use of islets from mice was approved by the local ethics committee. Islets from mice pancreas were isolated as described by Kelly *et al* (147). After 24 h incubation and recovery from the isolation procedure, the cells were dispersed by trypsin (0.25%) for 8 min to obtain single cells. Total separation of the cells was verified microscopically, and the cells were transferred to multi-well plates (2×10^5 cells/well). For attachment, the cells were incubated for 24 h in 11 mM glucose. A washing procedure repeated three times with KRBH containing 3.3 mM glucose, and 15 min of preincubation in 3.3 mM glucose preceded the stimulation. According to the different treatments tested, the wells were divided into 4 groups. Group 1 was incubated with 3.3 mM glucose, group 2 with 16.7 mM glucose, group 3 with 3.3 mM glucose and 80 µM ADPr, and group 4 was incubated with 16.7 mM glucose and 80 µM ADPr. Insulin concentration in the collected samples was measured by ELISA using a commercial kit (Crystal Chem Inc).

7.6 Whole-blood flow cytometric assays

The experiments were approved by local ethics committee. We tested blood from three individuals between the ages of 24 and 42. Venous blood was collected by venepuncture. Within 5 min of blood collection, the blood samples were processed for flow cytometric measurements. We used whole-blood flow cytometry to evaluate the effect of ADPr on platelet shape change, aggregability (fibrinogen binding), and secretion (P-selectin expression). Whole-blood flow cytometric assays of platelet P-selectin expression and fibrinogen binding have been described previously (148). Platelets were gated by their characteristic light scattering signals, and the gated cells were confirmed with fluorescein isothiocyanate (FITC) conjugated anti-CD42a (GPIX) monoclonal antibody (MAb) Beb1 (Becton Dickinson, San Jose, CA, USA). Please see details in paper II on how the platelet shape change was monitored. Platelet shape change was expressed as percentage calculated according to the following formula: % of platelet shape change=100×((platelet counts within the innergate after stimulation-platelet counts within the innergate before stimulation)/(platelet counts within the inner gate before stimulation)).

7.7 Western blot analysis

Western blot was used to study the expression of TRPV1 protein in the INS-1E cells and in the human islets. The primary anti-TRPV1 antibody used was affinity-purified rabbit polyclonal IgG antibody (BIOMOL international, U.K., BML-SA564-0050, Lot # P9604a, cat. no. SA-6564). The antibody was directed against the peptide sequence DASTRDRHATQQEEV, which represents the amino acid residues 824-838 in the C-

terminal region of the rat TRPV1. The specific blocking peptide antigen (TRPV1 blocking peptide, BIOMOL international, U.K., BML-SA564-0050, Lot #P9604a, SA-564) was used to test the specificity of the antibody. Please see detailed information of the procedures in paper III.

7.8 Immunohistochemistry

Immunohistochemistry was used to detect TRPV1 protein in the human islet cells and the human insulinoma cells. Human pancreas resection specimens were collected from the Laboratory of Pathology at the Uppsala University Hospital, Sweden. They were from surgical specimens that were stored in the biobank after approval from the local ethics committee. The samples were fixed in formalin and embedded in paraffin wax. Sections from the tissue microarray blocks were cut at 4 μm thickness and immunostained. Primary antibodies and a dextran polymer visualization system (UltraVision LP HRP polymer®, Lab Vision) were incubated for 30 min each at RT. Diaminobenzidine (Lab Vision) was used as chromogen, and slides were developed for 10 min. For details of the immunostaining procedures, please see paper III.

We used eight different antibodies that were affinity purified rabbit polyclonal IgG antibodies raised against synthetic peptides corresponding to either the C-terminus or the N-terminus of TRPV1. The antibodies were from: 1. Biosensis (cat. no. R-076-100), 2. Alomone (cat. no. ACC-03), 3. Sigma (cat. no. V2764), 4. and 5. Santa Cruz Biotechnologies (cat. no. Sc-20813 and Sc-28759), 6. and 7. Chemicon (cat. no. AB5889 and AB5370P) and 8. the human protein atlas project (HRPK2180179, not published in the Protein Atlas, yet).

7.9 Statistical analysis

The data were expressed as means ± SEM. When comparison between two groups was made, Student's unpaired t-test was used, and when comparison was made within groups paired *t*-test was used. The *p*-value was considered as significant when <0.05. The concentration-response curves were made by using Graph Pad software.

8 Results and discussion

The detailed results of experiments and discussions of their interpretation and importance are in the two published papers and one manuscript that constitute this thesis. In the following paragraphs, I shall briefly mention only the results of some of the key experiments.

8.1 RyRs operate activation of TRP-like channels

RyRs amplify Ca^{2+} signals by CICR and thereby increase insulin secretion (63;74;89;149). However, any possible role of RyRs in triggering Ca^{2+} entry through the plasma membrane remained unknown. Many groups have used caffeine to activate RyRs, but caffeine inhibits many ion channels, enzymes, and receptors. It also inhibits K_{ATP} channels, voltage-gated Ca^{2+} channels, and store operated Ca^{2+} channels (65;66). We used a more specific agonist of RyR, namely MBED, to study the consequences of RyR activation in the β-cells.

In paper I, we showed that MBED activated RyRs in the β-cells and elicited a pattern of $[Ca^{2+}]_i$ increases that could be divided into three distinct components. First, there was an initial peak, which declined to a plateau phase with regenerative spikes superimposed on the plateau (fig. 3). We found that the different phases of $[Ca^{2+}]_i$ increases were due to different underlying mechanisms. The initial peak was present even when the extracellular Ca^{2+} was omitted, but was abolished when the ER Ca^{2+} pools were depleted by thapsigargin, a specific inhibitor of the SERCA (150). Thus, the initial peak was due to a transient Ca^{2+} release from the ER caused by RyR activation. These results were in accordance with earlier studies (69;151).

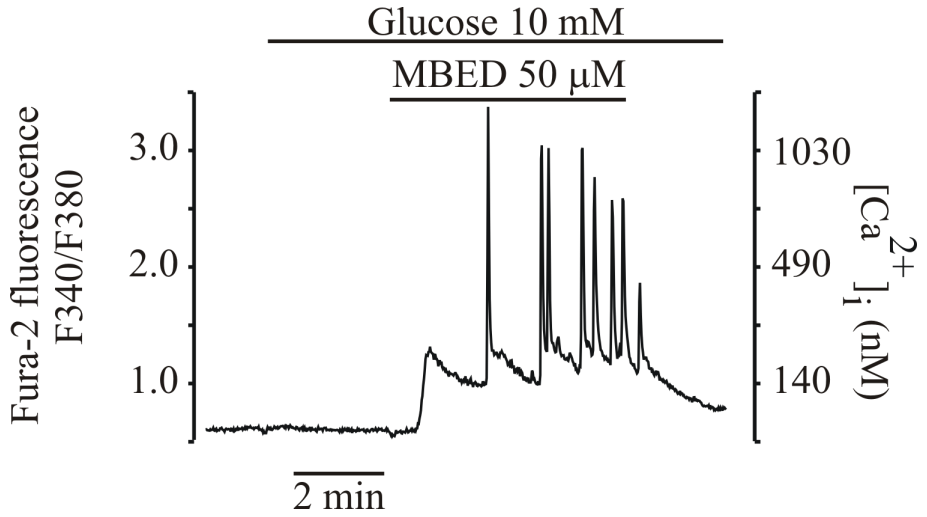

Figure 3. Activation of RyRs elicited a characteristic pattern of $[Ca^{2+}]_i$ changes. The figure is reproduced from Jabin Gustafsson *et al* 2004. MBED activated the RyRs in INS-1E cells, which resulted in a characteristic pattern of changes in $[Ca^{2+}]_i$. After addition of MBED (50μM) in the presence 10 mM glucose, there was an initial rapid rise of $[Ca^{2+}]_i$, which declined to a plateau. A series of large $[Ca^{2+}]_i$ spikes were superimposed on the $[Ca^{2+}]_i$ plateau.

The plateau phase was the most important finding in this study. It was abolished by omission of extracellular Ca^{2+}, and by SKF 96365, an inhibitor of SOCE and several TRP channels (152;153). Hence, we concluded that RyR activation also led to a prolonged $[Ca^{2+}]_i$ increase that was due to Ca^{2+} entry through some TRP-like Ca^{2+} channels in the plasma membrane. In comparison to the carbachol-induced capacitative Ca^{2+} entry (SOCE), the RyR-operated Ca^{2+} influx was much larger. When the cells were treated with thapsigargin, there was still a $[Ca^{2+}]_i$ plateau after stimulation by MBED. This suggests that the Ca^{2+} influx through the plasma membrane was not entirely dependent on the filling state of the ER. Instead, protein-protein interactions and conformational coupling could possibly be the link between activation of RyRs in the ER and the activation of Ca^{2+} channels in the plasma membrane. Such gating of the putative TRP channels by RyRs has previously been reported in other systems (154;155).

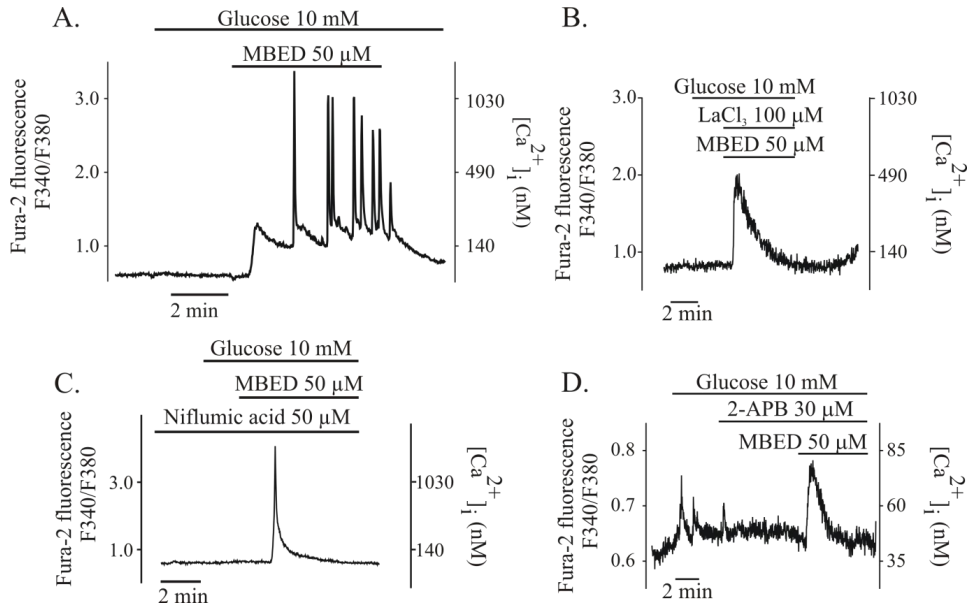

Figure 4. $LaCl_3$, niflumic acid, and 2-APB inhibited the $[Ca^{2+}]_i$ plateau that followed the activation of RyRs. The figures are reproduced from Jabin Gustafsson *et al* 2004. Activation of RyRs by MBED (50 µM) in the continued presence of $LaCl_3$ (100 µM) (B) or niflumic acid (50 µM) (C) caused the initial rise of $[Ca^{2+}]_i$, but the plateau phase of $[Ca^{2+}]_i$ increase was inhibited. The plateau phase was also inhibited by 2-APB (30 µM) (D).

More recently, Rosker *et al* have reported that the Ca^{2+} entry in the plateau phase is mediated by RyR2 located on the plasma membrane (75). However, the reported currents do not mimic any earlier reported currents of RyRs (156;157). It has been suggested that the channels described by Rosker *et al*, may represent a novel, non-selective ion-channel (158). In our study, the Ca^{2+} entry was blocked by SKF 96365, a compound that does not block RyRs. Therefore, it is unlikely that the Ca^{2+} entry was due to RyR in the plasma membrane. To rule out whether the plateau phase was due to activation of voltage-gated Ca^{2+} channels, nimodipine was used. But nimodipine did not inhibit the Ca^{2+} plateau. La^{3+}, Gd^{3+}, SKF 96365, niflumic acid, and 2-APB are non-selective inhibitors of different channels including several TRP channels (159;160), and they all inhibited the Ca^{2+} plateau. These results suggest that the plateau phase was due to activation of some Ca^{2+} channels belonging to the TRP family.

TRP channels and intracellular Ca^{2+} channels of β-cells

The third pattern of changes in $[Ca^{2+}]_i$ was the regenerative spikes that were superimposed on the plateau phase. Our results demonstrated that after activation of the RyR, the plasma membrane was depolarized to about -40 mV as a result of Ca^{2+} entry through the putative TRP-like channels. Such depolarization in turn activated the L-type voltage-gated Ca^{2+} channels. Since the spikes were inhibited by nimodipine, they required Ca^{2+} entry through the L-type voltage-gated channels. Also, the spikes were caused by CICR through the RyRs, as evidenced by the fact that high concentrations of ryanodine inhibited the spikes.

After the paper was published, we studied whether the plateau phase was due to the activation of TRPM2 or TRPV1, two TRP channels that we identified in the INS-1E cells. But neither ACA, a specific inhibitor of TRPM2, nor capsazepine, a specific inhibitor of TRPV1, were able to inhibit the plateau phase (data not shown). Thus, the identity of the TRP-like channels that mediate the Ca^{2+} entry in response to the activation of the RyRs remains unclear. Transcripts for several TRP channels have been found in the β-cells. Also, the possibility of different types of TRP forming homo- and heterotetramers yields many optional channels (161).

Under physiological conditions, the glucose metabolism is sensed by RyRs through molecules such as cADPr and fructose 1,6 diphosphate, among others. When the RyRs are activated, this will lead to $[Ca^{2+}]_i$ increase by activation of the putative TRP channels, membrane depolarization, and activation of L-type voltage-gated Ca^{2+} channels. The $[Ca^{2+}]_i$ increase will trigger exosytosis of insulin (fig. 5). It is of great importance that the role of TRP channels in Ca^{2+} signaling in the β-cells is elucidated and its physiological importance further investigated.

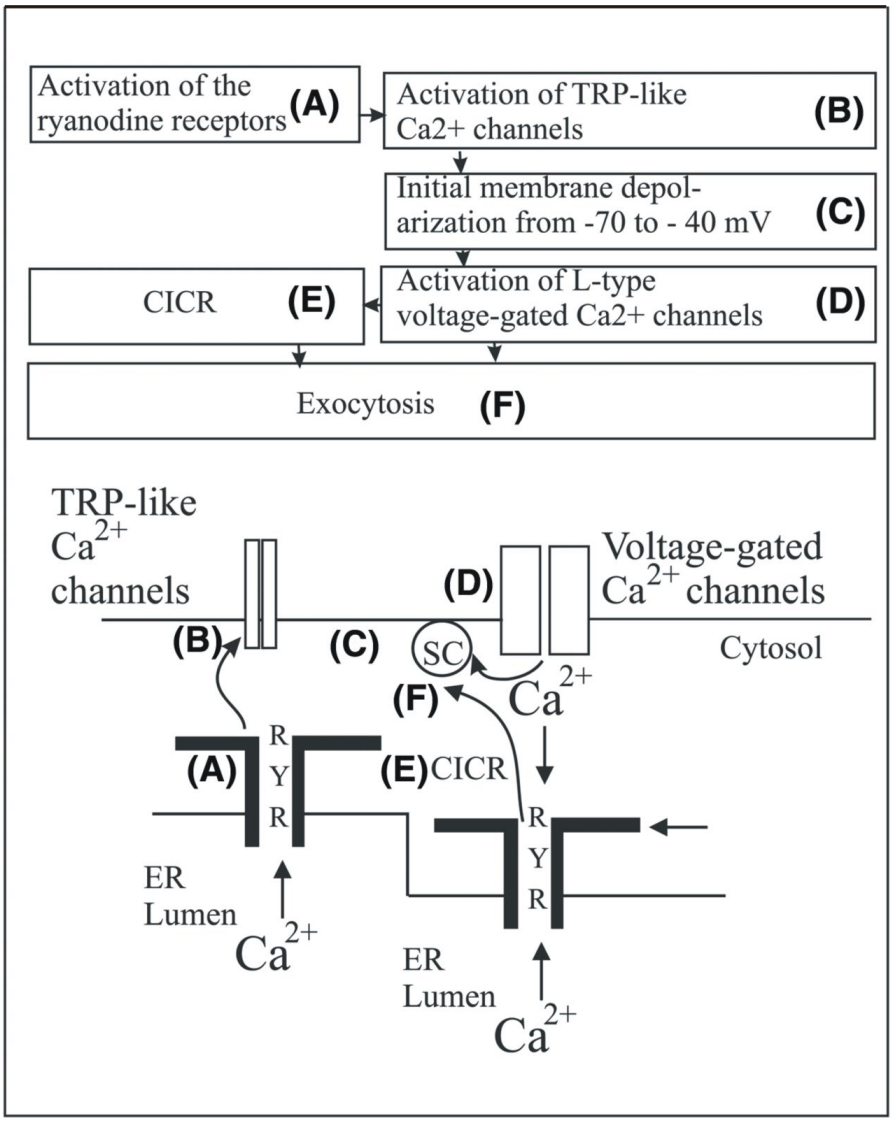

Figure 5. Schematic diagram of hypothesized involvement of RyRs and TRP-like channels in Ca^{2+} entry and membrane depolarization in β-cells. The figure is reproduced from Jabin Gustafsson *et al* 2005: The cartoon illustrates a sequence of events, whereby activation of RyRs (A) leads to the activation of TRP-like channels (B), an initial -membrane depolarization to about -40 mV (C), activation of the L-type voltage-gated Ca^{2+} channels (D), CICR (E), and exocytosis of insulin (F).

8.2 Extracellular ADPr activates P2Y1 receptors

Our study on the effect of ADPr on $[Ca^{2+}]_i$ in the β-cells was a side track from the main focus of this thesis. During our search for TRP channels in the β-cells we used ADPr as a tool to activate TRPM2, and to our surprise we found that extracellular ADPr increases $[Ca^{2+}]_i$ in the β-cells. This effect of ADPr was so obvious that we decided to identify the cell surface receptor involved in mediating the $[Ca^{2+}]_i$ response. ADPr increased $[Ca^{2+}]_i$ in a concentration-dependent manner (EC_{50} of ~ 30 μM). The $[Ca^{2+}]_i$ increase was observed in the INS-1E cells, as well as in the primary rat and human β-cells. Our first suspicion was that commercially available ADPr might contain ADP as a contaminant, which could elicit the observed $[Ca^{2+}]_i$ increase. Therefore, we synthesized highly purified ADPr that was free from ADP, but still similar $[Ca^{2+}]_i$ increase by ADPr was observed. The concentration of ADPr required for $[Ca^{2+}]_i$ increase in our experiments was much higher than that of ADP, the cognate agonist of P2Y1 receptors. The EC_{50} for ADP-induced activation of the P2Y1 receptor is 1 μM (162). However, ADPr concentrations in the range of 30 μM have been used in the past to demonstrate biological effects of ADPr in different tissues (112;163-166). It is possible that the concentration of ADPr at its local sites of actions is in the micromolar range, but we do not have any proof for that.

NAD^+, cADPr or breakdown products of ADPr did not increase $[Ca^{2+}]_i$. Neither PADPr, a phosphonate analogue of ADPr, nor 8-bromo-ADPr, increased $[Ca^{2+}]_i$. Non of them altered the ADPr-induced $[Ca^{2+}]_i$ changes.

ADPr increased $[Ca^{2+}]_i$ in the form of an initial peak followed by a plateau that depended on extracellular Ca^{2+}. Such biphasic $[Ca^{2+}]_i$ increase resembles the $[Ca^{2+}]_i$ changes upon activation of receptors coupled to PI-PLC. When the ER Ca^{2+} pool was depleted by thapsigargin, the $[Ca^{2+}]_i$ increase was abolished, indicating that the $[Ca^{2+}]_i$ rise was due to release of Ca^{2+} from the ER. Furthermore, this $[Ca^{2+}]_i$ increase was abolished by the PI-PLC inhibitor U73122, and by 2-APB, which inhibits the IP_3 receptor. These results suggest that the ADPr-induced $[Ca^{2+}]_i$ increase was due to activation of the PI-PLC-IP_3 pathway.

When Ca^{2+} was omitted from the extracellular medium, the plateau phase of the ADPr-induced $[Ca^{2+}]_i$ increase was abolished, indicating that this phase was due to Ca^{2+} entry from outside the cell. The plateau phase was not inhibited by inhibitors of TRPM2, namely flufenamic acid, niflumic acid, and ACA. Inhibition of the L-type voltage-gated Ca^{2+} channels also did not inhibit the plateau phase. These results indicate lack of involvement of both TRPM2 channels and L-type voltage-gated Ca^{2+} channels in mediating the Ca^{2+} entry.

The most important findings in this study were that MRS 2179 and MRS 2279, two specific inhibitors of the purinergic receptor P2Y1 (167;168), completely blocked the ADPr-induced $[Ca^{2+}]_i$ increase (fig. 6). MRS2279 only inhibits P2Y1, but MRS2179 also inhibits P2X1 and P2X3 (137). These results are strong evidence for the involvement of the P2Y1 receptor in the ADPr-induced $[Ca^{2+}]_i$ increase.

To further establish that we were dealing with P2Y1 receptors, we used 1321N1 human astrocytoma cells that stably overexpress human P2Y1 receptors. ADPr increased $[Ca^{2+}]_i$ in these cells, but did not increase $[Ca^{2+}]_i$ in the wild type astrocytoma cells that do not express P2Y1 receptors. Biological effects of ADPr-induced $[Ca^{2+}]_i$ increase were tested in the platelets, which express native P2Y1 receptors. ADPr induced platelet shape change as a result of $[Ca^{2+}]_i$ increase through P2Y1 activation.

The role of P2Y1 in insulin secretion is controversial. Depending on experimental conditions, cell types used, choice of P2Y1 agonist and its dosage, P2Y1 activation can either increase or inhibit the insulin secretion (169-172). The $[Ca^{2+}]_i$ increase leading to the insulin secretion is mainly due to Ca^{2+} entry through the voltage gated Ca^{2+} channels (85). In our study ADPr did not alter the basal or glucose-induced insulin secretion. We conclude that ADPr is a novel endogenous and specific agonist of P2Y1 receptors that increases the $[Ca^{2+}]_i$ in the insulin-secreting cells (fig. 7). The physiological importance of this finding needs further investigations.

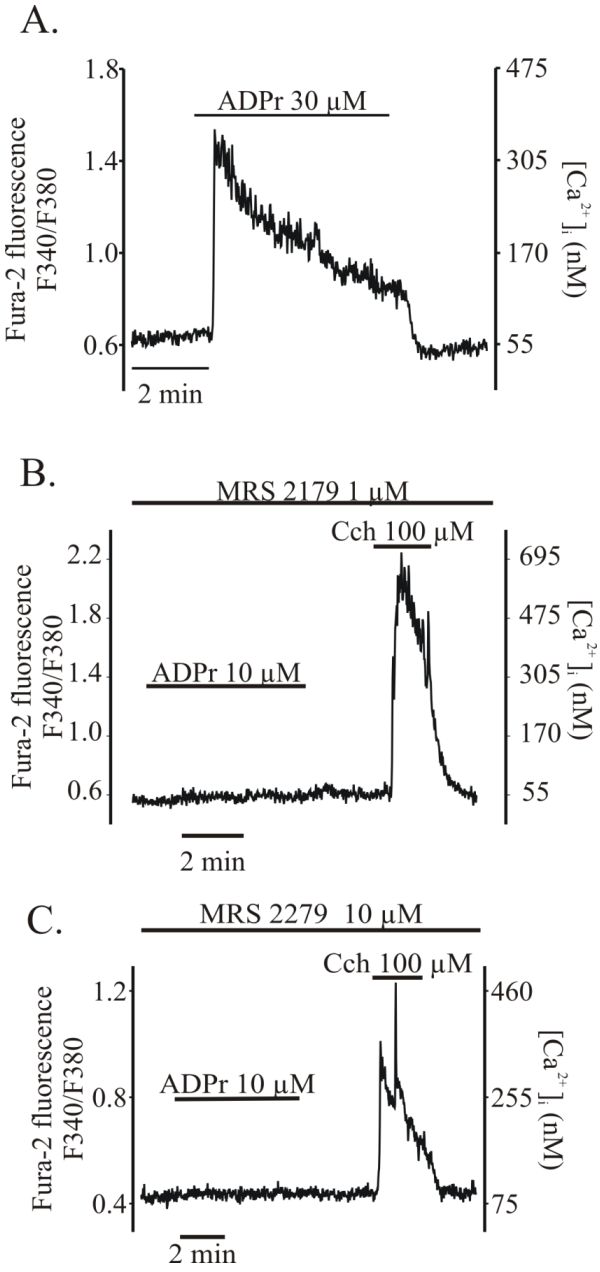

Figure 6. ADPr-induced $[Ca^{2+}]_i$ increase was due to the activation of P2Y1 receptors. The figure is reproduced from Jabin Gustafsson *et al* 2011. The INS-1E cells were incubated for 10 min with either MRS 2179 (1 and 10 µM) (B) or MRS 2279(10 µM) (C). The inhibitors were also present in the perfusion during the experiment. Both MRS2179 and MRS2279 completely inhibited the $[Ca^{2+}]_i$ increase by ADPr (10 µM). Fig. A is a control experiment that shows ADPr-induced $[Ca^{2+}]_i$ increase in the absence of the inhibitors. MRS2179 and MRS2279 did not block the carbachol- induced $[Ca^{2+}]_i$ increase. The traces are representatives of at least three experiments each.

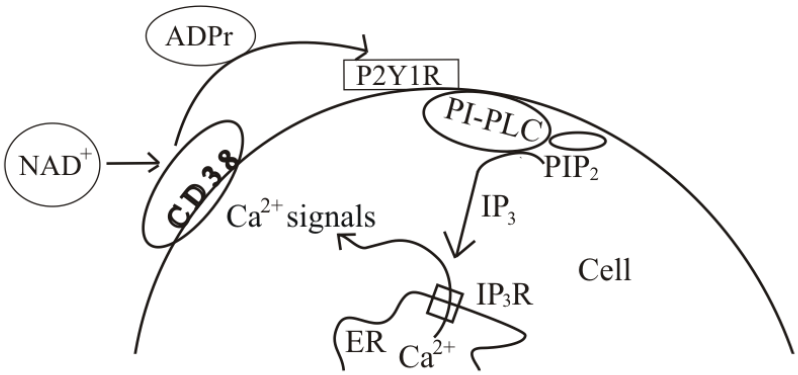

Figure 7. Schematic figure of ADPr as a ligand of the P2Y1 receptor. Extracellular ADPr activates the P2Y1 receptor (P2Y1R) and the PI-PLC, leading to the formation of IP_3 produced from PIP_2. The IP_3R is activated, and Ca^{2+} is released from the ER.

8.3 INS-1E cells express functional TRPV1 channels

In paper III, we studied whether β-cells have functional TRPV1 channels. We tested whether TRPV1 activation leads to $[Ca^{2+}]_i$ increase. Capsaicin, a specific agonist of TRPV1, increased $[Ca^{2+}]_i$ in the INS-1E cells in a concentration-dependent manner. The $[Ca^{2+}]_i$ increase was dependent on extracellular Ca^{2+}.These results indicated that we were dealing with Ca^{2+} channels in the plasma membrane. AM404, another known TRPV1 agonist, also increased $[Ca^{2+}]_i$ in the INS-1E cells. However, the precursors *p*-aminopenol and arachidonic acid did not increase $[Ca^{2+}]_i$. Capsazepine, a specific inhibitor of TRPV1, completely blocked both the capsaicin-induced and the AM404-induced $[Ca^{2+}]_i$ increase. These results together suggest that TRPV1 channels are located in the plasma membrane in the INS-1E cells, and causes Ca^{2+} entry and $[Ca^{2+}]_i$ increase upon activation.

Capsaicin elicited inward currents in the INS-1E cells, and the currents were inhibited by capsazepine. Since the permeability of TRPV1 is higher for Ca^{2+} than for Na^+ (PNa^+/PCa^{2+} = 1:9) (24), Ca^{2+} was probably the main carrier of the current in our experiments. This is consistent with microfluorometry experiments where capsaicin induced robust increase in $[Ca^{2+}]_i$.

The expression of TRPV1 protein in the INS-1E cells and the human islets was detected by Western blot analysis. The bands that were seen at ~94 kDa in the INS-1E cells and at ~96 kDa in the human islets were compared with the expected molecular weight of TRPV1 estimated from the mRNA. According to the comparison, the bands represented TRPV1. Our results were also in accordance with several earlier studies (173-177).

The existence of TRPV1 in primary β-cells is debated. Akiba *et al* have demonstrated TRPV1 immunoreactivity in primary β-cells from Sprague-Dawley rats, but they did not report the effect of capsaicin in these cells (35). Gram *et al* reported TRPV1 immunoreactivity in the nerve fibres in the islets, but not in the β-cells (51). In our study, we used primary β-cells from Wistar rat, but capsaicin did not induce any $[Ca^{2+}]_i$ increase in these cells. These results suggest that primary β-cells do not have TRPV1 channels.

The existence of TRPV1 in human β-cells is questionable. In our study, capsaicin did not increase $[Ca^{2+}]_i$ in human β-cells. Also, no TRPV1 immunoreactivity was detected in the human islets or human insulinoma cells. We used eight different antibodies that all detected TRPV1 immunoreactivity in the dorsal root ganglion cells, which were used as controls. Thus, TRPV1 is not expressed in the human β-cells, at least not at as high level as in the dorsal root ganglion cells. We conclude that functional TRPV1 channels are expressed at high level in the INS-1E cells, but not in the primary β-cells from rat or human.

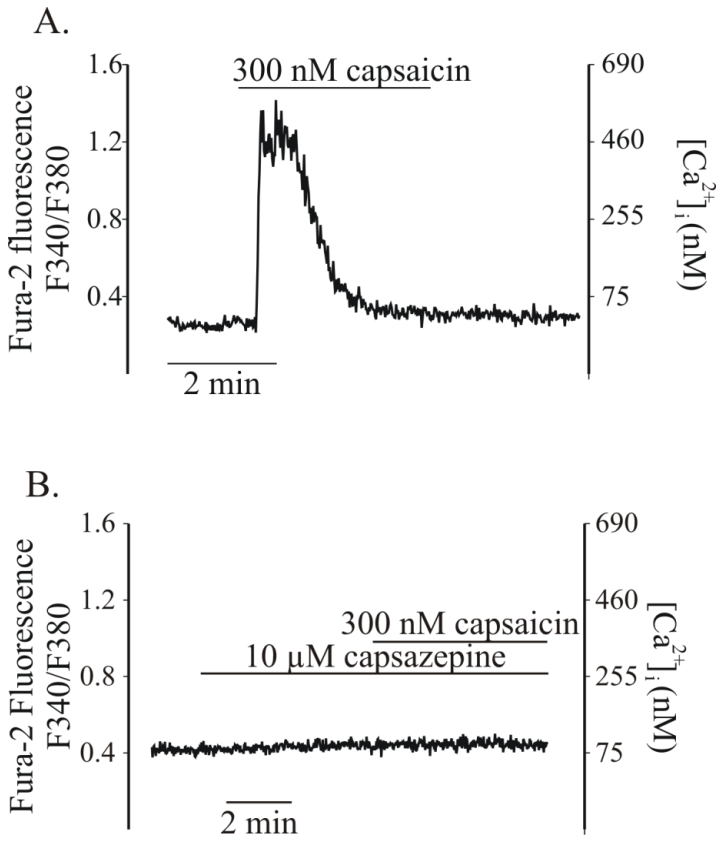

Figure 8. Effect of capsaicin and capsazepine on $[Ca^{2+}]_i$ in the INS-1E cells. The figure is reproduced from Jabin Fågelskiöld *et al* 2011. Capsaicin (300 nM) increased $[Ca^{2+}]_i$ (A). In the presence of capsazepine (10 μM), capsaicin failed to increase $[Ca^{2+}]_i$ (B).

9 Conclusions

1. The activation of RyRs induces a series of distinct signaling events, which include release of Ca^{2+} from the ER, activation of putative Ca^{2+}-permeable TRP-like channels in the plasma membrane, membrane depolarization, Ca^{2+} entry through the voltage-gated Ca^{2+} channels, and regenerative CICR.

2. Extracellular ADPr increases $[Ca^{2+}]_i$ in the insulin-secreting cells by activation of the P2Y1 purinergic receptors.

3. Functional Ca^{2+} permeable TRPV1 channels are present in the INS-1E cells, but not in the primary rat or human β-cells or the human insulinoma cells.

10 Future perspectives

It is important to identify which TRP channels are present and functional in the β-, α-, and δ-cells of the islets. Several TRP channels have already been identified in the β-cells and their role in the Ca^{2+} signaling and stimulus-secretion coupling needs to be studied in detail. The TRP channels might play an important role in mediating the depolarizing currents that lead to depolarization to the threshold for activation of the voltage-gated Ca^{2+} channels. Diverse physical second messengers like heat, swelling, stretch, and chemical factors like arachidonic acid, cAMP, PIP_2, and Ca^{2+} could act as links between insulin-secretagogues and activation of the TRP-channels. One of the challenges in the future will be to investigate the quantitative contribution of different second messengers and different TRP channels in stimulus-secretion coupling in the β-cells under different physiological and pathological conditions. The availability of more specific pharmacological tools and use of TRP channel knock-out mice models will hopefully give answers to many of the remaining questions. Eventually, some of these TRP channels may turn out to be molecular targets for the development of drugs for the treatment of impaired insulin secretion in diabetes.

11 Acknowledgements

I am grateful to Karolinska Institutet and Karolinska University Hospital as my PhD studies have been funded by Karolinska Institutet´s MD PhD program and Karolinska Institutet/University Hospital Research Internship. This work was performed at the Research centre, Department of Clinical Science and Education, Södersjukhuset, Karolinska Institutet. I want to thank all the people who have helped me and supported me during these years. In particular, I want to express my warm and sincere gratitude to:

Md Shahidul Islam, my supervisor, for his excellent and never-ending support and patience in teaching me research. He is always there for me willing to discuss experimental design, results, manuscript or any other topic.

Håkan Westerblad, my co-supervisor, for his encouragement and enthusiasm for science.

Sari Ponzer, professor and former prefect, for creating a good scientific environment and being a role-model for women in academic research and life.

Göran Elinder, professor and prefect, for creating a fruitful research environment.

Hans Olivecrona, former head of the Research Centre, for providing excellent research facilities.

Michael Eberhardson, head of the Research Centre, for development of the research facilities.

Anita Stålsäter-Pettersson, Jeanette Brynholt-Öhrman, Lina Rejnö, Mats Jonsson, Monica Dahlberg, Ingrid Iliou, Anne Edgren, Lena Guldevall and all the staff at KI SÖS, for helping me with warm hands with all the practicalities around my PhD studies.

Viveca "Pipsan" Holmberg, research coordinator, for helping me with the ethical applications, and for introducing me to the beautiful horse "Prippen"!

Mohamed Eweida, senior researcher, for kindly teaching me Western Blot analysis, for nice discussions about research and life.

Mensur Dzabic, Hanna Ingelman-Sundberg, Justina Awasum, Christina Pierro, Patrizia Tedeschi, Orison Woolcott, Shiue Chiounan, Lucia Muraro, Carin Dahlberg, Mohammad R Bari, Sanian Akbar, Kristina Kannisto, Peter Frykestig, Anna Boström, Banina Hadrovic, Shiva Mansouri, Paola Rabellato,Ousman Ndaw, Md Abdul Halim, and Kalaiselvan Krishnan who all have been students in our group and created a vivid and creative atmosphere.

All the summer research school students, who have made it easy to enter the dark lab during sunny summer days.

Özlem Erdogdu, Nina Grankvist, Viktoria Rosengren, Liselotte Fransson, Linnea Eriksson, Peter Rodhe, Anna Olverling, Camilla Kappe, Petra Wolbert, Hanna Dahlin, Hans Pettersson, Qimin Zhang, Fan"Tony" Zhang, Åke Sjöholm, Henrik Ortsäter, Cesare Patrone, Lotta Larsson,

Kristina Häll, Monica Nordlund, Thomas Nyström, Mikael Lehtihet and David Nathanson for creating a pleasant atmosphere to work in.

*Marie*the *"Mia" Ehnlund and Jeannette Lundblad Magnusson,* lab coordinators, for all the practical help in the lab.

Olof Larsson, Per-Eric Lund and Cecilia Farre, for introducing me to the patch-clamp technique.

Kenneth Wester, for introducing me to immunohistochemistry.

Hoa Nguyen Khahn, for helping me with insulin secretion measurements.

Nailin Li, for helping me with the platelet study.

Olivier Chevallier and Marie Migaud, for synthesis of PADPr and important feedback on my work.

Anders Wall and Anders Wall Foundation, who believe in me as a young researcher and for a generous friendship and scholarship.

Friends outside the hospital and research, thank you for being so fantastic. I specially want to thank *Johanna, Viktoria, Sofia, Elin, Natalie, Maria, Caroline, Annie, Hamedeh, Jeanette, Anikó, Linn, and Nina* and your families, for all that you are. I hope that our friendships are everlasting!

My lovely family , including my grandmother *"Mommi"* and my aunts *Rositha, Inga-Lill, Mai, and Zaima,* and their families for all love and fun together.

My brother *Amandus,* for being the best big brother one can wish for that helps me solve all my problems. And *Anna,* of course, who will marry my brother this summer and already is my favourite sister in law.

My sister *Matilda,* who always reminds me about the important things in life, and my brother in law, *Emil,* who always makes me laugh.

Lucia, my pretty little black cat, who has kept me company night and day during my thesis writing period. You bring joy into my life!

Most of all, I would like to thank my parents *Anitha Jabin and Carl-Lennart Gustafsson,* who always encourage me to achieve my goals in life, support me when things are difficult and celebrate me when I succeed. Dear Mum and Dad, I love you so!

Finally, I want to express my love to *Peter,* my wonderful husband, who has been my best friend for six years now. Peter, meeting you has been my greatest discovery, when I found the meaning of Love. You are the most caring, intelligent, honest and loving person I have ever met. Thank you for your patience during these years. I am looking forward to build a family with you.

12 References

1. **Fossati P** 2004 [Edouard Laguesse at Lille in 1893 created the term "endocrine" and opened the endocrinology era]. Hist Sci Med 38:433-439
2. **Iki K, Pour PM** 2006 Distribution of Pancreatic Endocrine Cells, Including IAPP-expressing Cells in Nondiabetic and Type 2 Diabetic Cases. J Histochem Cytochem
3. **Kin T, Murdoch TB, Shapiro AM, Lakey JR** 2006 Estimation of pancreas weight from donor variables. Cell Transplant 15:181-185
4. **Wittingen J, Frey CF** 1974 Islet concentration in the head, body, tail and uncinate process of the pancreas. Ann Surg 179:412-414
5. **Hellman B** 1959 Actual distribution of the number and volume of the islets of Langerhans in different size classes in non-diabetic humans of varying ages. Nature 184(Suppl 19):1498-1499
6. **Wierup N, Svensson H, Mulder H, Sundler F** 2002 The ghrelin cell: a novel developmentally regulated islet cell in the human pancreas. Regul Pept 107:63-69
7. **Pombo M, Pombo CM, Garcia A, Caminos E, Gualillo O, Alvarez CV, Casanueva FF, Dieguez C** 2001 Hormonal control of growth hormone secretion. Horm Res 55 Suppl 1:11-16
8. **Leprini A, Valente U, Celada F, Fontana I, Barocci S, Nocera A** 1987 Morphology, cytochemical features, and membrane phenotype of HLA-DR+ interstitial cells in the human pancreas. Pancreas 2:127-135
9. **Weir GC, Bonner-Weir S** 1990 Islets of Langerhans: the puzzle of intraislet interactions and their relevance to diabetes. J Clin Invest 85:983-987
10. **Ravier MA, Guldenagel M, Charollais A, Gjinovci A, Caille D, Sohl G, Wollheim CB, Willecke K, Henquin JC, Meda P** 2005 Loss of connexin36 channels alters beta-cell coupling, islet synchronization of glucose-induced Ca^{2+} and insulin oscillations, and basal insulin release. Diabetes 54:1798-1807
11. **Islam MS** 2010 An estimated 285 million people in the world have islet failure. Islets 2:209
12. **Porksen N, Nyholm B, Veldhuis JD, Butler PC, Schmitz O** 1997 In humans at least 75% of insulin secretion arises from punctuated insulin secretory bursts. Am J Physiol 273:E908-E914
13. **Song SH, McIntyre SS, Shah H, Veldhuis JD, Hayes PC, Butler PC** 2000 Direct measurement of pulsatile insulin secretion from the portal vein in human subjects. J Clin Endocrinol Metab 85:4491-4499
14. **Vaxillaire M, Froguel P** 2006 Genetic basis of maturity-onset diabetes of the young. Endocrinol Metab Clin North Am 35:371-384
15. **Grapengiesser E, Gylfe E, Hellman B** 1991 Cyclic AMP as a determinant for glucose induction of fast Ca^{2+} oscillations in isolated pancreatic beta-cells. J Biol Chem 266:12207-12210
16. **Roe MW, Worley JF, III, Mittal AA, Kuznetsov A, DasGupta S, Mertz RJ, Witherspoon SM, III, Blair N, Lancaster ME, McIntyre MS, Shehee WR, Dukes ID, Philipson LH** 1996 Expression and function of pancreatic beta-cell delayed rectifier K^+ channels. Role in stimulus-secretion coupling. J Biol Chem 271:32241-32246
17. **Thorens B, Sarkar HK, Kaback HR, Lodish HF** 1988 Cloning and functional expression in bacteria of a novel glucose transporter present in liver, intestine, kidney, and beta-pancreatic islet cells. Cell 55:281-290
18. **De Vos A, Heimberg H, Quartier E, Huypens P, Bouwens L, Pipeleers D, Schuit F** 1995 Human and rat beta cells differ in glucose transporter but not in glucokinase gene expression. J Clin Invest 96:2489-2495
19. **Detimary P, Gilon P, Henquin JC** 1998 Interplay between cytoplasmic Ca2+ and the ATP/ADP ratio: a feedback control mechanism in mouse pancreatic islets. Biochem J 333 (Pt 2):269-274

20. **Ainscow EK, Rutter GA** 2002 Glucose-stimulated oscillations in free cytosolic ATP concentration imaged in single islet beta-cells: evidence for a Ca^{2+}-dependent mechanism. Diabetes 51 Suppl 1:S162-S170
21. **Sturgess NC, Ashford ML, Cook DL, Hales CN** 1985 The sulphonylurea receptor may be an ATP-sensitive potassium channel. Lancet 2:474-475
22. **Shyng S, Ferrigni T, Nichols CG** 1997 Regulation of K_{ATP} channel activity by diazoxide and MgADP. Distinct functions of the two nucleotide binding folds of the sulfonylurea receptor. J Gen Physiol 110:643-654
23. **Minke B** 1982 Light-induced reduction in excitation efficiency in the trp mutant of Drosophila. J Gen Physiol 79:361-385
24. **Montell C** 2005 The TRP Superfamily of Cation Channels. Sci STKE 2005:re3
25. **Minke B, Wu C, Pak WL** 1975 Induction of photoreceptor voltage noise in the dark in Drosophila mutant. Nature 258:84-87
26. **Launay P, Fleig A, Perraud AL, Scharenberg AM, Penner R, Kinet JP** 2002 TRPM4 is a Ca^{2+}-activated nonselective cation channel mediating cell membrane depolarization. Cell 109:397-407
27. **Sakura H, Ashcroft FM** 1997 Identification of four trp1 gene variants murine pancreatic beta-cells. Diabetologia 40:528-532
28. **Roe MW, Worley JF, III, Qian F, Tamarina N, Mittal AA, Dralyuk F, Blair NT, Mertz RJ, Philipson LH, Dukes ID** 1998 Characterization of a Ca^{2+} release-activated nonselective cation current regulating membrane potential and $[Ca^{2+}]_i$ oscillations in transgenically derived beta-cells. J Biol Chem 273:10402-10410
29. **Li F, Zhang ZM** 2009 Comparative identification of Ca^{2+} channel expression in INS-1 and rat pancreatic beta cells. World J Gastroenterol 15:3046-3050
30. **Bari MR, Akbar S, Eweida M, Kühn FJP, Gustafsson AJ, Lückhoff A, Islam MS** 2009 H_2O_2-induced Ca^{2+} influx and its inhibition by N-(p-amylcinnamoyl) anthranilic acid in the beta-cells: involvement of TRPM2 channels. J Cell Mol Med 13:3260-3267
31. **Togashi K, Hara Y, Tominaga T, Higashi T, Konishi Y, Mori Y, Tominaga M** 2006 TRPM2 activation by cyclic ADP-ribose at body temperature is involved in insulin secretion. EMBO J 25:1804-1815
32. **Wagner TF, Loch S, Lambert S, Straub I, Mannebach S, Mathar I, Dufer M, Lis A, Flockerzi V, Philipp SE, Oberwinkler J** 2008 Transient receptor potential M3 channels are ionotropic steroid receptors in pancreatic beta cells. Nat Cell Biol 10:1421-1430
33. **Cheng H, Beck A, Launay P, Gross SA, Stokes AJ, Kinet JP, Fleig A, Penner R** 2007 TRPM4 controls insulin secretion in pancreatic beta-cells. Cell Calcium 41:51-61
34. **Colsoul B, Schraenen A, Lemaire K, Quintens R, Van Lommel L, Segal A, Owsianik G, Talavera K, Voets T, Margolskee RF, Kokrashvili Z, Gilon P, Nilius B, Schuit FC, Vennekens R** 2010 Loss of high-frequency glucose-induced Ca^{2+} oscillations in pancreatic islets correlates with impaired glucose tolerance in Trpm5-/- mice. Proc Natl Acad Sci U S A 107:5208-5213
35. **Akiba Y, Kato S, Katsube KI, Nakamura M, Takeuchi K, Ishii H, Hibi T** 2004 Transient receptor potential vanilloid subfamily 1 expressed in pancreatic islet beta cells modulates insulin secretion in rats. Biochem Biophys Res Commun 321:219-225
36. **Hisanaga E, Nagasawa M, Ueki K, Kulkarni RN, Mori M, Kojima I** 2009 Regulation of Calcium-Permeable TRPV2 Channel by Insulin in Pancreatic beta-Cells. Diabetes 58:174-184
37. **Casas S, Novials A, Reimann F, Gomis R, Gribble FM** 2008 Calcium elevation in mouse pancreatic beta cells evoked by extracellular human islet amyloid polypeptide involves activation of the mechanosensitive ion channel TRPV4. Diabetologia 51:2252-2262
38. **Perraud AL, Fleig A, Dunn CA, Bagley LA, Launay P, Schmitz C, Stokes AJ, Zhu Q, Bessman MJ, Penner R, Kinet JP, Scharenberg AM** 2001 ADP-ribose gating of the calcium-permeable LTRPC2 channel revealed by Nudix motif homology. Nature 411:595-599
39. **Perraud AL, Shen B, Dunn CA, Rippe K, Smith MK, Bessman MJ, Stoddard BL, Scharenberg AM** 2003 NUDT9, a member of the Nudix hydrolase family, is an evolutionarily conserved mitochondrial ADP-ribose pyrophosphatase. J Biol Chem 278:1794-1801

40. **Kraft R, Harteneck C** 2005 The mammalian melastatin-related transient receptor potential cation channels: an overview. Pflugers Arch 451:204-211
41. **Kühn FJP, Heiner I, Lückhoff A** 2005 TRPM2: a calcium influx pathway regulated by oxidative stress and the novel second messenger ADP-ribose. Pflugers Arch 451:212-219
42. **McNulty S, Fonfria E** 2005 The role of TRPM channels in cell death. Pflugers Arch 451:235-242
43. **Du J, Xie J, Yue L** 2009 Intracellular calcium activates TRPM2 and its alternative spliced isoforms. Proc Natl Acad Sci U S A 106:7239-7244
44. **Hill K, Benham CD, McNulty S, Randall AD** 2004 Flufenamic acid is a pH-dependent antagonist of TRPM2 channels. Neuropharmacology 47:450-460
45. **Hill K, McNulty S, Randall AD** 2004 Inhibition of TRPM2 channels by the antifungal agents clotrimazole and econazole. Naunyn Schmiedebergs Arch Pharmacol 370:227-237
46. **Togashi K, Inada H, Tominaga M** 2008 Inhibition of the transient receptor potential cation channel TRPM2 by 2-aminoethoxydiphenyl borate (2-APB). Br J Pharmacol 153:1324-1330
47. **Xu SZ, Zeng F, Boulay G, Grimm C, Harteneck C, Beech DJ** 2005 Block of TRPC5 channels by 2-aminoethoxydiphenyl borate: a differential, extracellular and voltage-dependent effect. Br J Pharmacol 145:405-414
48. **Zhang W, Chu X, Tong Q, Cheung JY, Conrad K, Masker K, Miller BA** 2003 A Novel TRPM2 Isoform Inhibits Calcium Influx and Susceptibility to Cell Death. J Biol Chem 278:16222-16229
49. **Lange I, Yamamoto S, Partida-Sanchez S, Mori Y, Fleig A, Penner R** 2009 TRPM2 functions as a lysosomal Ca2+-release channel in beta cells. Sci Signal 2:ra23
50. **Razavi R, Chan Y, Afifiyan FN, Liu XJ, Wan X, Yantha J, Tsui H, Tang L, Tsai S, Santamaria P, Driver JP, Serreze D, Salter MW, Dosch HM** 2006 TRPV1+ sensory neurons control beta cell stress and islet inflammation in autoimmune diabetes. Cell 127:1123-1135
51. **Gram DX, Ahren B, Nagy I, Olsen UB, Brand CL, Sundler F, Tabanera R, Svendsen O, Carr RD, Santha P, Wierup N, Hansen AJ** 2007 Capsaicin-sensitive sensory fibers in the islets of Langerhans contribute to defective insulin secretion in Zucker diabetic rat, an animal model for some aspects of human type 2 diabetes. Eur J Neurosci 25:213-223
52. **Planells-Cases R, Valente P, Ferrer-Montiel A, Qin F, Szallasi A** 2011 Complex Regulation of TRPV1 and Related Thermo-TRPs: Implications for Therapeutic Intervention. Adv Exp Med Biol 704:491-515
53. **Jung J, Hwang SW, Kwak J, Lee SY, Kang CJ, Kim WB, Kim D, Oh U** 1999 Capsaicin binds to the intracellular domain of the capsaicin-activated ion channel. J Neurosci 19:529-538
54. **Jordt SE, Julius D** 2002 Molecular basis for species-specific sensitivity to "hot" chili peppers. Cell 108:421-430
55. **Bertolini A, Ferrari A, Ottani A, Guerzoni S, Tacchi R, Leone S** 2006 Paracetamol: new vistas of an old drug. CNS Drug Rev 12:250-275
56. **Zygmunt PM, Chuang H, Movahed P, Julius D, Högestätt ED** 2000 The anandamide transport inhibitor AM404 activates vanilloid receptors. Eur J Pharmacol 396:39-42
57. **Högestätt ED, Jönsson BA, Ermund A, Andersson DA, Björk H, Alexander JP, Cravatt BF, Basbaum AI, Zygmunt PM** 2005 Conversion of acetaminophen to the bioactive N-acylphenolamine AM404 via fatty acid amide hydrolase-dependent arachidonic acid conjugation in the nervous system. J Biol Chem 280:31405-31412
58. **Bevan S, Hothi S, Hughes G, James IF, Rang HP, Shah K, Walpole CS, Yeats JC** 1992 Capsazepine: a competitive antagonist of the sensory neurone excitant capsaicin. Br J Pharmacol 107:544-552
59. **Savidge J, Davis C, Shah K, Colley S, Phillips E, Ranasinghe S, Winter J, Kotsonis P, Rang H, McIntyre P** 2002 Cloning and functional characterization of the guinea pig vanilloid receptor 1. Neuropharmacology 43:450-456
60. **Johnson JD, Kuang S, Misler S, Polonsky KS** 2004 Ryanodine receptors in human pancreatic beta cells: localization and effects on insulin secretion. FASEB J 18:878-880
61. **Kermode H, Chan WM, Williams AJ, Sitsapesan R** 1998 Glycolytic pathway intermediates activate cardiac ryanodine receptors. FEBS Lett 431:59-62

62. **Jones PM, Persaud SJ** 1993 Arachidonic acid as a second messenger in glucose-induced insulin secretion from pancreatic beta-cells. J Endocrinol 137:7-14
63. **Islam MS** 2002 The Ryanodine Receptor Calcium Channel of β-Cells: Molecular Regulation and Physiological Significance. Diabetes 51:1299-1309
64. **Rousseau E, Meissner G** 1989 Single cardiac sarcoplasmic reticulum Ca2+-release channel: activation by caffeine. Am J Physiol 256:H328-H333
65. **Islam MS, Larsson O, Nilsson T, Berggren PO** 1995 Effects of caffeine on cytoplasmic free Ca^{2+} concentration in pancreatic β-cells are mediated by interaction with ATP-sensitive K^+ channels and L-type voltage-gated Ca^{2+} channels but not the ryanodine receptor. Biochem J 306 (Pt 3):679-686
66. **Bennett DL, Bootman MD, Berridge MJ, Cheek TR** 1998 Ca^{2+} entry into PC12 cells initiated by ryanodine receptors or inositol 1,4,5-trisphosphate receptors. Biochem J 329 (Pt 2):349-357
67. **Kobayashi J, Ishibashi M, Nagai U, Ohizumi Y** 1989 9-Methyl-7-bromoeudistomin D, a potent inducer of calcium release from sarcoplasmic reticulum of skeletal muscle. Experientia 45:782-783
68. **Seino-Umeda A, Fang YI, Ishibashi M, Kobayashi J, Ohizumi Y** 1998 9-Methyl-7-bromoeudistomin D induces Ca^{2+} release from cardiac sarcoplasmic reticulum. Eur J Pharmacol 357:261-265
69. **Bruton JD, Lemmens R, Shi CL, Persson-Sjögren S, Westerblad H, Ahmed M, Pyne NJ, Frame M, Furman BL, Islam MS** 2002 Ryanodine receptors of pancreatic beta-cells mediate a distinct context-dependent signal for insulin secretion. FASEB J10.1096/fj.02-0481fje
70. **Bach AG, Wolgast S, Muhlbauer E, Peschke E** 2005 Melatonin stimulates inositol-1,4,5-trisphosphate and Ca^{2+} release from INS1 insulinoma cells. J Pineal Res 39:316-323
71. **Blondel O, Moody MM, Depaoli AM, Sharp AH, Ross CA, Swift H, Bell GI** 1994 Localization of inositol trisphosphate receptor subtype 3 to insulin and somatostatin secretory granules and regulation of expression in islets and insulinoma cells. Proc Natl Acad Sci U S A 91:7777-7781
72. **McPherson PS, Campbell KP** 1993 The ryanodine receptor/Ca^{2+} release channel. J Biol Chem 268:13765-13768
73. **Dror V, Kalynyak TB, Bychkivska Y, Frey MH, Tee M, Jeffrey KD, Nguyen V, Luciani DS, Johnson JD** 2008 Glucose and endoplasmic reticulum calcium channels regulate HIF-1beta via presenilin in pancreatic beta-cells. J Biol Chem 283:9909-9916
74. **Mitchell KJ, Lai FA, Rutter GA** 2003 Ryanodine receptor type I and nicotinic acid adenine dinucleotide phosphate receptors mediate Ca^{2+} release from insulin-containing vesicles in living pancreatic beta-cells (MIN6). J Biol Chem 278:11057-11064
75. **Rosker C, Meur G, Taylor EJ, Taylor CW** 2009 Functional ryanodine receptors in the plasma membrane of RINm5F pancreatic beta-cells. J Biol Chem 284:5186-5194
76. **Miura Y, Henquin JC, Gilon P** 1997 Emptying of intracellular Ca^{2+} stores stimulates Ca^{2+} entry in mouse pancreatic beta-cells by both direct and indirect mechanisms. J Physiol 503 (Pt 2):387-398
77. **Dyachok O, Gylfe E** 2001 Store-operated influx of Ca^{2+} in pancreatic beta-cells exhibits graded dependence on the filling of the endoplasmic reticulum. J Cell Sci 114:2179-2186
78. **Collins SR, Meyer T** 2011 Evolutionary origins of STIM1 and STIM2 within ancient Ca^{2+} signaling systems. Trends Cell Biol
79. **Potier M, Trebak M** 2008 New developments in the signaling mechanisms of the store-operated calcium entry pathway. Pflugers Archiv-European Journal of Physiology 457:405-415
80. **Kiselyov K, Shin DM, Shcheynikov N, Kurosaki T, Muallem S** 2001 Regulation of Ca^{2+}-release-activated Ca^{2+} current (Icrac) by ryanodine receptors in inositol 1,4,5-trisphosphate-receptor-deficient DT40 cells. Biochem J 360:17-22
81. **Tamarina NA, Kuznetsov A, Philipson LH** 2008 Reversible translocation of EYFP-tagged STIM1 is coupled to calcium influx in insulin secreting beta-cells. Cell Calcium 44:533-544
82. **Birnbaumer L, Boulay G, Brown D, Jiang M, Dietrich A, Mikoshiba K, Zhu X, Qin N** 2000 Mechanism of capacitative Ca^{2+} entry (CCE): interaction between IP_3 receptor and

TRP links the internal calcium storage compartment to plasma membrane CCE channels. Recent Prog Horm Res 55:127-161

83. **Bokvist K, Eliasson L, Ämmälä C, Renström E, Rorsman P** 1995 Co-localization of L-type Ca^{2+} channels and insulin-containing secretory granules and its significance for the initiation of exocytosis in mouse pancreatic B-cells. EMBO J 14:50-57
84. **Davalli AM, Biancardi E, Pollo A, Socci C, Pontiroli AE, Pozza G, Clementi F, Sher E, Carbone E** 1996 Dihydropyridine-sensitive and -insensitive voltage-operated calcium channels participate in the control of glucose-induced insulin release from human pancreatic beta cells. J Endocrinol 150:195-203
85. **Braun M, Ramracheya R, Bengtsson M, Zhang Q, Karanauskaite J, Partridge C, Johnson PR, Rorsman P** 2008 Voltage-gated ion channels in human pancreatic beta-cells: electrophysiological characterization and role in insulin secretion. Diabetes 57:1618-1628
86. **Braun M** 2009 The alphabetadelta of ion channels in human islet cells. Islets 1:160-162
87. **Swatton JE, Morris SA, Cardy TJ, Taylor CW** 1999 Type 3 inositol trisphosphate receptors in RINm5F cells are biphasically regulated by cytosolic Ca^{2+} and mediate quantal Ca2+ mobilization. Biochem J 344 Pt 1:55-60
88. **Dyachok O, Tufveson G, Gylfe E** 2004 Ca^{2+}-induced Ca^{2+} release by activation of inositol 1,4,5-trisphosphate receptors in primary pancreatic beta-cells. Cell Calcium 36:1-9
89. **Kang G, Holz GG** 2003 Amplification of exocytosis by Ca^{2+}-induced Ca^{2+} release in INS-1 pancreatic beta cells. J Physiol 546:175-189
90. **Islam MS, Leibiger I, Leibiger B, Rossi D, Sorrentino V, Ekström TJ, Westerblad H, Andrade FH, Berggren PO** 1998 *In situ* activation of the type 2 ryanodine receptor in pancreatic beta cells requires cAMP-dependent phosphorylation. Proc Natl Acad Sci U S A 95:6145-6150
91. **Holz GG, Leech CA, Heller RS, Castonguay M, Habener JF** 1999 cAMP-dependent mobilization of intracellular Ca^{2+} stores by activation of ryanodine receptors in pancreatic β-cells. A Ca^{2+} signalling system stimulated by the insulinotropic hormone glucagon-like peptide-1-(7-37). J Biol Chem 274:14147-14156
92. **Kang G, Joseph JW, Chepurny OG, Monaco M, Wheeler MB, Bos JL, Schwede F, Genieser HG, Holz GG** 2003 Epac-selective cAMP analog 8-pCPT-2'-O-Me-cAMP as a stimulus for Ca^{2+}-induced Ca^{2+} release and exocytosis in pancreatic beta-cells. J Biol Chem 278:8279-8285
93. **Calcraft PJ, Ruas M, Pan Z, Cheng X, Arredouani A, Hao X, Tang J, Rietdorf K, Teboul L, Chuang KT, Lin P, Xiao R, Wang C, Zhu Y, Lin Y, Wyatt CN, Parrington J, Ma J, Evans AM, Galione A, Zhu MX** 2009 NAADP mobilizes calcium from acidic organelles through two-pore channels. Nature 459:596-600
94. **Koch-Nolte F, Haag F, Guse AH, Lund F, Ziegler M** 2009 Emerging roles of NAD^+ and its metabolites in cell signaling. Sci Signal 2:mr1
95. **Lee HC** 2006 Structure and enzymatic functions of human CD38. Mol Med 12:317-323
96. **Howard M, Grimaldi JC, Bazan JF, Lund FE, Santos-Argumedo L, Parkhouse RM, Walseth TF, Lee HC** 1993 Formation and hydrolysis of cyclic ADP-ribose catalyzed by lymphocyte antigen CD38. Science 262:1056-1059
97. **Berthelier V, Tixier JM, Muller-Steffner H, Schuber F, Deterre P** 1998 Human CD38 is an authentic $NAD(P)^+$ glycohydrolase. Biochem J 330 (Pt 3):1383-1390
98. **Lund FE, Muller-Steffner HM, Yu NX, Stout CD, Schuber F, Howard MC** 1999 CD38 signaling in B lymphocytes is controlled by its ectodomain but occurs independently of enzymatically generated ADP-ribose or cyclic ADP-ribose. J Immunol 162:2693-2702
99. **Bonicalzi ME, Haince JF, Droit A, Poirier GG** 2005 Regulation of poly(ADP-ribose) metabolism by poly(ADP-ribose) glycohydrolase: where and when? Cell Mol Life Sci 62:739-750
100. **Lin W, Ame JC, Aboul-Ela N, Jacobson EL, Jacobson MK** 1997 Isolation and characterization of the cDNA encoding bovine poly(ADP-ribose) glycohydrolase. J Biol Chem 272:11895-11901
101. **Lee HC** 1997 Mechanisms of calcium signaling by cyclic ADP-ribose and NAADP. Physiol Rev 77:1133-1164

102. **De Flora A, Zocchi E, Guida L, Franco L, Bruzzone S** 2004 Autocrine and paracrine calcium signaling by the CD38/NAD+/cyclic ADP-ribose system. Ann N Y Acad Sci 1028:176-191
103. **Hotta T, Asai K, Fujita K, Kato T, Higashida H** 2000 Membrane-bound form of ADP-ribosyl cyclase in rat cortical astrocytes in culture. J Neurochem 74:669-675
104. **Snell CR, Snell PH, Richards CD** 1984 Degradation of NAD by synaptosomes and its inhibition by nicotinamide mononucleotide: implications for the role of NAD as a synaptic modulator. J Neurochem 43:1610-1615
105. **Smyth LM, Bobalova J, Mendoza MG, Lew C, Mutafova-Yambolieva VN** 2004 Release of beta-nicotinamide adenine dinucleotide upon stimulation of postganglionic nerve terminals in blood vessels and urinary bladder. J Biol Chem 279:48893-48903
106. **Kato I, Yamamoto Y, Fujimura M, Noguchi N, Takasawa S, Okamoto H** 1999 CD38 disruption impairs glucose-induced increases in cyclic ADP-ribose, $[Ca^{2+}]_i$, and insulin secretion. J Biol Chem 274:1869-1872
107. **Lee HC, Munshi C, Graeff R** 1999 Structures and activities of cyclic ADP-ribose, NAADP and their metabolic enzymes. Mol Cell Biochem 193:89-98
108. **Polzonetti V, Orsomando G, Micossi L, Vita A, Egidi D, Natalini P** 2002 NAD^+ catabolism in pheochromocytoma rat cells. J Biol Regul Homeost Agents 16:196-201
109. **Kim UH, Han MK, Park BH, Kim HR, An NH** 1993 Function of NAD glycohydrolase in ADP-ribose uptake from NAD by human erythrocytes. Biochim Biophys Acta 1178:121-126
110. **Dunn CA, O'Handley SF, Frick DN, Bessman MJ** 1999 Studies on the ADP-ribose pyrophosphatase subfamily of the nudix hydrolases and tentative identification of trgB, a gene associated with tellurite resistance. J Biol Chem 274:32318-32324
111. **Bernet D, Pinto RM, Costas MJ, Canales J, Cameselle JC** 1994 Rat liver mitochondrial ADP-ribose pyrophosphatase in the matrix space with low Km for free ADP-ribose. Biochem J 299 (Pt 3):679-682
112. **Zhang DX, Zou AP, Li PL** 2001 Adenosine diphosphate ribose dilates bovine coronary small arteries through apy. J Vasc Res 38:64-72
113. **Zimmermann H** 1992 5'-Nucleotidase: molecular structure and functional aspects. Biochem J 285 (Pt 2):345-365
114. **Fredholm BB, Abbracchio MP, Burnstock G, Daly JW, Harden TK, Jacobson KA, Leff P, Williams M** 1994 Nomenclature and classification of purinoceptors. Pharmacol Rev 46:143-156
115. **Londos C, Wolff J** 1977 Two distinct adenosine-sensitive sites on adenylate cyclase. Proc Natl Acad Sci U S A 74:5482-5486
116. **Zhou QY, Li C, Olah ME, Johnson RA, Stiles GL, Civelli O** 1992 Molecular cloning and characterization of an adenosine receptor: the A3 adenosine receptor. Proc Natl Acad Sci U S A 89:7432-7436
117. **Burnstock G, Kennedy C** 1985 Is there a basis for distinguishing two types of P2-purinoceptor? Gen Pharmacol 16:433-440
118. **Bean BP** 1992 Pharmacology and Electrophysiology of ATP-Activated Ion Channels. Trends in Pharmacological Sciences 13:87-90
119. **Burnstock G, Knight GE** 2004 Cellular distribution and functions of P2 receptor subtypes in different systems. Int Rev Cytol 240:31-304
120. **Jacques-Silva MC, Correa-Medina M, Cabrera O, Rodriguez-Diaz R, Makeeva N, Fachado A, Diez J, Berman DM, Kenyon NS, Ricordi C, Pileggi A, Molano RD, Berggren PO, Caicedo A** 2010 ATP-gated P2X3 receptors constitute a positive autocrine signal for insulin release in the human pancreatic beta cell. Proc Natl Acad Sci U S A 107:6465-6470
121. **Glas R, Sauter NS, Schulthess FT, Shu L, Oberholzer J, Maedler K** 2009 Purinergic P2X7 receptors regulate secretion of interleukin-1 receptor antagonist and beta cell function and survival. Diabetologia 52:1579-1588
122. **Richards-Williams C, Contreras JL, Berecek KH, Schwiebert EM** 2008 Extracellular ATP and zinc are co-secreted with insulin and activate multiple P2X purinergic receptor channels expressed by islet beta-cells to potentiate insulin secretion. Purinergic Signal 4:393-405

123. **Hollopeter G, Jantzen HM, Vincent D, Li G, England L, Ramakrishnan V, Yang RB, Nurden P, Nurden A, Julius D, Conley PB** 2001 Identification of the platelet ADP receptor targeted by antithrombotic drugs. Nature 409:202-207
124. **Communi D, Gonzalez NS, Detheux M, Brezillon S, Lannoy V, Parmentier M, Boeynaems JM** 2001 Identification of a novel human ADP receptor coupled to G(i). J Biol Chem 276:41479-41485
125. **Zhang FL, Luo L, Gustafson E, Palmer K, Qiao X, Fan X, Yang S, Laz TM, Bayne M, Monsma F, Jr.** 2002 P2Y(13): identification and characterization of a novel Galphai-coupled ADP receptor from human and mouse. J Pharmacol Exp Ther 301:705-713
126. **Lugo-Garcia L, Filhol R, Lajoix AD, Gross R, Petit P, Vignon J** 2007 Expression of purinergic P2Y receptor subtypes by INS-1 insulinoma beta-cells: A molecular and binding characterization. Eur J Pharmacol 568:54-60
127. **Verspohl EJ, Johannwille B, Waheed A, Neye H** 2002 Effect of purinergic agonists and antagonists on insulin secretion from INS-1 cells (insulinoma cell line) and rat pancreatic islets. Can J Physiol Pharmacol 80:562-568
128. **Hillaire-Buys D, Bertrand G, Chapal J, Puech R, Ribes G, Loubatieres-Mariani MM** 1993 Stimulation of insulin secretion and improvement of glucose tolerance in rat and dog by the P2y-purinoceptor agonist, adenosine-5'-O-(2-thiodiphosphate). Br J Pharmacol 109:183-187
129. **Ribes G, Bertrand G, Petit P, Loubatieres-Mariani MM** 1988 Effects of 2-methylthio ATP on insulin secretion in the dog in vivo. Eur J Pharmacol 155:171-174
130. **Oconnor SE, Dainty IA, Leff P** 1991 Further Subclassification of Atp Receptors Based on Agonist Studies. Trends in Pharmacological Sciences 12:137-141
131. **van der Geer P, Hunter T, Lindberg RA** 1994 Receptor protein-tyrosine kinases and their signal transduction pathways. Annu Rev Cell Biol 10:251-337
132. **Kelley GG, Reks SE, Ondrako JM, Smrcka AV** 2001 Phospholipase C(epsilon): a novel Ras effector. EMBO J 20:743-754
133. **Dzhura I, Chepurny OG, Kelley GG, Leech CA, Roe MW, Dzhura E, Afshari P, Malik S, Rindler MJ, Xu X, Lu Y, Smrcka AV, Holz GG** 2010 Epac2-dependent mobilization of intracellular Ca2+ by glucagon-like peptide-1 receptor agonist exendin-4 is disrupted in β-cells of phospholipase C- knockout mice. J Physiol 588:4871-4889
134. **Berridge MJ** 1983 Rapid accumulation of inositol trisphosphate reveals that agonists hydrolyse polyphosphoinositides instead of phosphatidylinositol. Biochem J 212:849-858
135. **Takai Y, Kishimoto A, Kikkawa U, Mori T, Nishizuka Y** 1979 Unsaturated diacylglycerol as a possible messenger for the activation of calcium-activated, phospholipid-dependent protein kinase system. Biochem Biophys Res Commun 91:1218-1224
136. **Missiaen L, Callewaert G, De Smedt H, Parys JB** 2001 2-Aminoethoxydiphenyl borate affects the inositol 1,4,5-trisphosphate receptor, the intracellular Ca2+ pump and the non-specific Ca^{2+} leak from the non-mitochondrial Ca^{2+} stores in permeabilized A7r5 cells. Cell Calcium 29:111-116
137. **Brown SG, King BF, Kim YC, Jang SY, Burnstock G, Jacobson KA** 2000 Activity of novel adenine nucleotide derivatives as agonists and antagonists at recombinant rat P2X receptors. Drug Develop Res 49:253-259
138. **Boland LM, Brown TA, Dingledine R** 1991 Gadolinium block of calcium channels: influence of bicarbonate. Brain Res 563:142-150
139. **Caldwell RA, Clemo HF, Baumgarten CM** 1998 Using gadolinium to identify stretch-activated channels: technical considerations. Am J Physiol 275:C619-C621
140. **Clapham DE** 2007 SnapShot: mammalian TRP channels. Cell 129:220
141. **Klose C, Straub I, Riehle M, Ranta F, Krautwurst D, Ullrich S, Meyerhof W, Harteneck C** 2010 Fenamates as TRP channel blockers: mefenamic acid selectively blocks TRPM3. Br J Pharmacol
142. **Kraft R, Grimm C, Frenzel H, Harteneck C** 2006 Inhibition of TRPM2 cation channels by N-(p-amylcinnamoyl)anthranilic acid. Br J Pharmacol 148:264-273
143. **Grubisha O, Rafty LA, Takanishi CL, Xu X, Tong L, Perraud AL, Scharenberg AM, Denu JM** 2006 Metabolite of SIR2 reaction modulates TRPM2 ion channel. J Biol Chem 281:14057-14065

144. **Grynkiewicz G, Poenie M, Tsien RY** 1985 A new generation of Ca^{2+} indicators with greatly improved fluorescence properties. J Biol Chem 260:3440-3450
145. **Poenie M** 1990 Alteration of intracellular Fura-2 fluorescence by viscosity: a simple correction. Cell Calcium 11:85-91
146. **Lippiat JD** 2008 Whole-cell recording using the perforated patch clamp technique. Methods Mol Biol 491:141-149
147. **Kelly CB, Blair LA, Corbett JA, Scarim AL** 2003 Isolation of islets of Langerhans from rodent pancreas. Methods Mol Med 83:3-14
148. **Li N, Wallén NH, Hjemdahl P** 1999 Evidence for prothrombotic effects of exercise and limited protection by aspirin. Circulation 100:1374-1379
149. **Lemmens R, Larsson O, Berggren PO, Islam MS** 2001 Ca^{2+}-induced Ca^{2+} release from the endoplasmic reticulum amplifies the Ca^{2+} signal mediated by activation of voltage-gated L-type Ca^{2+} channels in pancreatic β-cells. J Biol Chem 276:9971-9977
150. **Thastrup O, Cullen PJ, Drobak BK, Hanley MR, Dawson AP** 1990 Thapsigargin, a tumor promoter, discharges intracellular Ca2+ stores by specific inhibition of the endoplasmic reticulum Ca^{2+}-ATPase. Proc Natl Acad Sci U S A 87:2466-2470
151. **Ohi Y, Atsuki K, Tori Y, Ohizumi Y, Watanabe M, Imaizumi Y** 2001 Imaging of Ca^{2+} release by caffeine and 9-methyl-7-bromoeudistomin D and the associated activation of large conductance Ca^{2+}-dependent K^+ channels in urinary bladder smooth muscle cells of the guinea pig. Jpn J Pharmacol 85:382-390
152. **Zhu X, Jiang M, Birnbaumer L** 1998 Receptor-activated Ca_{2+} influx via human Trp3 stably expressed in human embryonic kidney (HEK)293 cells. Evidence for a non-capacitative Ca^{2+} entry. J Biol Chem 273:133-142
153. **Merritt JE, Armstrong WP, Benham CD, Hallam TJ, Jacob R, Jaxa-Chamiec A, Leigh BK, McCarthy SA, Moores KE, Rink TJ** 1990 SK&F 96365, a novel inhibitor of receptor-mediated calcium entry. Biochem J 271:515-522
154. **Guerrero A, Singer JJ, Fay FS** 1994 Simultaneous measurement of Ca^{2+} release and influx into smooth muscle cells in response to caffeine. A novel approach for calculating the fraction of current carried by calcium. J Gen Physiol 104:395-422
155. **Kiselyov KI, Shin DM, Wang Y, Pessah IN, Allen PD, Muallem S** 2000 Gating of store-operated channels by conformational coupling to ryanodine receptors. Mol Cell 6:421-431
156. **Tinker A, Sutko JL, Ruest L, Deslongchamps P, Welch W, Airey JA, Gerzon K, Bidasee KR, Besch HR, Jr., Williams AJ** 1996 Electrophysiological effects of ryanodine derivatives on the sheep cardiac sarcoplasmic reticulum calcium-release channel. Biophys J 70:2110-2119
157. **Lindsay AR, Manning SD, Williams AJ** 1991 Monovalent cation conductance in the ryanodine receptor-channel of sheep cardiac muscle sarcoplasmic reticulum. J Physiol 439:463-480
158. **Sitsapesan R** 2009 In pursuit of ryanodine receptors gating in the plasma membrane of RINm5F pancreatic beta-cells. Islets 1:84-86
159. **Walker RL, Koh SD, Sergeant GP, Sanders KM, Horowitz B** 2002 TRPC4 currents have properties similar to the pacemaker current in interstitial cells of Cajal. Am J Physiol Cell Physiol 283:C1637-C1645
160. **Peppiatt CM, Collins TJ, MacKenzie L, Conway SJ, Holmes AB, Bootman MD, Berridge MJ, Seo JT, Roderick HL** 2003 2-Aminoethoxydiphenyl borate (2-APB) antagonises inositol 1,4,5-trisphosphate-induced calcium release, inhibits calcium pumps and has a use-dependent and slowly reversible action on store-operated calcium entry channels. Cell Calcium 34:97-108
161. **Strubing C, Krapivinsky G, Krapivinsky L, Clapham DE** 2003 Formation of novel TRPC channels by complex subunit interactions in embryonic brain. J Biol Chem
162. **Waldo GL, Harden TK** 2004 Agonist binding and Gq-stimulating activities of the purified human P2Y1 receptor. Mol Pharmacol 65:426-436
163. **Miller JS, Cervenka T, Lund J, Okazaki IJ, Moss J** 1999 Purine metabolites suppress proliferation of human NK cells through a lineage-specific purine receptor. J Immunol 162:7376-7382

164. **Hoyle CH, Edwards GA** 1992 Activation of P1- and P2Y-purinoceptors by ADP-ribose in the guinea-pig taenia coli, but not of P2X-purinoceptors in the vas deferens. Br J Pharmacol 107:367-374
165. **Bortell R, Moss J, McKenna RC, Rigby MR, Niedzwiecki D, Stevens LA, Patton WA, Mordes JP, Greiner DL, Rossini AA** 2001 Nicotinamide adenine dinucleotide (NAD) and its metabolites inhibit T lymphocyte proliferation: role of cell surface NAD glycohydrolase and pyrophosphatase activities. J Immunol 167:2049-2059
166. **Broetto-Biazon AC, Bracht F, Sa-Nakanishi AB, Lopez CH, Constantin J, Kelmer-Bracht AM, Bracht A** 2008 Transformation products of extracellular NAD^+ in the rat liver: kinetics of formation and metabolic action. Mol Cell Biochem 307:41-50
167. **Moro S, Guo D, Camaioni E, Boyer JL, Harden TK, Jacobson KA** 1998 Human P2Y1 receptor: molecular modeling and site-directed mutagenesis as tools to identify agonist and antagonist recognition sites. J Med Chem 41:1456-1466
168. **Boyer JL, Adams M, Ravi RG, Jacobson KA, Harden TK** 2002 2-Chloro N(6)-methyl-(N)-methanocarba-2'-deoxyadenosine-3',5'-bisphosphate is a selective high affinity P2Y(1) receptor antagonist. Br J Pharmacol 135:2004-2010
169. **Fischer B, Shahar L, Chulkin A, Boyer JL, Harden KT, Gendron FP, Beaudoin AR, Chapal J, Hillaire-Buys D, Petit P** 2000 2-Thioether-5'-O-(1-thiotriphosphate)-adenosine derivatives: new insulin secretagogues acting through P2Y-receptors. Isr Med Assoc J 2 Suppl:92-98
170. **Petit P, Hillaire-Buys D, Manteghetti M, Debrus S, Chapal J, Loubatieres-Mariani MM** 1998 Evidence for two different types of P2 receptors stimulating insulin secretion from pancreatic B cell. Br J Pharmacol 125:1368-1374
171. **Poulsen CR, Bokvist K, Olsen HL, Hoy M, Capito K, Gilon P, Gromada J** 1999 Multiple sites of purinergic control of insulin secretion in mouse pancreatic beta-cells. Diabetes 48:2171-2181
172. **Verspohl EJ, Blackburn GM, Hohmeier N, Hagemann J, Lempka M** 2003 Synthetic, nondegradable diadenosine polyphosphates and diinosine polyphosphates: their effects on insulin-secreting cells and cultured vascular smooth muscle cells. J Med Chem 46:1554-1562
173. **Andaloussi-Lilja J, Lundqvist J, Forsby A** 2009 TRPV1 expression and activity during retinoic acid-induced neuronal differentiation. Neurochem Int 55:768-774
174. **Lazzeri M, Vannucchi MG, Spinelli M, Bizzoco E, Beneforti P, Turini D, Faussone-Pellegrini MS** 2005 Transient receptor potential vanilloid type 1 (TRPV1) expression changes from normal urothelium to transitional cell carcinoma of human bladder. Eur Urol 48:691-698
175. **Tominaga M, Caterina MJ, Malmberg AB, Rosen TA, Gilbert H, Skinner K, Raumann BE, Basbaum AI, Julius D** 1998 The cloned capsaicin receptor integrates multiple pain-producing stimuli. Neuron 21:531-543
176. **Vos MH, Neelands TR, McDonald HA, Choi W, Kroeger PE, Puttfarcken PS, Faltynek CR, Moreland RB, Han P** 2006 TRPV1b overexpression negatively regulates TRPV1 responsiveness to capsaicin, heat and low pH in HEK293 cells. J Neurochem 99:1088-1102
177. **Wang YX, Wang J, Wang C, Liu J, Shi LP, Xu M, Wang C** 2008 Functional expression of transient receptor potential vanilloid-related channels in chronically hypoxic human pulmonary arterial smooth muscle cells. J Membr Biol 223:151-159

I A

The FASEB Journal • FJ Express

Ryanodine receptor-operated activation of TRP-like channels can trigger critical Ca^{2+} signaling events in pancreatic β-cells

Amanda Jabin Gustafsson,[1] Hanna Ingelman-Sundberg,* Mensur Dzabic, Justina Awasum, Nguyen Khanh Hoa,* Claes-Göran Östenson,* Cristina Pierro, Patrizia Tedeschi, Orison Woolcott, Shiue Chiounan, Per-Eric Lund,† Olof Larsson,† and Md. Shahidul Islam

Karolinska Institutet, *Department of Molecular Medicine, Karolinska Hospital; Department of Medicine, Stockholm Söder Hospital, Research Center, Stockholm, Sweden; and †AstraZeneca R&D, Södertälje, Sweden

To read the full text of this article, go to http://www.fasebj.org/cgi/doi/10.1096/fj.04-2621fje; doi: 10.1096/fj.04-2621fje

SPECIFIC AIMS

Pancreatic β-cells possess ryanodine (RY) receptors, but there is little detailed information available concerning the link between the activation of these channels to membrane excitability and downstream Ca^{2+} signaling events. We tested the hypothesis that activation of RY receptors may lead to activation of the transient receptor potential (TRP) channels and that such activation may contribute to membrane depolarization, Ca^{2+} entry through voltage-gated Ca^{2+} channels, and Ca^{2+}-induced Ca^{2+} release (CICR) in the β-cells.

PRINCIPAL FINDINGS

1. Activation of RY receptors triggers Ca^{2+} entry through TRP-like channels

Activation of RY receptors by 9-methyl 5,7-dibromo eudistomin D (MBED) in the presence of glucose (10 mM) increased $[Ca^{2+}]_i$ in INS-1E cells in a characteristic pattern (**Fig. 1*A***). There was an initial rapid increase of $[Ca^{2+}]_i$ followed by a prolonged $[Ca^{2+}]_i$ plateau. A third feature of MBED-induced $[Ca^{2+}]_i$ increase was large regenerative $[Ca^{2+}]_i$ spikes superimposed on the $[Ca^{2+}]_i$ plateau. Similar $[Ca^{2+}]_i$ changes were observed when we used primary β-cells obtained from Wistar rats (Fig. 1*B*). In the absence of extracellular Ca^{2+}, MBED caused a transient increase of $[Ca^{2+}]_i$ and the $[Ca^{2+}]_i$ plateau was absent (Fig. 1*C*). The plateau phase of $[Ca^{2+}]_i$ increase was completely blocked by SKF 96365, which blocks several TRP channels. When applied in the presence of SKF 96365 (10 μM), MBED induced only a transient $[Ca^{2+}]_i$ increase that was abolished by thapsigargin. La^{3+} or Gd^{3+} abolished the $[Ca^{2+}]_i$ plateau that followed activation of RY receptors. Niflumic acid and 2-aminoethoxydiphenyl borate (2-APB), which inhibit several TRP channels, inhibited the $[Ca^{2+}]_i$ plateau. The $[Ca^{2+}]_i$ plateau was also inhibited when MBED was applied to cells depolarized by KCl (30 mM).

Nimodipine did not inhibit the initial rapid rise of $[Ca^{2+}]_i$ and the $[Ca^{2+}]_i$ plateau that followed activation of RY receptors. Ruthenium red (10 μM), a blocker of TRPV channels, did not reduce the $[Ca^{2+}]_i$ plateau induced by MBED.

These results suggest that activation of RY receptors by MBED releases Ca^{2+} from the ER as well as activates Ca^{2+} influx across the plasma membrane. The fact that Ca^{2+} influx was inhibited by SKF 96365, La^{3+}, Gd^{3+}, 2-APB, and niflumic acid suggests that Ca^{2+} entry after activation of RY receptors is likely due to Ca^{2+} entry through channels that belong to the TRP family.

2. Activation of TRP-like channels that follows activation of RY receptors is not due to depletion of ER Ca^{2+} stores

We investigated whether activation of the phosphatidylinositol-specific phospholipase C (PI-PLC) and IP_3 system could be involved in MBED-induced $[Ca^{2+}]_i$ changes. Carbachol (100 μM), a muscarinic agonist that activates PI-PLC, caused a biphasic increase in $[Ca^{2+}]_i$ with an initial peak reflecting Ca^{2+} release from the ER and a small plateau phase representing the Ca^{2+} influx. Application of MBED in the presence of carbachol resulted in a pattern of $[Ca^{2+}]_i$ increase that was similar to that observed when MBED was used without prior application of carbachol. The $[Ca^{2+}]_i$ plateau induced by MBED was larger than that induced by carbachol. These results suggest that activation of RY receptors triggers $[Ca^{2+}]_i$-influx mechanisms that are

[1] Correspondence: Department of Medicine, Karolinska Inst., Stockholm Söder Hospital, Stockholm 118 83, Sweden. E-mail: amajab@ki.se

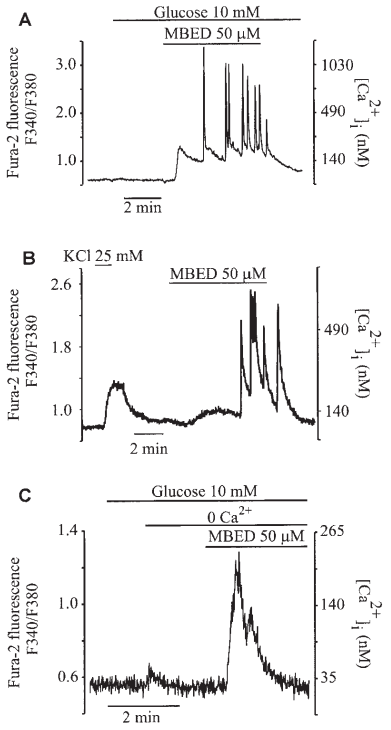

Figure 1. Activation of RY receptors caused a characteristic pattern of $[Ca^{2+}]_i$ changes. $[Ca^{2+}]_i$ was measured from fura-2-loaded single rat insulinoma cells. *A)* Activation of RY receptor by MBED resulted in a characteristic pattern of changes in $[Ca^{2+}]_i$. After addition of MBED (50 μM) in the presence 10 mM glucose, there was an initial rapid rise of $[Ca^{2+}]_i$, followed by a plateau. Superimposed on the $[Ca^{2+}]_i$ plateau was a series of large $[Ca^{2+}]_i$ spikes. *B)* Similar $[Ca^{2+}]_i$ changes were observed when MBED was applied to primary β-cells obtained from Wistar rats. *C)* MBED increased $[Ca^{2+}]_i$ only transiently when extracellular Ca^{2+} was chelated. Note that the scales are different in the graphs. Traces are representative of experiments repeated at least 10 times.

different from those triggered by agonists that engage the PI-PLC and IP_3 pathway.

To test whether activation of TRP channels was due to depletion of the ER or due to an increase of $[Ca^{2+}]_i$, we first depleted ER Ca^{2+} pools by treatment with thapsigargin. Under such condition, MBED would activate RY receptors but such activation would not deplete the ER Ca^{2+} pool further. There would be no release of Ca^{2+} from the ER and thus no increase of $[Ca^{2+}]_i$ attributable to release of Ca^{2+}. Activation of RY receptors in thapsigargin-treated cells resulted in a plateau-like increase in $[Ca^{2+}]_i$. This $[Ca^{2+}]_i$ plateau was due to Ca^{2+} entry through the plasma membrane since it was abolished by SKF 96365. These results suggest that activation of RY receptors may lead to activation of TRP-channels by a mechanism that can operate without involving depletion of the ER Ca^{2+} pools.

3. Activation of TRP-like channels after activation of RY receptors changes membrane potential from −80 mV to −40 mV

We tested the effect of activation of RY receptors on plasma membrane potential using perforated patch current-clamp technique and found that such activation depolarized plasma membrane potential from ~ −80 mV to ~ −40 mM in a reversible manner (**Fig. 2**).

4. Activation of RY receptors and consequent activation of TRP-like channels cause membrane depolarization, activation of L-type voltage-gated Ca^{2+} channels and Ca^{2+} induced Ca^{2+} release

Nimodipine (5 μM) inhibited regenerative $[Ca^{2+}]_i$ spikes that were superimposed on the $[Ca^{2+}]_i$ plateau, indicating that Ca^{2+} entry through the L-type voltage-gated Ca^{2+} channels is essential for generation of these spikes. Ryanodine (50 μM) inhibited regenerative $[Ca^{2+}]_i$ spikes in a use-dependent manner.

Large $[Ca^{2+}]_i$ spikes that are indicative of membrane depolarization and Ca^{2+} influx through the L-type Ca^{2+} channels were observed even when MBED was added in the presence of diazoxide, an agent that hyperpolarizes membrane potential by opening K_{ATP} channels. These data indicate that MBED-induced membrane depolarization was not due to inhibition of K_{ATP} channels by the eudistomin compound and that Ca^{2+} influx through TRP channels can depolarize membrane potential even when K_{ATP} channels are open.

CONCLUSIONS AND SIGNIFICANCE

Whereas much is known about the role of the PI-PLC/IP_3-pathway in mediating Ca^{2+} entry in β-cells, little information is available concerning the role of RY

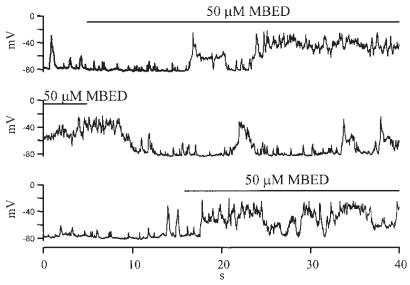

Figure 2. Activation of RY receptors and consequent activation of TRP-like channels depolarized membrane potential. Membrane potential was recorded at room temperature (21–23°C) using the perforated-patch whole cell approach. Activation of RY receptors by MBED (50 μM) depolarized membrane potential from ~ −80 mV to ~ −40 mV.

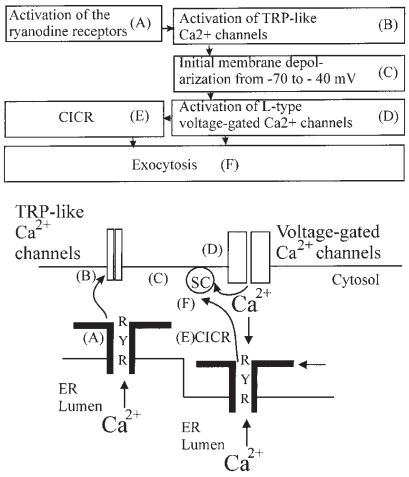

Figure 3. Schematic diagram of hypothesized involvement of RY receptor and TRP-like channels in Ca^{2+} entry and membrane depolarization in β-cells. The diagram illustrates a sequence of events whereby activation of RY receptors *(A)* leads to the activation of TRP-like channels *(B)*, an initial membrane depolarization to ~ −40 mV *(C)*, activation of the L-type voltage-gated Ca^{2+} channels *(D)*, CICR *(E)*, and exocytosis *(F)*.

receptors in triggering Ca^{2+} influx across the plasma membrane. For activation of RY receptors, previous studies have used caffeine, which inhibits plasma membrane Ca^{2+} channels including voltage-gated Ca^{2+} channels and store-operated channels. Unlike caffeine, MBED, a potent caffeine-like activator of RY receptors does not inhibit plasma membrane Ca^{2+} channels, cAMP-phosphodiesterases, IP_3 receptors, or K_{ATP} channels. These properties make MBED a suitable probe for mechanistic studies of RY receptors. Activation of RY receptors of β-cells by MBED caused changes in $[Ca^{2+}]_i$ that consisted of three components: *1)* an initial rapid rise of $[Ca^{2+}]_i$; *2)* a prolonged plateau of $[Ca^{2+}]_i$; and *3)* a series of $[Ca^{2+}]_i$ spikes superimposed on the plateau. Initial rapid increase of $[Ca^{2+}]_i$ was due to release of Ca^{2+} from the ER.

The most important finding of this study was that activation of RY receptors resulted in a prolonged $[Ca^{2+}]_i$ increase after the initial rise of $[Ca^{2+}]_i$. This $[Ca^{2+}]_i$ plateau was dependent on extracellular Ca^{2+}. These results demonstrate that activation of RY receptors leads to the activation of Ca^{2+} permeable channels in the plasma membrane. In thapsigargin-treated cells, MBED did not increase $[Ca^{2+}]_i$ by releasing Ca^{2+} from the ER but there was still activation of Ca^{2+} entry. This finding argues against the possibility that Ca^{2+} influx was triggered by the increase in $[Ca^{2+}]_i$ itself. It is unlikely that Ca^{2+} entry was due to activation of any RY receptors located on the plasma membrane since Ca^{2+} influx was blocked by SKF 96365, which does not block RY receptors. The Ca^{2+} entry responsible for the $[Ca^{2+}]_i$ plateau was not mediated by the voltage-gated Ca^{2+} channels since it was not blocked by nimodipine. La^{3+}, Gd^{3+}, SKF 96365, niflumic acid, and 2-APB, which block many TRP channels, blocked the Ca^{2+} entry that followed the activation of RY receptors. Together, these pharmacological properties suggest that the Ca^{2+} channels that are activated as a consequence of activation of RY receptors belong to the TRP family of cation channels.

Another consequence of activation of RY receptors was the appearance of regenerative $[Ca^{2+}]_i$ spikes superimposed on the $[Ca^{2+}]_i$ plateau. Ca^{2+} entry through the L-type voltage-gated Ca^{2+} channels was essential for generation of these spikes. This is evident from the fact that the spikes were abolished by nimodipine. After activation of RY receptor, membrane potential was depolarized to ~ −40 mV as a result of Ca^{2+} current through the TRP channels (Fig. 2). Such depolarization in turn activated L-type Ca^{2+} channels. The generation of these spikes required CICR through RY receptors. This is evident from the fact that the spikes were inhibited in a use-dependent manner by ryanodine.

The RY receptor-operated Ca^{2+} influx described in this study is much larger than the small capacitative Ca^{2+} entry observed in β-cells after application of high concentrations of carbachol. Consistent with this, the RY receptor-operated Ca^{2+} influx readily depolarized membrane potential to the threshold potential for activation of L-type Ca^{2+} channels. The molecular identity of the Ca^{2+} channel(s) activated as a result of activation of RY receptors in β-cells is not fully known from our study. Members of the TRP family appear to be the best candidates.

Ca^{2+} influx described in the present study is different from the store-operated Ca^{2+} entry described earlier. This is evident from the fact that prior depletion of ER stores by thapsigargin or carbachol did not eliminate the Ca^{2+} plateau elicited by RY receptor activation. This suggests that activation of RY receptors likely stimulates TRP channels through a mechanism that is not essentially dependent on the filling state of the ER. Rather, it is likely that putative TRP channels are activated by their linkage to RY receptors as has been proposed in regards to other cells. It is unclear how activation of RY receptors couples to and gates TRP channels in β-cells. This may involve protein-protein interactions and conformational coupling.

Molecules generated from glucose metabolism (e.g., fructose 1,6-diphosphate and long-chain Acyl CoA can activate RY receptors). Thus, RY receptors are potential links between nutrient metabolism and membrane excitability. We demonstrate that activation of RY receptor by pharmacological tools leads to a series of distinct signaling events that include not only release of Ca^{2+} from the ER but activation of TRP-like channels, membrane depolarization, and Ca^{2+} entry through voltage-gated Ca^{2+} channels and CICR. CICR mediated by RY receptors has been implicated in mediating amplification of exocytosis in β-cells. Activation of RY receptors in β-cells may be an important signaling event that is transduced into a coherent cellular response by participation of TRP-like channels and voltage-gated Ca^{2+} channels. FJ

IB

The FASEB Journal express article 10.1096/fj.04-2621fje. Published online November 30, 2004.

Ryanodine receptor-operated activation of TRP-like channels can trigger critical Ca^{2+} signaling events in pancreatic β-cells

Amanda Jabin Gustafsson, Hanna Ingelman-Sundberg,* Mensur Dzabic, Justina Awasum, Nguyen Khanh Hoa,* Claes-Göran Östenson,* Cristina Pierro, Patrizia Tedeschi, Orison Woolcott, Shiue Chiounan, Per-Eric Lund,† Olof Larsson,† and Md. Shahidul Islam*

*Karolinska Institutet, Department of Medicine, Stockholm Söder Hospital, Research Center, 118 83 Stockholm, Sweden; Department of Molecular Medicine, Karolinska University Hospital; and †AstraZeneca R&D, S-151 85, Södertälje, Sweden

Corresponding author: Amanda Jabin Gustafsson, Karolinska Institutet, Department of Medicine, Stockholm Söder Hospital S-118 83 Stockholm, Sweden. E-mail: amajab@ki.se

ABSTRACT

There is little information available concerning the link between the ryanodine (RY) receptors and the downstream Ca^{2+} signaling events in β-cells. In fura-2 loaded INS-1E cells, activation of RY receptors by 9-methyl 5,7-dibromoeudistomin D (MBED) caused a rapid rise of $[Ca^{2+}]_i$ followed by a plateau and repetitive $[Ca^{2+}]_i$ spikes on the plateau. The $[Ca^{2+}]_i$ plateau was abolished by omission of extracellular Ca^{2+} and by SKF 96365. In the presence of SKF 96365, MBED produced a transient increase of $[Ca^{2+}]_i$, which was abolished by thapsigargin. Activation of RY receptors caused Ca^{2+} entry even when the ER Ca^{2+} pool was depleted by thapsigargin. The $[Ca^{2+}]_i$ plateau was not inhibited by nimodipine or ruthenium red, but was inhibited by membrane depolarization, La^{3+}, Gd^{3+}, niflumic acid, and 2-aminoethoxydiphenyl borate, agents that inhibit the transient receptor potential channels. The $[Ca^{2+}]_i$ spikes were inhibited by nimodipine and ryanodine, indicating that they were due to Ca^{2+} influx through the voltage-gated Ca^{2+} channels and Ca^{2+}-induced Ca^{2+} release (CICR). Activation of RY receptors depolarized membrane potential as measured by patch clamp. Thus, activation of RY receptors leads to coherent changes in Ca^{2+} signaling, which includes activation of TRP-like channels, membrane depolarization, activation of the voltage-gated Ca^{2+} channels and CICR.

Key words: islets of Langerhans • Ca^{2+}-induced Ca^{2+} release • transient receptor potential channels

In the pancreatic β-cells, a cascade of signaling events participates in transducing the effects of glucose and incretin hormones into the exocytosis of insulin. Such events include progressive membrane depolarization, Ca^{2+} entry through the voltage-gated Ca^{2+} channels and Ca^{2+} -induced Ca^{2+} release (CICR) (1). Among the mechanisms that mediate initial depolarization to the threshold potential for the activation of the voltage-gated Ca^{2+} channels, closure of the ATP-sensitive potassium (K_{ATP}) channel is most well known. It is, however, not

always appreciated that depolarization by closure of the K_{ATP} channels requires a second event, namely the existence of a depolarizing inward current primarily carried by Na^+ or Ca^{2+}. The identity of the channels that mediate such depolarizing currents and their regulation remain unclear.

Several members of the transient receptor potential (TRP) superfamily of cation channels are known to mediate membrane depolarization in different cells (2, 3). TRP channels are conserved from worms to humans and are present in both electrically nonexcitable and excitable cells including the β-cells (4–7). The biophysical properties, regulation mechanisms, and functions of these channels remain enigmatic. Much evidence has been presented that different TRP channels can be activated by depletion of the endoplasmic reticulum (ER) Ca^{2+} stores, conformational coupling to the inositol 1,4,5-trisphosphate receptor (IP_3 receptor), and ryanodine receptor (RY receptor) and by diacylglycerol (8–10). β-cells possess IP_3 receptors, RY receptors and probably other intracellular Ca^{2+} release channels. Depletion of the IP_3-sensitive ER Ca^{2+} store induces a small capacitative or store-operated Ca^{2+} influx in these cells (11, 12). Candidate subunits of the store-operated Ca^{2+} channels belong to the TRPC (TRP-canonical) or TRPV (TRP-vanilloid) family (13, 14). Recent studies demonstrate that RY receptors of β-cells are activated as a consequence of glucose metabolism and in response to stimulation by some incretin hormones (15–17). However, it is unknown whether activation of RY receptors could lead to the activation of ion channels in the plasma membrane of β-cells. In previous studies, investigators have used caffeine to activate RY receptors of β-cells (18). The consequences of activation of RY receptors on the downstream Ca^{2+} signaling events were difficult to elucidate in those studies because of the numerous side effects of the xanthine compound. 9-methyl 5,7-dibromoeudistomin D (MBED) is a compound derived from the natural product eudistomin D. MBED is a more specific and more potent activator of RY receptors and is thus suitable for mechanistic studies of these channels (19). We tested the hypothesis that activation of RY receptors may lead to the activation of the TRP channels and that such activation may contribute to the membrane depolarization, Ca^{2+} entry through the voltage-gated Ca^{2+} channels and CICR in the β-cells.

MATERIALS AND METHODS

Chemicals

Fura-2 acetoxymethyl ester was from Molecular Probes Europe. Ryanodine (98% pure), SKF 96365 and thapsigargin were from Calbiochem. 2-aminoethoxydiphenyl borate (2-APB, also called diphenylboric acid 2-aminoethyl ester), N-propargylnitrendipene (MRS 1845) and niflumic acid were from Sigma. Gadolinium (III) chloride hexahydrate was from Aldrich. 9-methyl 5,7-dibromo eudistomin D (MBED) was synthesized. INS-1E cells were a gift from C. B. Wollheim and P. Maechler, Geneva. Cell culture materials were from Life Technologies.

Cell culture

We used a highly differentiated rat insulinoma cell line (S5-cells). This clone of cells was derived from INS-1E cells (20). The cells were cultured in RPMI-1640 medium supplemented with fetal bovine serum (2.5%, v/v), penicillin (50 i.u./ml), streptomycin (50 µg/ml), 2-mercaptoethanol (500 µM), HEPES (10 mM), and sodium pyruvate (1 mM). Cells were

incubated at 37°C in humidified incubator in 5% CO_2. The medium was changed every other day and cells were passaged every other week.

Preparation of rat β-cells

Male Wister rats were killed by decapitation after anesthesia with CO_2. The islets were isolated by injecting collagenase A in Hanks' solution (9 mg/10 ml) into pancreas through the pancreatic duct. The gland was removed, incubated for 24 min at 37°C, washed with Hanks' solution and islets were picked up after separation on Histopaque gradient. Islets were dispersed by trypsin digestion and the cells were plated on glass cover slips. For measurement of $[Ca^{2+}]_I$, only large cells were used to exclude as much as possible non-β-cells.

Measurement of cytosolic free $[Ca^{2+}]$ ($[Ca^{2+}]_i$) by microfluorometry

Cells (~20,000/ml) plated on glass cover slips were incubated in RPMI-1640 medium supplemented with 0.1% bovine serum albumin and 1 μM fura-2 acetoxymethyl ester for 35 min at 37°C. Cells were then incubated for an additional 10 min in the basal medium containing 140 NaCl, 3.6 KCl, 0.5 NaH_2PO_4, 0.5 $MgSO_4$, 1.5 $CaCl_2$, 10 HEPES, 3 glucose (in mM), and 0.1% bovine serum albumin (pH 7.4). Cover slips were mounted as the exchangeable bottom of an open perifusion chamber on the stage of an inverted epifluorescence microscope (Olympus CK 40). The superfusion chamber was designed to allow rapid exchange of fluids. The chamber was thermostatically controlled to maintain a temperature of 37°C in the perifusate. The microscope was connected to a fluorescence system (M-39/2000 RatioMaster, PhotoMed) for dual wavelength excitation fluorometry. The excitation wavelengths generated by a monochromator (DeltaRam, PhotoMed) were directed to the cell by a dichroic mirror. The emitted light selected by a 510-nm filter was monitored by a photomultiplier. The excitation wavelengths were alternated at a frequency of 1 Hz, and the duration of data collection at each wavelength was 0.33 s. The emission at the excitation wavelength of 340 nm (*F*340) and that of 380 nm (*F*380) were used to calculate the fluorescence ratio (*R*340/380). Single cells isolated optically by means of a diaphragm, were studied by using a 40× 1.3 NA oil immersion objective (40× UV APO). The background fluorescence was measured and subtracted from the traces before calculation of $[Ca^{2+}]_i$. $[Ca^{2+}]_i$ was calculated from *R*340/380 according to Grynkiewicz et al. (21). R_{max} and R_{min} were determined by using thin films of external standards containing fura-2 and 2 M sucrose (22). The K_d for Ca^{2+}-fura-2 was taken as 225 nM.

Patch clamp experiments

The cells were detached and seeded on 60-mm dishes and used within two days. Membrane potential was recorded at room temperature (21–23°C) using the perforated-patch whole cell approach with a computer based EPC-10/2 patch amplifier together with PULSE 8.63 (HEKA Elektronik, Lambrecht, Germany). Cells were continuously perifused with a saline solution containing 137 NaCl, 5 KCl, 1.2 $MgCl_2$, 1 $CaCl_2$, 10 HEPES-NaOH (in mM), pH 7.4, and 10 glucose. Patch pipettes were pulled from borosilicate glass, fire-polished, and had resistances between 3 and 4 MΩ after filling the pipettes with the standard intracellular solution containing 140 KCl, 3 NaCl, 1.2 $MgCl_2$, 1 EGTA, 10 HEPES-NaOH (in mM), pH 7.2, and 200 μg/ml amphotericin B. Membrane potential recordings were started when R_S < 30 MΩ, at which time

the amplifier was switched from voltage-clamp to current clamp. MBED was applied by a local pressure application device from a wide-tipped micropipette placed within 100 μm from the cell.

RESULTS

Application of glucose (10 mM) to fura-2 loaded single INS-1E cells for two minutes increased $[Ca^{2+}]_i$ in ~50% of cells by ~50 nM. In the rest of the cells there was no $[Ca^{2+}]_i$ increase. Activation of RY receptors by MBED (50 μM) in the presence of glucose (10 mM), increased $[Ca^{2+}]_i$ immediately and in a characteristic pattern (Fig. 1*A*). There was an initial rapid increase of $[Ca^{2+}]_i$ followed by a prolonged $[Ca^{2+}]_i$ signal which remained elevated during the period of application of MBED. A third and more conspicuous feature of MBED-induced $[Ca^{2+}]_i$ increase was large regenerative $[Ca^{2+}]_i$ spikes superimposed on the $[Ca^{2+}]_i$ plateau. $[Ca^{2+}]_i$ changes returned to the baseline when MBED was washed away in the continued presence of 10 mM glucose. Similar $[Ca^{2+}]_i$ changes were observed when we used primary β-cells obtained from Wister rats (Fig. 1*B*). When extracellular Ca^{2+} was chelated by addition of EGTA, MBED still caused a transient increase of $[Ca^{2+}]_i$ but the $[Ca^{2+}]_i$ plateau was absent (Fig. 1*C*). Under this condition, the transient increase in $[Ca^{2+}]_i$ continuously declined and reached the baseline in less than 2 min. MBED was dissolved in DMSO (final concentration 1.6%). At this concentration DMSO alone caused only a small increase in the basal $[Ca^{2+}]_i$ (~50 nM). 25-μM MBED also increased $[Ca^{2+}]_i$, the magnitude of which was smaller compared with that obtained with 50 μM MBED. Six and twelve μM MBED did not increase $[Ca^{2+}]_i$. The effect of MBED reversed on washout and repeated application of MBED caused repeated $[Ca^{2+}]_i$ increase showing similar pattern. During continued stimulation by MBED, the $[Ca^{2+}]_i$ plateau returned to the baseline over a period of four to 10 min (Fig. 10*C*). Taken together, these results suggest that activation of RY receptors by MBED releases Ca^{2+} from the intracellular stores as well as activation of Ca^{2+} influx across the plasma membrane.

Next we investigated whether the voltage-gated Ca^{2+} channels were involved in mediating Ca^{2+} entry following the activation of RY receptors. In these cells, L-type Ca^{2+} channels constitute the main type of voltage-gated Ca^{2+} channels. We inhibited the L-type Ca^{2+} channels by treating the cells with nimodipine (5 μM). The effectiveness of the inhibition of the voltage-gated Ca^{2+} channels was verified in separate experiments by demonstrating that nimodipine completely blocked the $[Ca^{2+}]_i$-increase induced by 30 mM KCl. As shown in Fig. 2, nimodipine did not inhibit the initial rapid rise of $[Ca^{2+}]_i$ and the $[Ca^{2+}]_i$ plateau that followed activation of RY receptors. Nimodipine inhibited the regenerative $[Ca^{2+}]_i$ spikes that were superimposed on the $[Ca^{2+}]_i$ plateau (Fig. 1*A*), indicating that Ca^{2+} entry through the L-type Ca^{2+} channels is required for the generation of these spikes. However, it should be noted that the large transient Ca^{2+} spikes were generated mainly by CICR rather than by Ca^{2+} entry through the L-type voltage gated Ca^{2+} channels (Fig. 10*B*). We tested the effect of MBED on plasma membrane potential using perforated patch current-clamp technique and found that MBED depolarized plasma membrane potential from approximately –80 mV to approximately –40 mM in a reversible manner (Fig. 3).

The plateau phase of $[Ca^{2+}]_i$ increase was completely blocked by SKF 96365 that blocks several TRP channels as well as the voltage-gated Ca^{2+} channels (23, 24). When applied in the presence of SKF 96365 (10 μM), MBED induced only a transient $[Ca^{2+}]_i$ increase (Fig. 4*A*). This transient $[Ca^{2+}]_i$ increase by MBED, observed in the SKF 96365-treated cells, was due to Ca^{2+} release

from the ER. This is evident from the observation that this $[Ca^{2+}]_i$ increase was abolished when the ER Ca^{2+} pool was depleted by treatment with thapsigargin (Fig. 4*B*). Thus, the results obtained from experiments with nimodipine and SKF 96365 suggest that the $[Ca^{2+}]_i$ plateau that follows activation of RY receptors is due to Ca^{2+} influx through the TRP family of Ca^{2+} permeable channels.

In β-cells carbachol and thapsigargin releases Ca^{2+} from ER Ca^{2+} stores (Fig. 5*A*). To test whether activation of the TRP channels was due to the depletion of the ER or due to an increase of $[Ca^{2+}]_i$, we first depleted the ER Ca^{2+} pools by treatment with thapsigargin. Under such condition, MBED would activate RY receptors but such activation would not deplete the ER Ca^{2+} pool further. There would be no release of Ca^{2+} from the ER and thus no increase of $[Ca^{2+}]_i$ attributable to the release of Ca^{2+}. Consistent with our previous reports (18), treatment of cells with thapsigargin (500 nM- 1 μM) for 45 min completely emptied the ER Ca^{2+} pools as evidenced from the fact that carbachol did not increase $[Ca^{2+}]_i$ (Fig. 5*B*). The basal $[Ca^{2+}]_i$ in the thapsigargin-treated cells was similar to that in the control cells. The plasma membrane potential of the thapsigargin-treated cells is similar to that of the untreated cells (25). As shown in Fig. 5*B*, activation of RY receptors in the thapsigargin-treated cells also resulted in a plateau increase in $[Ca^{2+}]_i$. This $[Ca^{2+}]_i$ plateau was due to Ca^{2+} entry through the plasma membrane since it was abolished by SKF 96365 (Fig. 4*B*). The initial rapid increase of $[Ca^{2+}]_i$ and the large regenerative $[Ca^{2+}]_i$ spikes were absent in the thapsigargin-treated cells. These results suggest that activation of RY receptors can lead to the activation of TRP-channels by a mechanism that can operate without involving depletion of the ER Ca^{2+} pools.

We investigated whether activation of the phosphatidylinositol-specific phospholipase C (PI-PLC) and IP_3 system could be involved in the MBED-induced $[Ca^{2+}]_i$ changes. Carbachol (100 μM), a muscarinic agonist that activates PI-PLC, caused a biphasic increase in $[Ca^{2+}]_i$ with an initial peak reflecting Ca^{2+} release from the ER and a small plateau phase representing the capacitative Ca^{2+} influx (Fig. 6). Application of MBED in the continued presence of carbachol resulted in a pattern of $[Ca^{2+}]_i$ increase that was similar to that observed when the eudistomin was used without prior application of carbachol (Fig. 1*A*). The $[Ca^{2+}]_i$ plateau induced by MBED was larger than that induced by carbachol. These results suggest that activation of RY receptors triggers $[Ca^{2+}]_i$-entry mechanisms which are different from those triggered by agonists that engage the PI-PLC and IP_3 pathway.

Ca^{2+} entry through the TRP channels should be reduced when plasma membrane is depolarized because of the reduced driving force for Ca^{2+}. In Fig. 7*A*, the membrane potential was clamped at a depolarized level by 30 mM KCl. This increased $[Ca^{2+}]_i$ to a plateau of ~265 nM. Activation of RY receptors by MBED in the depolarized cells caused a transient $[Ca^{2+}]_i$ increase, but it did not affect the plateau level. The repetitive $[Ca^{2+}]_i$ spikes that are normally elicited by MBED (Fig. 1*A*) were absent when MBED was added to the depolarized cells. Diazoxide, an agent that hyperpolarizes membrane potential by opening the K_{ATP} channels, did not alter the $[Ca^{2+}]_i$ response to MBED (Fig. 7*B*). The large $[Ca^{2+}]_i$ spikes that are indicative of membrane depolarization and Ca^{2+} influx through the L-type Ca^{2+} channels were observed even when MBED was added in the presence of diazoxide (Fig. 7*B*). Taken together, these data indicate that the MBED-induced membrane depolarization was not due to the inhibition of K_{ATP} channels by the eudistomin compound and that Ca^{2+} influx through the TRP channels can depolarize membrane potential even when the K_{ATP} channels are open (Fig. 7*B*).

We examined the role of extracellular Na^+ on $[Ca^{2+}]_i$ changes induced by MBED. In Figure 8, the superfusion solution was changed to one that did not contain Na^+. Choline chloride was used to replace NaCl. On switching to choline chloride solution, a small increase in $[Ca^{2+}]_i$ was observed. Addition of MBED in the absence of extracellular Na^+ resulted in $[Ca^{2+}]_i$ changes which were similar to those observed when MBED was applied in the presence of extracellular Na^+. The large regenerative $[Ca^{2+}]_i$ spikes which are due to plasma membrane depolarization and activation of the voltage-gated Ca^{2+} channels were present even when cells were activated by MBED in the Na^+-free medium. These results indicate that RY receptor-operated plasma membrane current through the TRP-like channels is not dependent on Na^+ permeation.

La^{3+} (100 μM) abolished the $[Ca^{2+}]_i$ plateau that followed activation of the RY receptors (Fig. 9*A*). Gd^{3+} (10 μM) also inhibited the $[Ca^{2+}]_i$ plateau induced by MBED (data not shown). Ruthenium red (10 μM), a blocker of TRPV channels, did not reduce the $[Ca^{2+}]_i$ plateau induced by MBED (data not shown). Niflumic acid inhibits TRPC4 and several other TRP channels (26). Niflumic acid (30 μM) inhibited the Ca^{2+} plateau induced by MBED (Fig. 9*B*). 2-APB inhibits or activates different channels, for example, IP_3 receptors and some TRP channels (27, 28). This substance has multiple effects on different ion channels and pumps and is difficult to use under many experimental conditions (29). We used 2-APB at concentrations of 1, 5, 10, 20, 30, 40, 50, and 100 μM. The effects of 2-APB on MBED-induced $[Ca^{2+}]_i$ increase were complex. 2-APB (30 and 40 μM) by itself caused a transient increase of $[Ca^{2+}]_i$. When applied in the presence of 2-APB, MBED still increased $[Ca^{2+}]_i$ in 15 out of 16 experiments. In one experiment 2-APB (100μM) completely blocked Ca^{2+} release by MBED. The $[Ca^{2+}]_i$ plateau that follows the activation of RY receptors was completely absent in four out of nine experiments where we used 2-APB at a concentration of 30–40 μM (Fig. 9*C*). In the remaining five experiments the $[Ca^{2+}]_i$ plateau was reduced almost to the baseline. N-Propargylnitrendipene (5 μM), a dihydropyridine blocker of store-operated Ca^{2+} channels (30) did not block MBED-induced $[Ca^{2+}]_i$ changes (data not shown). High concentrations of N-Propargylnitrendipene (e.g., 20 μM) by itself increased $[Ca^{2+}]_i$ in these cells.

To confirm that MBED-induced Ca^{2+}-changes were due to activation of RY receptors, we pretreated the cells with ryanodine (50 μM) in the presence of caffeine (10 mM) and KCl (25 mM) for 45 min. The treated cells were activated by MBED (50 μM). Under such conditions there was no increase of $[Ca^{2+}]_i$ by MBED (Fig. 10*A*). Figure 10*B* provides further evidence that MBED-induced $[Ca^{2+}]_i$ increase was inhibited by ryanodine (50 μM) in a use-dependent manner (refer to Figure 10*C*). In the cells that were incubated with ryanodine the initial $[Ca^{2+}]_i$ response to MBED was similar to that in the control cells but the $[Ca^{2+}]_i$ spikes became progressively smaller and the plateau $[Ca^{2+}]_i$ returned to the baseline during the continued presence of ryanodine (Fig. 10*B*).

DISCUSSION

Whereas much is known about the role of the PI-PLC/IP_3-pathway in mediating a small Ca^{2+} entry in β-cells (5, 12, 31, 32), by comparison, little detailed information is available concerning the role of RY receptors in triggering Ca^{2+} influx across plasma membrane. This is true even though it has been known for some time that β-cells have RY receptors and that these channels

amplify Ca^{2+} signals and exocytosis (25, 33–35). Part of the difficulty in addressing the issue arises from lack of suitable pharmacological agonists of RY receptors. For activation of RY receptors, previous studies have used caffeine, which inhibits many ion channels, enzymes and receptors. In fact, caffeine inhibits plasma membrane Ca^{2+} entry pathways, including both the voltage-gated Ca^{2+} channels and the store-operated channels (18, 36). MBED is more potent than caffeine in its action on the RY receptors. The compound has been used as an activator of RY receptors for nearly 20 years, and so far no major nonspecific effects have been reported. Unlike caffeine, MBED does not inhibit cAMP-phosphodiesterases of β-cells and does not inhibit the IP_3 receptors or the K_{ATP} channels (15). These properties make MBED a suitable probe for mechanistic studies of RY receptors. We found that activation of RY receptors of β-cells by MBED caused a characteristic pattern of changes in $[Ca^{2+}]_i$ that consisted of three distinct components: (a) an initial rapid rise of $[Ca^{2+}]_i$ (b) a prolonged plateau of $[Ca^{2+}]_i$ and (c) a series of high amplitude $[Ca^{2+}]_i$ spikes superimposed on the plateau. These effects of MBED were reversible, and a similar pattern of $[Ca^{2+}]_i$ changes was observed on repeated application of MBED.

The initial rapid increase of $[Ca^{2+}]_i$ observed after application of MBED was due to the release of Ca^{2+} from the ER, since it was present even when the extracellular Ca^{2+} was omitted or when Ca^{2+} influx was blocked by SKF 96365. This initial increase of $[Ca^{2+}]_i$ was also abolished when the ER Ca^{2+} pool was depleted by thapsigargin. Consistent with previous reports, these results confirm that MBED causes a transient Ca^{2+} release from the ER by activation of RY receptors of β-cells (15, 37).

The most important finding of this study was that activation of RY receptors resulted in a prolonged $[Ca^{2+}]_i$ increase after the initial rapid rise of $[Ca^{2+}]_i$. This $[Ca^{2+}]_i$ plateau was dependent on extracellular Ca^{2+}. These results demonstrate that activation of RY receptors not only releases Ca^{2+} from the ER but also leads to the activation of Ca^{2+} permeable cation channels in the plasma membrane. In thapsigargin-treated cells, MBED did not increase $[Ca^{2+}]_i$ by releasing Ca^{2+} from the ER but there was still activation of Ca^{2+} entry across the plasma membrane. This finding argues against the possibility that Ca^{2+} influx was triggered by the increase in $[Ca^{2+}]_i$ itself. It is also unlikely that Ca^{2+} entry was due to activation of any RY receptors located on the plasma membrane since Ca^{2+} influx was blocked by SKF 96365 (Fig. 4*A*), which does not block RY receptors. The Ca^{2+} entry responsible for the $[Ca^{2+}]_i$ plateau was not mediated by the voltage-gated Ca^{2+} channels since it was not blocked by nimodipine. N-propargylnitrendipene, a dihydropyridine that blocks store-operated Ca^{2+} influx did not reduce the $[Ca^{2+}]_i$ plateau. La^{3+} (100 μM), Gd^{3+} (10 μM), SKF 96365, niflumic acid and 2-APB (30 μM) which block store-operated Ca^{2+} channels and many TRP channels, blocked Ca^{2+} entry (26, 29). Taken together, these pharmacological properties suggest that the Ca^{2+} channels that are activated as a consequence of activation of RY receptors belong to the TRP family of cation channels.

Another dramatic consequence of activation of RY receptors was the appearance of large regenerative $[Ca^{2+}]_i$ spikes that were superimposed on the $[Ca^{2+}]_i$ plateau. Multiple mechanisms contributed to the generation of these spikes. First, Ca^{2+} entry through the L- type voltage-gated Ca^{2+} channels was essential for generation of these spikes. This is evidenced from the fact that the spikes were abolished by nimodipin. Our results demonstrate that following activation of RY receptor, plasma membrane is depolarized to about –40 mV as a result of Ca^{2+} current through

the TRP channels (Fig. 3). Such depolarization in turn activates L-type Ca^{2+} channels. Second, the generation of these spikes required CICR through RY receptors. This is evident from the fact that the spikes were inhibited in a use-dependent manner by high concentration of ryanodine or when the ER Ca^{2+} pool was emptied by thapsigargin.

Previous studies have shown that glucose and glucagon-like peptide-1 can induce a cationic inward current in β-cells (31, 38). The pharmacological property or molecular identity of the channels that mediate such inward current has not been elucidated in these studies. Other studies have demonstrated that depletion of the IP_3-sensitive ER Ca^{2+} pools induces a small capacitative Ca^{2+} influx in β-cells (11, 12). In the present study, we have demonstrated a mechanism of Ca^{2+} entry that involves the RY receptors. The RY receptor-operated Ca^{2+} influx described in the present study is much larger compared with the small capacitative Ca^{2+} entry that is observed in β-cells after application of high concentrations of carbachol (Fig. 6). Consistent with this, the RY receptor-operated Ca^{2+} influx readily depolarizes membrane potential to the threshold potential for activation of the L-type Ca^{2+} channels. In this study we have depended primarily on fluorescence methods and characterization of the inward current by patch-clamp technique is planned for future studies. The molecular identity of the Ca^{2+} channel(s) that are activated as a result of the activation of RY receptors in β-cells is not fully known from our study. In this respect, members of the TRP family appear to be the best candidates. In β-cells, transcripts for TRPC1-6, TRPM2, TRPM5, TRPV1, and TRPV5 have been found (4–7, 31). TRPV5 is abundant in β-cells where it is located on the secretory granules (39). However, TRPV channels are unlikely candidates because the Ca^{2+} influx was not blocked by ruthenium red, a potent inhibitor of TRPV channels (40). It should be noted that assembly of different types of TRP channels into homo- and hetero-multimers is likely to yield a wide variety of channels with diverse regulation mechanisms (41).

The Ca^{2+} influx described in the present study is different from the store-operated Ca^{2+} entry described earlier in these cells (11, 12). This is evident from the fact that prior depletion of ER stores by thapsigargin or carbachol did not eliminate the Ca^{2+} plateau elicited by RY receptor activation. This suggests that activation of RY receptors likely stimulates TRP channels through a mechanism that is not essentially dependent on the filling state of the ER. Rather, it is likely that the putative TRP channels are activated by their linkage to the RY receptors as has been proposed in other cells (10, 42). At present, it is unclear how the activation of RY receptors couples to and gates the TRP channels in β-cells. This may involve protein–protein interactions and conformational coupling. Such gating of TRP channels by RY receptors has been demonstrated in other systems (10).

Thus, we describe a novel route of Ca^{2+} influx, which is coupled to the activation of RY receptors. The channels that mediate this Ca^{2+} influx are presumably members of the TRP family. Molecules generated from glucose metabolism for example, fructose 1,6-diphosphate (43) and long-chain Acyl CoA (44) can activate RY receptors. Thus, RY receptors are potential links between nutrient metabolism and membrane excitability. We demonstrate that activation of RY receptor by pharmacological tools leads to a series of distinct signaling events, which include not only the release of Ca^{2+} from the ER but also activation of TRP-like channels, membrane depolarization, Ca^{2+} entry through the voltage-gated Ca^{2+} channels, and CICR. This sequence of events has been illustrated in a model shown in Fig. 11. CICR mediated by RY receptors has

been implicated in mediating amplification of exocytosis in β-cells (34, 45). Thus, activation of RY receptors in β-cells may be an important signaling event that is transduced into a coherent cellular response by participation of the TRP-like channels and the voltage-gated Ca^{2+} channels.

ACKNOWLEDGMENTS

This work was supported in part by Swedish Medical Research Council Grant K2003-32X-14648-01A, funds of Karolinska Institutet, Swedish Medical Society, Novo Nordisk Foundation, Stiftelsen Irma och Arvid Larsson-Rösts minne. Svenska Diabetesstiftelsen and Swedish Diabetes Society has supported A. J. G. M. S. I. is a recipient of career development award from the Juvenile Diabetes Research Foundation, International. O. W. is a Swedish Institute guest researcher.

REFERENCES

1. Islam, M. S. (2000) Calcium and diabetes. In *Calcium: the molecular basis of calcium action in biology and medicine* (Pochet, R., Donato, R., Haiech, J., Heizmann, C., and Gerke, V., eds) Amersterdam: Kluwer Academic Publishers; pp. 402–413

2. Minke, B., Wu, C., and Pak, W. L. (1975) Induction of photoreceptor voltage noise in the dark in *Drosophila* mutant. *Nature* **258,** 84–87

3. Launay, P., Fleig, A., Perraud, A. L., Scharenberg, A. M., Penner, R., and Kinet, J. P. (2002) TRPM4 is a Ca^{2+}-activated nonselective cation channel mediating cell membrane depolarization. *Cell* **109,** 397–407

4. Qian, F., Huang, P., Ma, L., Kuznetsov, A., Tamarina, N., and Philipson, L. H. (2002) TRP genes: candidates for nonselective cation channels and store-operated channels in insulin-secreting cells. *Diabetes* **51,** Suppl 1**,** S183–S189

5. Sakura, H., and Ashcroft, F. M. (1997) Identification of four trp1 gene variants murine pancreatic beta-cells. *Diabetologia* **40,** 528–532

6. Inamura, K., Sano, Y., Mochizuki, S., Yokoi, H., Miyake, A., Nozawa, K., Kitada, C., Matsushime, H., and Furuichi, K. (2003) Response to ADP-ribose by activation of TRPM2 in the CRI-G1 insulinoma cell line. *J. Membr. Biol.* **191,** 201–207

7. Akiba, Y., Kato, S., Katsube, K., Nakamura, M., Takeuchi, K., Ishii, H., and Hibi, T. (2004) Transient receptor potential vanilloid subfamily 1 expressed in pancreatic islet beta cells modulates insulin secretion in rats. *Biochem. Biophys. Res. Commun.* **321,** 219–225

8. Putney, J. W., Jr., Broad, L. M., Braun, F. J., Lievremont, J. P., and Bird, G. S. (2001) Mechanisms of capacitative calcium entry. *J. Cell Sci.* **114,** 2223–2229

9. Kiselyov, K., Xu, X., Mozhayeva, G., Kuo, T., Pessah, I. N., Mignery, G., Zhu, X., Birnbaumer, L., and Muallem, S. (1998) Functional interaction between InsP3 receptors and store-operated Htrp3 channels. *Nature* **396,** 478–482

10. Kiselyov, K. I., Shin, D. M., Wang, Y., Pessah, I. N., Allen, P. D., and Muallem, S. (2000) Gating of store-operated channels by conformational coupling to ryanodine receptors. *Mol. Cell* **6,** 421–431

11. Miura, Y., Henquin, J. C., and Gilon, P. (1997) Emptying of intracellular Ca^{2+} stores stimulates Ca^{2+} entry in mouse pancreatic beta-cells by both direct and indirect mechanisms. *J. Physiol.* **503,** 387–398

12. Dyachok, O., and Gylfe, E. (2001) Store-operated influx of Ca^{2+} in pancreatic beta-cells exhibits graded dependence on the filling of the endoplasmic reticulum. *J. Cell Sci.* **114,** 2179–2186

13. Minke, B., and Cook, B. (2002) TRP channel proteins and signal transduction. *Physiol. Rev.* **82,** 429–472

14. Putney, J. W. (2003) Capacitative calcium entry in the nervous system. *Cell Calcium* **34,** 339–344

15. Bruton, J. D., Lemmens, R., Shi, C. L., Persson-Sjogren, S., Westerblad, H., Ahmed, M., Pyne, N. J., Frame, M., Furman, B. L., Islam, M. S. (2002) Ryanodine receptors of pancreatic beta-cells mediate a distinct context-dependent signal for insulin secretion. *FASEB J* 10.1096/fj.02-0481fje

16. Kang, G., and Holz, G. G. (2003) Amplification of exocytosis by Ca^{2+}-induced Ca^{2+} release in INS-1 pancreatic beta cells. *J. Physiol.* **546,** 175–189

17. Roe, M. W., Lancaster, M. E., Mertz, R. J., Worley, J. F., III, and Dukes, I. D. (1993) Voltage-dependent intracellular calcium release from mouse islets stimulated by glucose. *J. Biol. Chem.* **268,** 9953–9956

18. Islam, M. S., Larsson, O., Nilsson, T., and Berggren, P. O. (1995) Effects of caffeine on cytoplasmic free Ca^{2+} concentration in pancreatic β-cells are mediated by interaction with ATP-sensitive K^+ channels and L-type voltage-gated Ca^{2+} channels but not the ryanodine receptor. *Biochem. J.* **306,** 679–686

19. Seino-Umeda, A., Fang, Y. I., Ishibashi, M., Kobayashi, J., and Ohizumi, Y. (1998) 9-Methyl-7-bromoeudistomin D induces Ca^{2+} release from cardiac sarcoplasmic reticulum. *Eur. J. Pharmacol.* **357,** 261–265

20. Maechler, P., Antinozzi, P. A., and Wollheim, C. B. (2000) Modulation of glutamate generation in mitochondria affects hormone secretion in INS-1E beta cells. *IUBMB Life* **50,** 27–31

21. Grynkiewicz, G., Poenie, M., and Tsien, R. Y. (1985) A new generation of Ca^{2+} indicators with greatly improved fluorescence properties. *J. Biol. Chem.* **260,** 3440–3450

22. Poenie, M. (1990) Alteration of intracellular Fura-2 fluorescence by viscosity: a simple correction. *Cell Calcium* **11,** 85–91

23. Merritt, J. E., Armstrong, W. P., Benham, C. D., Hallam, T. J., Jacob, R., Jaxa-Chamiec, A., Leigh, B. K., McCarthy, S. A., Moores, K. E., and Rink, T. J. (1990) SK&F 96365, a novel inhibitor of receptor-mediated calcium entry. *Biochem. J.* **271,** 515–522

24. Zhu, X., Jiang, M., and Birnbaumer, L. (1998) Receptor-activated Ca^{2+} influx via human Trp3 stably expressed in human embryonic kidney (HEK)293 cells. Evidence for a non-capacitative Ca^{2+} entry. *J. Biol. Chem.* **273,** 133–142

25. Lemmens, R., Larsson, O., Berggren, P. O., and Islam, M. S. (2001) Ca^{2+}-induced Ca^{2+} release from the endoplasmic reticulum amplifies the Ca^{2+} signal mediated by activation of voltage-gated L-type Ca^{2+} channels in pancreatic β-cells. *J. Biol. Chem.* **276,** 9971–9977

26. Walker, R. L., Koh, S. D., Sergeant, G. P., Sanders, K. M., and Horowitz, B. (2002) TRPC4 currents have properties similar to the pacemaker current in interstitial cells of Cajal. *Am. J. Physiol. Cell Physiol.* **283,** C1637–C1645

27. Ma, H. T., Patterson, R. L., van Rossum, D. B., Birnbaumer, L., Mikoshiba, K., and Gill, D. L. (2000) Requirement of the inositol trisphosphate receptor for activation of store-operated Ca^{2+} channels. *Science* **287,** 1647–1651

28. Hermosura, M. C., Monteilh-Zoller, M. K., Scharenberg, A. M., Penner, R., and Fleig, A. (2002) Dissociation of the store-operated calcium current I(CRAC) and the Mg-nucleotide-regulated metal ion current MagNuM. *J. Physiol.* **539,** 445–458

29. Peppiatt, C. M., Collins, T. J., MacKenzie, L., Conway, S. J., Holmes, A. B., Bootman, M. D., Berridge, M. J., Seo, J. T., and Roderick, H. L. (2003) 2-Aminoethoxydiphenyl borate (2-APB) antagonises inositol 1,4,5-trisphosphate-induced calcium release, inhibits calcium pumps and has a use-dependent and slowly reversible action on store-operated calcium entry channels. *Cell Calcium* **34,** 97–108

30. Harper, J. L., Camerini-Otero, C. S., Li, A. H., Kim, S. A., Jacobson, K. A., and Daly, J. W. (2003) Dihydropyridines as inhibitors of capacitative calcium entry in leukemic HL-60 cells. *Biochem. Pharmacol.* **65,** 329–338

31. Roe, M. W., Worley, J. F., III, Qian, F., Tamarina, N., Mittal, A. A., Dralyuk, F., Blair, N. T., Mertz, R. J., Philipson, L. H., and Dukes, I. D. (1998) Characterization of a Ca^{2+} release-activated nonselective cation current regulating membrane potential and [Ca2+]i oscillations in transgenically derived beta-cells. *J. Biol. Chem.* **273,** 10,402–10,410

32. Worley, J. F., III, McIntyre, M. S., Spencer, B., and Dukes, I. D. (1994) Depletion of intracellular Ca^{2+} stores activates a maitotoxin-sensitive nonselective cationic current in beta-cells. *J. Biol. Chem.* **269,** 32,055–32,058

33. Islam, M. S. (2002) The ryanodine receptor calcium channel of β-cells: molecular regulation and physiological significance. *Diabetes* **51,** 1299–1309

34. Kang, G., and Holz, G. G. (2003) Amplification of exocytosis by Ca^{2+}-induced Ca^{2+} release in INS-1 pancreatic beta cells. *J. Physiol.* **546,** 175–189

35. Mitchell, K. J., Lai, F. A., and Rutter, G. A. (2003) Ryanodine receptor type I and nicotinic acid adenine dinucleotide phosphate receptors mediate Ca^{2+} release from insulin-containing vesicles in living pancreatic beta-cells (MIN6). *J. Biol. Chem.* **278,** 11,057–11,064

36. Bennett, D. L., Bootman, M. D., Berridge, M. J., and Cheek, T. R. (1998) Ca^{2+} entry into PC12 cells initiated by ryanodine receptors or inositol 1,4,5-trisphosphate receptors. *Biochem. J.* **329,** 349–357

37. Ohi, Y., Atsuki, K., Tori, Y., Ohizumi, Y., Watanabe, M., and Imaizumi, Y. (2001) Imaging of Ca^{2+} release by caffeine and 9-methyl-7-bromoeudistomin D and the associated activation of large conductance Ca^{2+}-dependent K+ channels in urinary bladder smooth muscle cells of the guinea pig. *Jpn. J. Pharmacol.* **85,** 382–390

38. Leech, C. A., and Habener, J. F. (1997) Insulinotropic glucagon-like peptide-1-mediated activation of non-selective cation currents in insulinoma cells is mimicked by maitotoxin. *J. Biol. Chem.* **272,** 17,987–17,993

39. Janssen, S. W., Hoenderop, J. G., Hermus, A. R., Sweep, F. C., Martens, G. J., and Bindels, R. J. (2002) Expression of the novel epithelial Ca^{2+} channel ECaC1 in rat pancreatic islets. *J. Histochem. Cytochem.* **50,** 789–798

40. Guler, A. D., Lee, H., Iida, T., Shimizu, I., Tominaga, M., and Caterina, M. (2002) Heat-evoked activation of the ion channel, TRPV4. *J. Neurosci.* **22,** 6408–6414

41. Strubing, C., Krapivinsky, G., Krapivinsky, L., Clapham, D. E. (2003) Formation of novel TRPC channels by complex subunit interactions in embryonic brain. *J Biol.Chem.* **278,** 39,014-39,019

42. Guerrero, A., Singer, J. J., and Fay, F. S. (1994) Simultaneous measurement of Ca^{2+} release and influx into smooth muscle cells in response to caffeine. A novel approach for calculating the fraction of current carried by calcium. *J. Gen. Physiol.* **104,** 395–422

43. Kermode, H., Chan, W. M., Williams, A. J., and Sitsapesan, R. (1998) Glycolytic pathway intermediates activate cardiac ryanodine receptors. *FEBS Lett.* **431,** 59–62

44. Mitchell, K. J., Pinton, P., Varadi, A., Tacchetti, C., Ainscow, E. K., Pozzan, T., Rizzuto, R., and Rutter, G. A. (2001) Dense core secretory vesicles revealed as a dynamic Ca^{2+} store in neuroendocrine cells with a vesicle-associated membrane protein aequorin chimaera. *J. Cell Biol.* **155,** 41–51

45. Graves, T. K., and Hinkle, P. M. (2003) Ca^{2+}-Induced Ca^{2+} Release in the Pancreatic beta-cell: Direct evidence of endoplasmic reticulum Ca^{2+} release. *Endocrinology* **144,** 3565–3574

Received June 24, 2004; accepted October 20, 2004.

Fig. 1

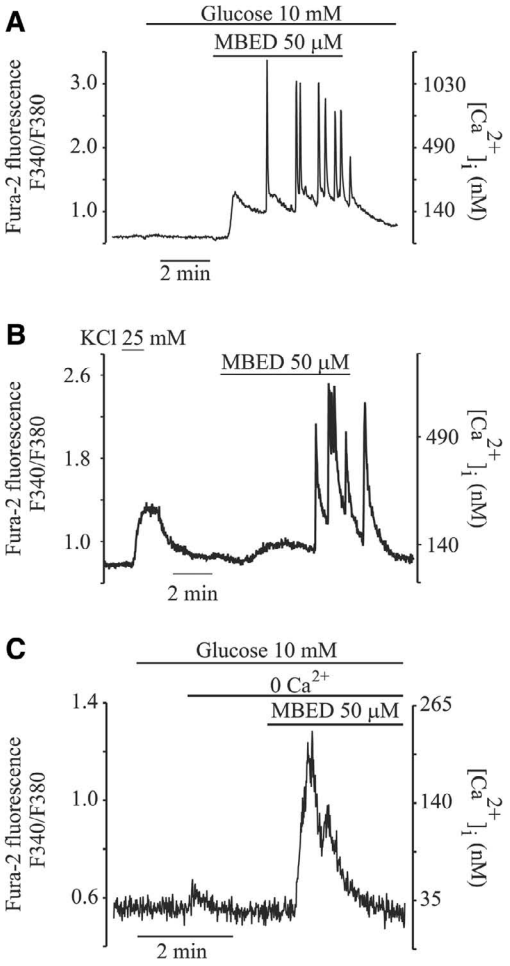

Figure 1. Activation of RY receptors causes a characteristic pattern of $[Ca^{2+}]_i$ changes. $[Ca^{2+}]_i$ was measured from fura-2-loaded single rat insulinoma cells as described in the materials and methods section. ***A***) Activation of RY receptor by 9-methyl 5,7-dibromoeudistomin D (MBED) resulted in a characteristic pattern of changes in $[Ca^{2+}]_i$. After addition of MBED (50 µM) in the presence 10 mM glucose, there was an initial rapid rise of $[Ca^{2+}]_i$, which was then followed by a plateau. Superimposed on the $[Ca^{2+}]_i$ plateau were a series of large $[Ca^{2+}]_i$ spikes. ***B***) Similar $[Ca^{2+}]_i$ changes were observed when MBED was applied to primary β-cells obtained from Wister rats. ***C***). MBED increased $[Ca^{2+}]_i$ only transiently when extracellular Ca^{2+} was chelated. Observe that the scales are different in the graphs. Traces are representative of experiments repeated at least 10 times.

Fig. 2

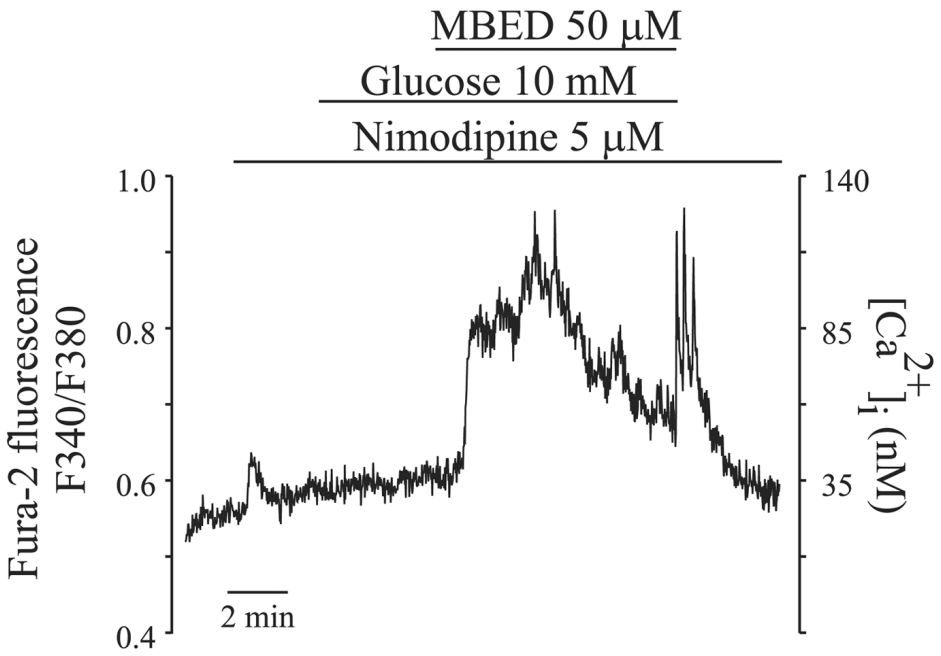

Figure 2. The $[Ca^{2+}]_i$ plateau that followed activation of RY receptors was not due to Ca^{2+} influx through the voltage-gated Ca^{2+} channels. Experimental protocols were as described in the legends to the **Fig. 1**. Nimodipine (5 μM) did not block the initial rapid rise of $[Ca^{2+}]_i$ and the $[Ca^{2+}]_i$ plateau that followed the activation of RY receptor by MBED (50 μM) but inhibited the repetitive $[Ca^{2+}]_i$ spikes that were normally seen in the absence of nimodipine (see **Fig. 1*A***). Similar results were obtained in 3 independent experiments.

Fig. 3

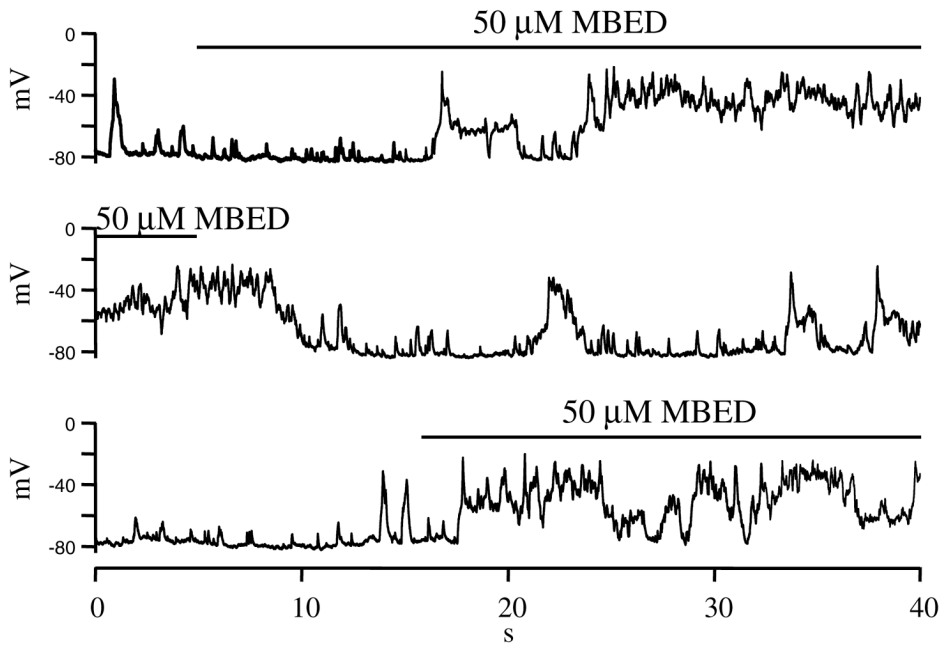

Figure 3. Activation of RY receptors depolarized membrane potential. Membrane potential was recorded at room temperature (21–23°C) using the perforated-patch whole cell approach. The concentration of glucose in the medium was 10 mM. Application of MBED (50 μM) depolarized membrane potential. The trace is representative of experiments repeated 3 times.

Fig. 4

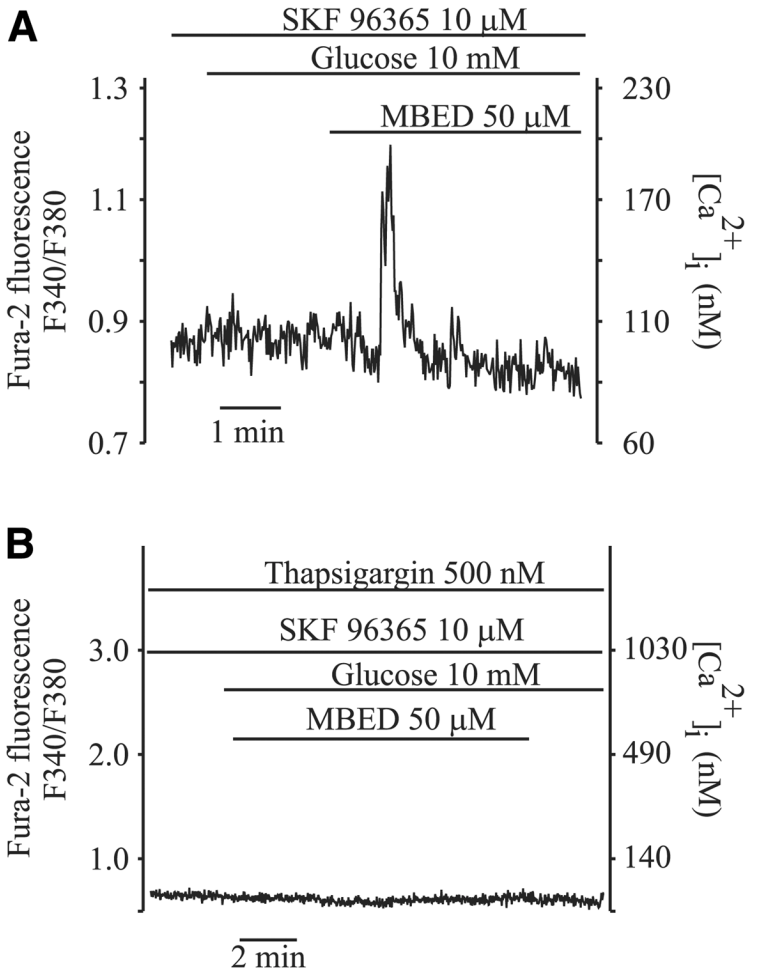

Figure 4. The plateau phase of $[Ca^{2+}]_i$ increase that follows activation of RY receptors was abolished by SKF 96365. ***A***) MBED (50 μM) was applied in the presence of SKF 96365 (10 μM). This resulted in a transient increase in $[Ca^{2+}]_i$. ***B***) The ER Ca^{2+} pool was depleted by thapsigargin treatment (500 nM for 45 min). SKF 96365 (10 μM) was present in the superfusate. The transient $[Ca^{2+}]_i$ increase induced by MBED as seen in (***A***) was now completely blocked. The traces are representatives of experiments repeated at least 3 times.

Fig. 5

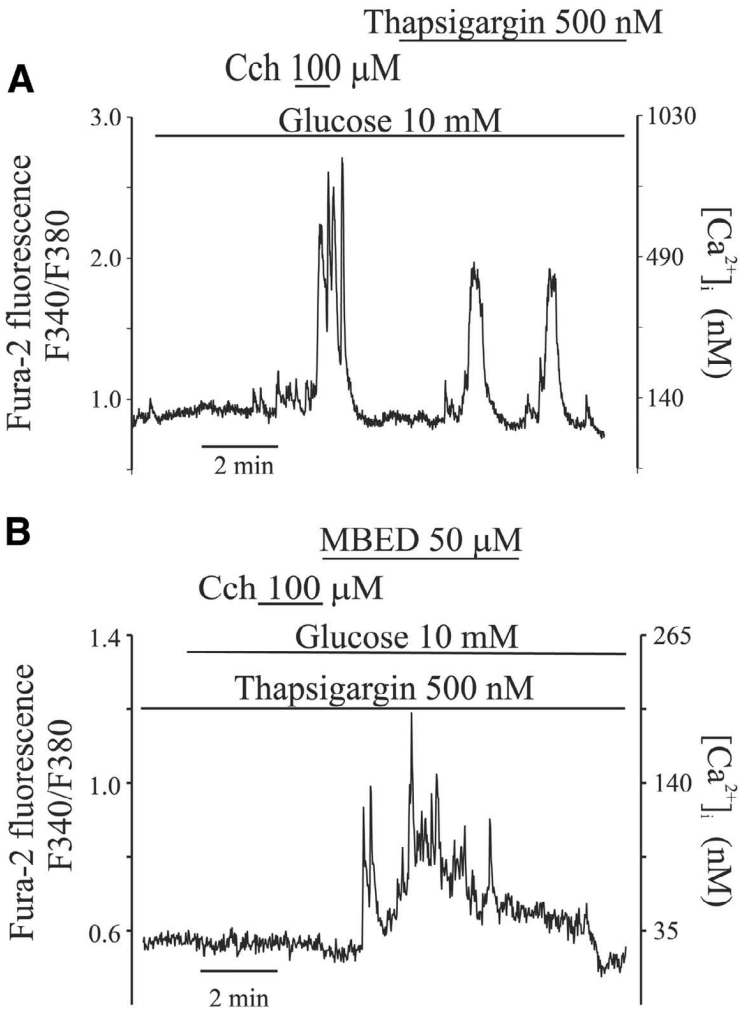

Figure 5. Activation of RY receptors caused Ca^{2+} influx even when the ER Ca^{2+} pools were depleted by inhibition of the SERCA. ***A***) Application of carbachol (100 μM) or thapsigargin (500 nM) released Ca^{2+} from ER Ca^{2+} stores. ***B***) Cells were treated by thapsigargin (500 nM) for 45 min. Such treatment depleted the ER Ca^{2+} pools as evidenced from the fact that carbachol (100 μM) failed to increase $[Ca^{2+}]_i$. Activation of RY receptors by MBED increased $[Ca^{2+}]_i$ to a plateau in the thapsigargin-treated cells. Such $[Ca^{2+}]_i$ increase was due to Ca^{2+} influx since it was blocked by SKF 96365 (see **Fig. 4*B***). Similar results were obtained in at least 3 independent experiments.

Fig. 6

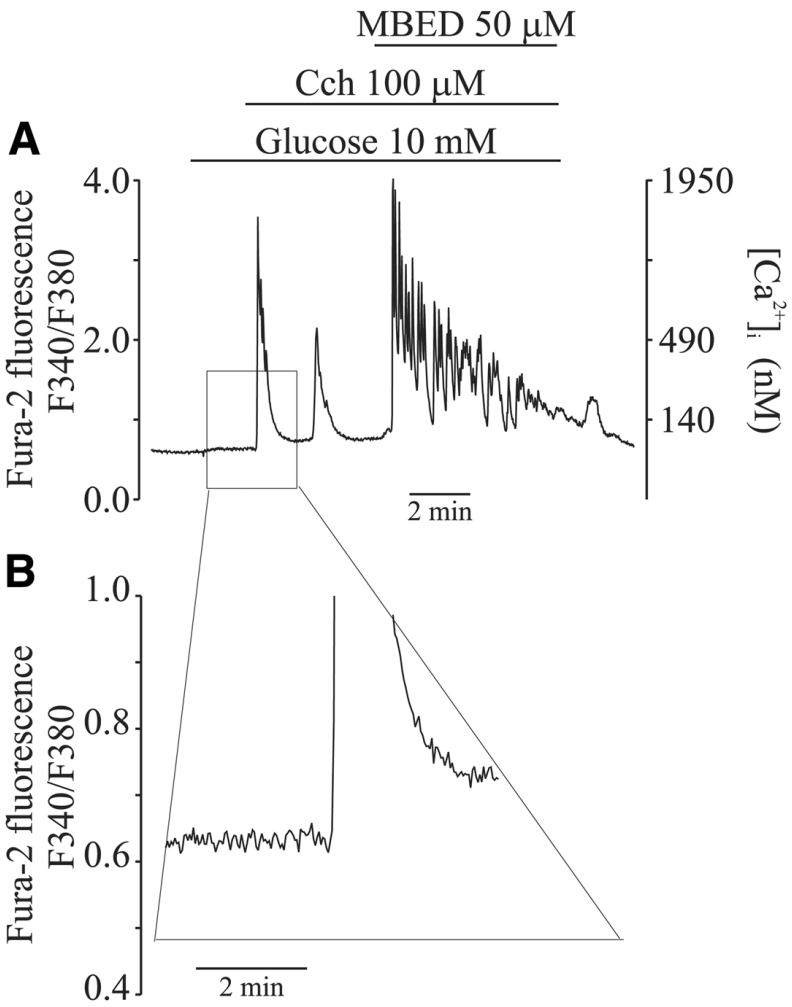

Figure 6. Effect of prior application of carbachol on $[Ca^{2+}]_i$-increase induced by RY receptor activation. ***A***) The cells were first stimulated by a high concentration of carbachol (100 μM), which resulted in two $[Ca^{2+}]_i$ transients. Carbachol caused rapid release of Ca^{2+} from the ER and a small $[Ca^{2+}]_i$ plateau representing capacitative Ca^{2+} entry shown on expanded scale in (***B***). When RY receptors were activated by MBED, in the continued presence of carbachol, there was a large increase of $[Ca^{2+}]_I$, followed by a plateau and $[Ca^{2+}]_i$ spikes superimposed on the plateau. The trace is representative of at least 3 different experiments.

Fig. 7

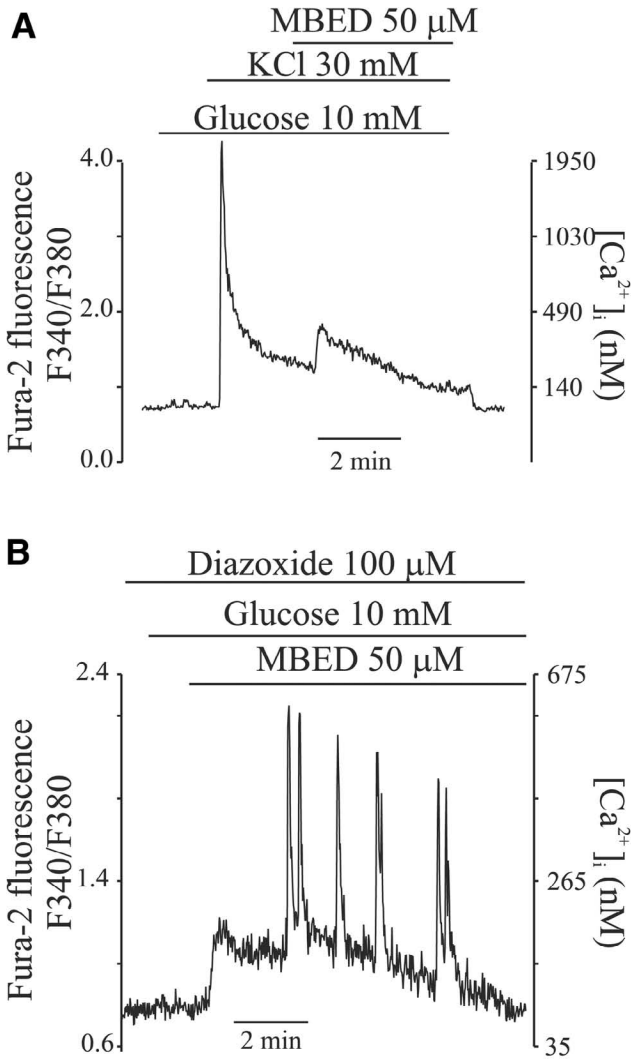

Figure 7. Effect of plasma membrane potential on Ca^{2+} influx induced by RY receptor activation. ***A)*** Cells were first depolarized by KCl (30 mM). Addition of MBED (50 μM) to the depolarized cell caused a transient increase in $[Ca^{2+}]_i$ without any effect on the plateau $[Ca^{2+}]_i$. ***B)*** Cells were first hyperpolarized by diazoxide (100 μM). Addition of MBED (50 μM) in the continued presence of diaxoxide caused an initial rapid rise of $[Ca^{2+}]_i$ followed by a plateau and $[Ca^{2+}]_i$ spikes superimposed on the plateau. Similar results were obtained in at least 3 independent experiments.

Fig. 8

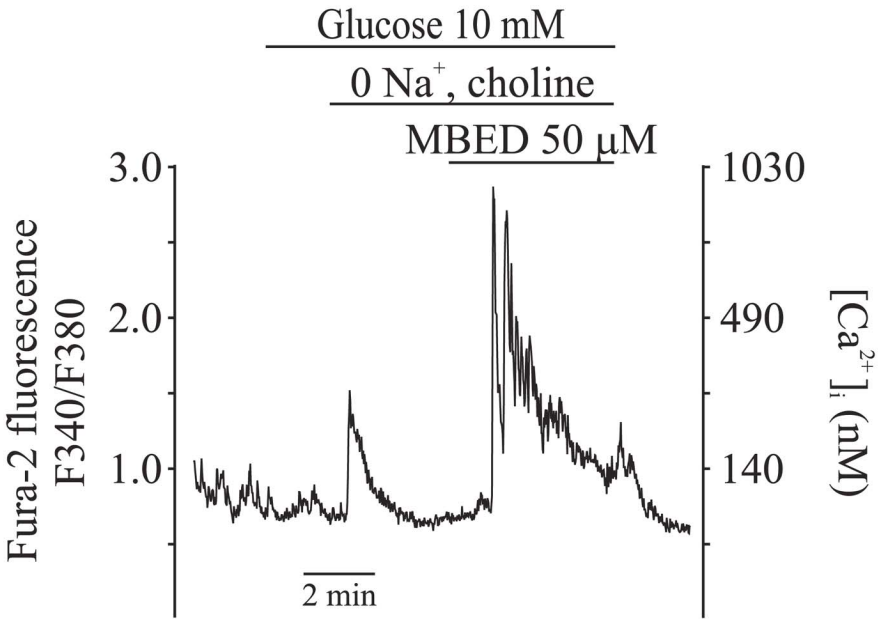

Figure 8. Effect of activation of RY receptors on $[Ca^{2+}]_i$ in Na^+-free extracellular medium. The cell was first perifused with the basal medium. At times indicated by the horizontal bar the solution was changed to one that contained choline chloride instead of NaCl. Choline chloride caused a transient increase of $[Ca^{2+}]_i$. Activation of RY receptor by MBED (50 µM) in the absence of extracellular Na^+ caused $[Ca^{2+}]_i$ changes that were similar to those observed when MBED was used in the presence of Na^+. The trace is representative of at least 3 different experiments.

Fig. 9

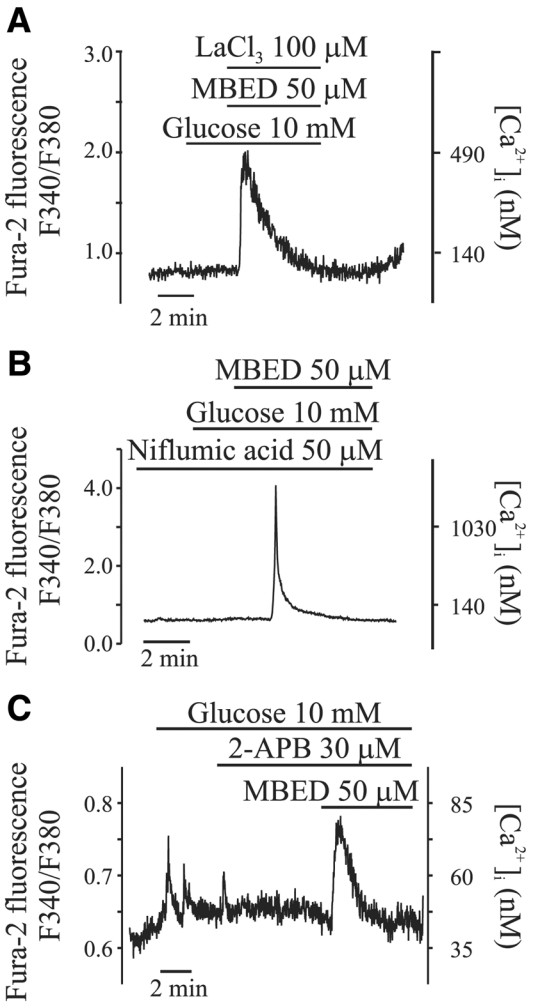

Figure 9. La^{3+}, niflumic acid and 2-APB inhibited the $[Ca^{2+}]_i$ plateau that followed activation of RY receptors. Activation of RY receptor by MBED (50 µM) in the continued presence of $LaCl_3$ (100 µM) (***A***) or niflumic acid (50 µM) (***B***) caused the initial rise of $[Ca^{2+}]_i$ but the plateau phase of $[Ca^{2+}]_i$ increase was inhibited. The traces are representative of experiments that has been repeated at least 3 times. Complete inhibition of the plateau phase of $[Ca^{2+}]_i$ by 2-APB (30 µM) (***C***) was seen in four out of nine experiments. In the remaining five experiments the plateau phase of $[Ca^{2+}]_i$ was partially inhibited.

Fig. 10

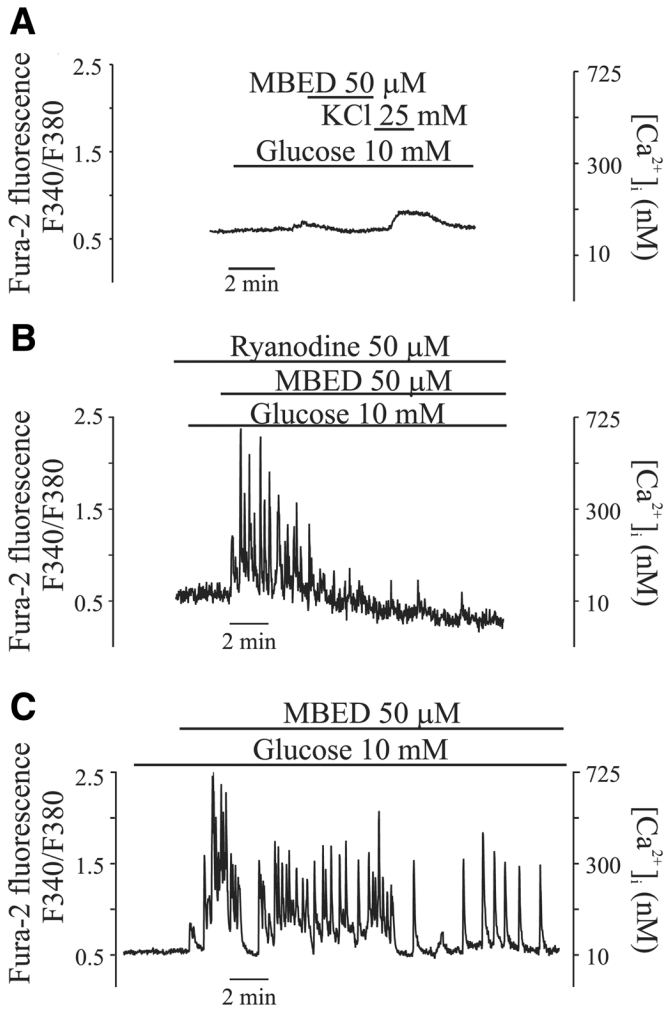

Figure 10. Effect of ryanodine on MBED-induced $[Ca^{2+}]_i$ changes. ***A*****)** Cells were pretreated with caffeine (10 mM), KCl (25 mM), and ryanodine (50 μM) for 45 min. Application of MBED (50 μM) to the treated cells failed to increase $[Ca^{2+}]_i$. ***B*****)** Acute application of ryanodine (50 μM) did not affect the initial rise of $[Ca^{2+}]_i$ that was triggered by MBED, but it inhibited the $[Ca^{2+}]_i$ spikes progressively in a use-dependent manner. The trace is representative of experiments repeated at least 3 times. ***C*****)** The control experiment, where ryanodine was not included.

Fig. 11

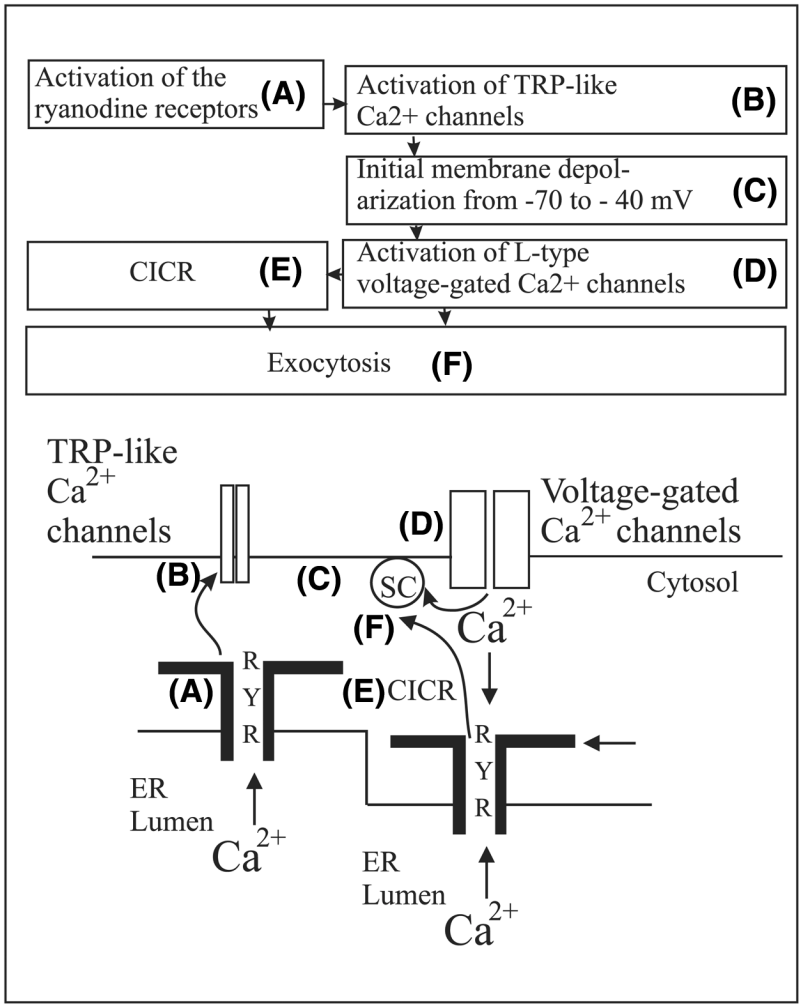

Figure 11. Schematic diagram of hypothesized involvement of RY receptor and TRP-like channels in Ca^{2+} entry and membrane depolarization in β-cells. The cartoon illustrates a sequence of events, whereby activation of RY receptors (***A***) leads to the activation of TRP-like channels (***B***), an initial membrane depolarization to approximately –40 mV (***C***), activation of the L-type voltage-gated Ca^{2+} channels (***D***), CICR (***E***) and exocytosis (***F***).

II

Molecular and Cellular Endocrinology 333 (2011) 8–19

Contents lists available at ScienceDirect

Molecular and Cellular Endocrinology

journal homepage: www.elsevier.com/locate/mce

ADP ribose is an endogenous ligand for the purinergic P2Y1 receptor

Amanda Jabin Gustafsson[a,*,1], Lucia Muraro[a,1], Carin Dahlberg[a,2], Marie Migaud[b,3], Olivier Chevallier[b,4], Hoa Nguyen Khanh[c], Kalaiselvan Krishnan[a], Nailin Li[d,5], Md. Shahidul Islam[a,e]

[a] Department of Clinical Science and Education, Karolinska Institutet, Research Centre, Stockholm South Hospital, 118 83 Stockholm, Sweden
[b] School of Chemistry and Chemical Engineering, Queen's University Belfast, BT9 5AG, Northern Ireland, United Kingdom
[c] Department of Molecular Medicine and Surgery, Karolinska Institutet, 171 76 Stockholm, Sweden
[d] Department of Medicine Solna, Clinical Pharmacology Unit, Karolinska University Hospital Institutet, 171 76 Stockholm, Sweden
[e] Uppsala University Hospital, AR division, Uppsala, Sweden

ARTICLE INFO

Article history:
Received 26 May 2010
Received in revised form 13 October 2010
Accepted 7 November 2010

Keywords:
Calcium
Cell signaling
ADPr
Purinergic receptors
TRPM2

ABSTRACT

The mechanism by which extracellular ADP ribose (ADPr) increases intracellular free Ca^{2+} concentration ($[Ca^{2+}]_i$) remains unknown. We measured $[Ca^{2+}]_i$ changes in fura-2 loaded rat insulinoma INS-1E cells, and in primary β-cells from rat and human. A phosphonate analogue of ADPr (PADPr) and 8-Bromo-ADPr (8Br-ADPr) were synthesized. ADPr increased $[Ca^{2+}]_i$ in the form of a peak followed by a plateau dependent on extracellular Ca^{2+}. NAD^+, cADPr, PADPr, 8Br-ADPr or breakdown products of ADPr did not increase $[Ca^{2+}]_i$. The ADPr-induced $[Ca^{2+}]_i$ increase was not affected by inhibitors of TRPM2, but was abolished by thapsigargin and inhibited when phospholipase C and IP_3 receptors were inhibited. MRS 2179 and MRS 2279, specific inhibitors of the purinergic receptor P2Y1, completely blocked the ADPr-induced $[Ca^{2+}]_i$ increase. ADPr increased $[Ca^{2+}]_i$ in transfected human astrocytoma cells (1321N1) that express human P2Y1 receptors, but not in untransfected astrocytoma cells. We conclude that ADPr is a specific agonist of P2Y1 receptors.

1. Introduction

Intracellular adenosine diphosphate ribose (ADPr) increases intracellular free calcium concentration ($[Ca^{2+}]_i$) by activating the type 2 melastatin-like transient receptor potential (TRPM2) channel in many cells, including insulin-secreting cells (Bari et al., 2009; Perraud et al., 2001; Togashi et al., 2006). It is, however, not widely known whether extracellular ADPr can increase $[Ca^{2+}]_i$ and in that case what could be the underlying mechanisms. ADPr is produced from NAD^+ by NAD glycohydrolases, and by hydrolysis of cyclic ADPr (cADPr) (Lee, 2006). Furthermore, ADPr can be produced from poly (ADPr) by poly (ADPr) glycohydrolase (Bonicalzi et al., 2005; Lin et al., 1997). CD38 and its homologues are enzymes with NADase, ADP-ribosyl cyclase and cADPr hydrolase activities (Lee, 2006). More than 99% of the products produced by the action of CD38 is ADPr (Berthelier et al., 1998; Howard et al., 1993; Lund et al., 1999). In the plasma membrane, CD38 is located with its catalytic site oriented extracellularly (De Flora et al., 2004; Lee, 1997). Thus, ADPr produced by CD38 and related enzymes is likely to be released extracellularly. In fact, in cortical astrocytes ADPr is released into the extracellular space (Hotta et al., 2000). NADase activity and production of ADPr have been reported in synaptosomes, giving rise to speculations that ADPr could be a neurotransmitter (Snell et al., 1984). Indeed, there is evidence that ADPr is released during nerve stimulation (Smyth et al., 2004). CD38 and related enzymes are present in the pancreatic β-cells too, and they are thought to play some roles in mediating insulin secretion (Kato et al., 1999). However, this role of CD38 in insulin secretion is generally attributed to the activation of ryanodine receptors by cADPr and NAADP (Lee et al., 1999). Whether extracellularly produced ADPr can signal by acting on cell surface receptors or whether it must enter into the cell, remains unclear. It has been postulated that ADPr can enter

Abbreviations: ACA, anthranilic acid; $[Ca^{2+}]_i$, intracellular free Ca^{2+} concentration; ER, endoplasmic reticulum; FBS, fetal bovine serum; F340/F380, fluorescence ratio; GPIX, conjugated anti CD42a; HBSS, Hanks' balanced salt solution; INS-1E, insulinoma cell line 1E; IP_3 receptor, inositol 1,4,5-triphosphate receptor; MRS 2179, 2′ deoxy-N^6-methyladenosine 3′,5′-bisphosphate; MRS 2279, 2-chloro N6-methyl-(N)-methanocarba-2′-deoxyadenosine-3′,5′-bisphosphate; OAADPr, O-acetyl adenosine diphosphate ribose; P2Y1, purinergic receptor type P2Y1; RIN-5F, a rat pancreatic β-cell line; TRPM2, type 2 melastatin-like transient receptor potential channel; 1321N1, human astrocytoma cells.

* Corresponding author. Tel.: +46 709 961 962; fax: +46 8 616 2933.
E-mail address: amajab@ki.se (A.J. Gustafsson).

[1] These authors contributed equally to the work.

[2] Present address: Karolinska Institutet, Department of medicine Solna, Clinical Allergy Research Unit, Karolinska University Hospital, Solna L2:04, 171 76 Stockholm, Sweden.

[3] Queen's University Belfast, Belfast BT9 5AG, Northern Ireland, United Kingdom.

[4] Institute of Agri-Food & Land Use, School of Biological Sciences, Queen's University Belfast, David Keir Building, Stranmillis Road, Belfast BT9 5AG, Northern Ireland, United Kingdom.

[5] Karolinska Institutet, Department of Medicine-Solna, Clinical Pharmacology Unit, 171 76 Stockholm, Sweden.

0303-7207/$ – see front matter © 2010 Elsevier Ireland Ltd. All rights reserved.
doi:10.1016/j.mce.2010.11.004

into the cells via CD38. However, the rate of transport is slow and this mechanism is not universal (Kim et al., 1993; Polzonetti et al., 2002). ADPr is degraded by ecto-nucleotide pyrophosphatases to AMP (Bernet et al., 1994; Dunn et al., 1999). Apyrase can also catalyse the conversion of ADPr to AMP that can be further metabolized to adenosine by 5′nucleotidase (Zhang et al., 2001; Zimmermann, 1992). Extracellular ADPr is thus a well-suited nucleotide for signaling by activating cell surface receptors.

A variety of biological effects of extracellularly applied ADPr have been described (Bortell et al., 2001; Breen et al., 2006; Broetto-Biazon et al., 2008; Hoyle and Edwards, 1992; Miller et al., 1999; Zhang et al., 2001). However, the signaling mechanisms that mediate the action of ADPr have remained largely unclear. Some actions of ADPr have been attributed to its breakdown product adenosine (Hoyle and Edwards, 1992). More recently, it has been shown that extracellular ADPr increases $[Ca^{2+}]_i$ in human monocytes and in rat insulinoma RIN-5F cells (Gerth et al., 2004; Ishii et al., 2006). RIN-5F cells are, however, not a suitable model of β-cells since these cells are highly undifferentiated (Trautmann and Wollheim, 1987). It is not known whether ADPr increases $[Ca^{2+}]_i$ in more differentiated insulinoma cell lines such as INS-1E cells, and in primary β-cells (Merglen et al., 2004). Thus, while there is considerable evidence for biological activity of extracellular ADPr, the cell-surface receptor that is activated by extracellular ADPr has not been identified. The aim of this study was to find out the effect of extracellular ADPr on $[Ca^{2+}]_i$ in differentiated insulin secreting cells and to elucidate the signaling mechanisms that alter $[Ca^{2+}]_i$ changes. We wanted to know the identity of the surface receptor with which ADPr interacts to increase $[Ca^{2+}]_i$. In this respect, the purinergic receptor P2Y1 was a possible candidate, since ADPr by virtue of its ADP moiety could interact with one of the purinergic receptors. The P2Y1 receptor is one of the purinergic receptors that is linked to the Ca^{2+} signaling system and has been extensively studied in insulin secreting cells. Our study shows that extracellular ADPr increases $[Ca^{2+}]_i$ specifically by activation of the purinergic P2Y1 receptors and in this respect ADPr shows stringent structural requirements for activation of the receptor.

2. Materials and methods

2.1. Chemicals

Fura-2 acetoxymethyl ester (AM), RPMI 1640, fetal bovine serum (FBS), penicillin, streptomycin and cell culture materials were from Invitrogen, Stockholm, Sweden. N-(p-amylcinnamoyl) anthranilic acid (ACA) and thapsigargin were from Calbiochem, Stockholm, Sweden. ELISA insulin kit was from Crystal Chem Inc., Santa Monica, CA, USA and collagenase type V was from Roche, Bromma, Sweden. An isopolar phosphonate analogue of ADPr (PADPr) was synthesized and purified as described before (Van derpoorten and Migaud, 2004). O-acetyl adenosine diphosphate ribose (OAADPr) was synthesized by J.M. Denu, Wisconsin (Borra et al., 2002) and 8-bromo (8Br)-ADPr was synthesized by T.F. Walseth, Minneapolis (Partida-Sanchez et al., 2007). All other chemicals were from Sigma–Aldrich, Stockholm, Sweden.

2.2. Preparation of ADP-free ADPr from β-NAD

The method for purification of ADP-free ADPr from β-NAD was based on anion exchange chromatography (Chevallier and Migaud, 2008; Oppenheimer, 1994). Commercially available β-NAD (52 mg, 78.4 μmol) was dissolved in mQ water (10 ml). The pH of the resulting solution was adjusted to 9 by addition of a 0.2 M solution of sodium hydroxide (7 ml) and the reaction mixture was stirred at room temperature for 4 days. The pH of the reaction solution was then adjusted to 7 by addition of a 0.1 M solution of hydrochloric acid (10 ml) and the solution was freeze-dried overnight. The white fluffy residue obtained was dissolved with mQ water (1 ml) and was purified using SAX anion exchange pre-packed column (Supelco DSC-SAX 6 ml/1 g) that was eluted first with mQ water (10 ml), then with an ammonium formate buffer (10 mM, pH 4.5, 10 ml), and finally with an ammonium formate buffer (20 mM, pH 3.5, 15 ml). The fractions containing ADPr were identified by HPLC using anion exchange chromatography (SAX column, 200 mm × 4.5 mm; phosphate buffer, KH_2PO_4 50 mM, pH 3.5, 5% MeOH; 1 ml/min; retention time = 11.4 min) and were pooled together. The combined fractions were freeze-dried to obtain ADPr as a fluffy powder (24.6 mmol, yield: 32% quantified by UV).

2.3. Cell culture

INS-1E cells were provided by C.B. Wollheim and P. Maechler, Geneva. A highly differentiated rat insulinoma cell line (S5) was subcloned from the INS-1E cells. The cells were cultured in RPMI-1640 medium supplemented with fetal bovine serum (2.5%, v/v), penicillin (50 IU/ml), streptomycin (50 μg/ml), 2-mercaptoethanol (500 μM), HEPES (10 mM) and sodium pyruvate (1 mM). The cells were cultured in a humidified incubator with 5% CO_2 at 37 °C. The medium was changed every other day and the cells were mildly trypsinized and split once weekly.

2.4. Preparation of β-cells from rat

The use of rat cells was approved by local ethics committee. Male Wistar rats were killed by decapitation after anaesthesia with CO_2. Collagenase A in Hanks' solution (9 mg/10 ml) was injected into the pancreas through the pancreatic duct. The gland was removed, incubated for 24 min at 37 °C, washed with Hanks' solution and islets were collected after separation on Histopaque gradient. The islets were dispersed by trypsin digestion and the cells were plated on glass coverslips. To exclude α-cells and δ-cells, only large cells, which are likely to be β-cells, were used for measurement of $[Ca^{2+}]_i$.

2.5. Preparation of human islets

The use of human islets for experiments was approved by local ethics committee. Human islets were obtained from Geneva University Hospital, Cell Isolation and Transplantation Center. Islets were isolated, cultured for 1–3 days and shipped overnight. Upon receipt, islets were checked for sterility and structural integrity. Approximately 2500 islets were placed in each centrifuge tube, centrifuged at 1300 rpm for 2 min at 18–20 °C and washed with HBSS 3 times. The islets were trypsinized (0.025% trypsin–EDTA, diluted with HBSS without Ca^{2+} and Mg^{2+}) and triturated with a sterile transfer pipette. RPMI 1640 medium supplemented as described above, and with 10% FBS, was added. Cells were centrifuged at 1500 rpm for 5 min at 4 °C. The medium was removed and cells were resuspended in new medium. The cells were plated on glass coverslips and incubated for 1 h to allow cell attachment. 2 ml of medium was added to each Petridish and the cells were incubated overnight before use.

2.6. Preparation of human astrocytoma cells stably expressing P2Y1

1321N1 human astrocytoma cells that stably overexpress recombinant human P2Y1, and wild type (WT) astrocytoma cells that do not express any P2Y1 were used. The 1321N1 astrocytoma cells that stably overexpress human P2Y1 receptor were originally developed by Prof. K. Harden (Schachter et al., 1996). The cells were stored at the Department of pharmacology at Karolinska Institutet and were, together with the WT astrocytoma cells, a gift from B.B. Fredholm, Stockholm. The cells were cultured in Dulbecco's Modified Eagle's Medium (DMEM) supplemented with FBS (5%, v/v), l-glutamine (2 mM), penicillin (100 IU/ml) and streptomycin (100 μg/ml). The cells were incubated in DMEM for 4 h to allow attachment of cells to bottom surface of a flask. The medium was changed and cells were cultured in DMEM for 5 days. When cells confluenced, they were trypsinized, plated on glass coverslips, and cultured for 3 days prior to experiments.

2.7. Measurement of $[Ca^{2+}]_i$ by microfluorometry

The cells were incubated for 35 min at 37 °C in RPMI-1640 medium supplemented with bovine serum albumin (0.1%) and fura-2 AM (1 μM). To allow de-esterification of the loaded dye, the cells were incubated for another 10 min in modified Krebs–Ringer bicarbonate–HEPES buffer (KRBH) containing (in mM): 140 NaCl, 3.6 KCl, 0.5 NaH_2PO_4, 0.5 $MgSO_4$, 1.5 $CaCl_2$, 10 HEPES, 3 glucose and 0.1% bovine serum albumin (pH 7.4). In some experiments nominally Ca^{2+} free medium was used. This medium was made by omission of Ca^{2+} and addition of EGTA (0.5 mM). A single coverslip was mounted as the exchangeable bottom of an open perfusion chamber on the stage of an inverted epifluorescence microscope (Olympus CK 40). Fluids were perfused through the chamber by a peristaltic pump and the temperature in the chamber was controlled by a temperature controller (Warner TC-344B) to maintain a temperature of 37 °C. The microscope was connected with a fluorescence system (PhotoMed M-39/2000 RatioMaster) for dual wavelength excitation fluorometry. The excitation wavelengths generated by a monochromator (PhotoMed DeltaRam) were directed to the cell by a dichroic mirror. Emitted light selected by a 510 nm filter was monitored by a photomultiplier tube detector. The excitation wavelengths were alternated to obtain one ratio per second. The emissions at the excitation wavelength of 340 nm ($F340$) and that of 380 nm ($F380$) were used to calculate the fluorescence ratio ($F340/F380$). Differentiated INS-1E cells were chosen on the basis on their size, shape and appearance during direct inspection under microscope. Such cells look like primary β-cells and constitute only about 10% of INS-1E cells in the microscopy field. Single cells were optically isolated and studied through a 40× 1.3 NA oil immersion objective (40× UV APO). Before calculation of $[Ca^{2+}]_i$, the background fluorescence was subtracted from the traces. $[Ca^{2+}]_i$ was calculated from $F340/F380$ according to Grynkiewicz et al. (1985). R_{max} and R_{min} were determined by using external standards containing

fura-2 free acid and sucrose (2 M) (Poenie, 1990). The K_d for Ca^{2+}-fura-2 was taken as 225 nM.

2.8. Measurement of insulin secretion

The use of islets from mice was approved by local ethics committee. Islets from mice pancreas were isolated following the procedure described before (Kelly et al., 2003). The islets were incubated for 24 h to recover from the isolation procedure, and then treated with trypsin 0.25% for 8 min to obtain single cells. Total separation of cells from islets was verified microscopically, and the cells were then seeded onto 6 well plates. There were 2×10^5 cells in each well. The cells were incubated for 24 h in 11 mM glucose for attachment. Before performing glucose stimulation, the cells were gently washed 3 times with KRBH containing 3.3 mM glucose and preincubated in 3.3 mM glucose for 15 min. The wells were divided into 4 groups and incubated for 1 h with different treatments. Group 1 was incubated with 3.3 mM glucose, group 2 with 16.7 mM glucose, group 3 with 3.3 mM glucose and 80 μM ADPr, and group 4 was incubated with 16.7 mM glucose and 80 μM ADPr. Samples were collected to measure insulin concentration using ELISA kit.

2.9. Whole-blood flow cytometric assays for measuring activation of platelets by ADPr

Blood samples from three individuals between the ages of 24 and 42 were tested, and the experiments were approved by local ethics committee. Venous blood was collected by clean venepuncture without stasis using a vacutainer containing 1/10 volume of 3.8% sodium citrate. Whole blood samples were processed for flow cytometric sample labelling within 5 min of blood collection. We used whole-blood flow cytometry to evaluate the effect of ADPr on platelet shape change, aggregability (fibrinogen binding), and secretion (P-selectin expression). Whole-blood flow cytometric assays of platelet P-selectin expression and fibrinogen binding have been described previously (Li et al., 1999). Platelets were gated by their characteristic light scattering signals, and the gated cells were confirmed with fluorescein isothiocyanate (FITC) conjugated anti-CD42a (GPIX) monoclonal antibody (MAb) Beb 1 (Becton Dickinson, San Jose, CA, USA). To monitor platelet shape change, an inner spindle shape gate was inserted into the centre of the total platelet gate. Increased proportion of platelets within the inner gate reflected platelet shape change. Platelet P-selectin expression was determined by PE-CD62P MAb AC1.2 (Becton Dickinson), while platelet fibrinogen binding was monitored by FITC-conjugated polyclonal rabbit anti-human fibrinogen antibody (DAKO, Glostrup, Denmark). Platelet shape change was expressed as percentage calculated according to the following formula: % of platelet shape change = 100 × ((platelet counts within the inner gate after stimulation − platelet counts within the inner gate before stimulation)/(platelet counts within the inner gate before stimulation)).

2.10. Statistical analysis

Data were expressed as means ± SEM. Comparison between two groups was made by Student's unpaired *t*-test, and within groups by paired *t*-test. *P*-value was considered as significant when <0.05. Graph Pad was used for making the concentration–response curve.

3. Results

3.1. Extracellular ADPr increased $[Ca^{2+}]_i$ in insulin secreting cells

Extracellular ADPr increased $[Ca^{2+}]_i$ in INS-1E cells in a dose-dependent manner (Fig. 1A and B). The ADPr-induced $[Ca^{2+}]_i$ increase was biphasic. The first phase consisted of a rapid rise of $[Ca^{2+}]_i$ to a peak and the second phase consisted of an elevated plateau (Fig. 1A). After washout of ADPr, $[Ca^{2+}]_i$ returned to the baseline. The minimal effective concentration of ADPr was 2.5 μM, but at this concentration $[Ca^{2+}]_i$ increase was observed in only 80% of the cells examined ($n = 5$). 10 μM ADPr increased $[Ca^{2+}]_i$ in all the cells examined ($n > 12$). Maximal effect was obtained by 80 μM ADPr and the EC_{50} was ∼30 μM (Fig. 1B). Repeated applications of ADPr elicited repeated $[Ca^{2+}]_i$ responses of similar pattern and amplitude. Commercially available ADPr is 95–98% pure. To exclude the possibility that the ADPr-induced $[Ca^{2+}]_i$ increase could be due to eventual contamination by ADP, we synthesized ADP-free ADPr and found that it also increased $[Ca^{2+}]_i$ in a pattern similar to that obtained with commercially available ADPr. We also tested whether the $[Ca^{2+}]_i$ increase was due to any of the precursors of ADPr, namely NAD^+ and cADPr. Extracellular NAD^+ (30 μM) did neither increase $[Ca^{2+}]_i$ nor did it alter the amplitude of the ADPr-induced $[Ca^{2+}]_i$ increase. The ADPr-induced $[Ca^{2+}]_i$ increase was in these experiments 79 ± 50 nM without NAD^+ and 152 ± 86 nM with NAD^+ ($p = 0.24$, $n = 10$) (Fig. 1C). Extracellular cADPr also did not increase $[Ca^{2+}]_i$ (Fig. 1D). ADPr increased $[Ca^{2+}]_i$ also in primary rat β-cells (Fig. 1E) and in human β-cells (Fig. 1F). In contrast, ADPr did not increase $[Ca^{2+}]_i$ in undifferentiated PC12 cells (data not shown).

3.2. Effects of repeated exposure to ADP and the effect of ADP on ADPr-induced $[Ca^{2+}]_i$ increase

ADP is the known agonist for P2Y1 receptors and is known to desensitize the receptor. Therefore, we tested the effect of repeated application of ADP and the effect of prior exposure to ADP on subsequent ADPr-induced $[Ca^{2+}]_i$ increase. ADP (5 μM) induced a $[Ca^{2+}]_i$ increase, and after prolonged washout when the $[Ca^{2+}]_i$ had returned to the baseline, ADP was added for a second time. This time also, there was a $[Ca^{2+}]_i$ increase similar to that obtained by the first exposure to ADP, indicating lack of desensitization of the receptor (Fig. 2A). The same results were seen with ADPr (Fig. 3B). In Fig. 2B, ADP was applied for a second time shortly after the $[Ca^{2+}]_i$ increase by the first application of ADP returned to the baseline. Under these conditions the $[Ca^{2+}]_i$ response to the second application of ADP was reduced, suggesting desensitization of the receptor involved. Under similar conditions, application of ADPr shortly after application of ADP elicited only a small $[Ca^{2+}]_i$ increase (Fig. 2C).

3.3. Effects of metabolites and analogues of ADPr on $[Ca^{2+}]_i$

To test whether the effect of ADPr on $[Ca^{2+}]_i$ could be mediated by breakdown products of ADPr such as 5′AMP, adenosine and D-ribose 5-phosphate, we examined the effect of these metabolites on $[Ca^{2+}]_i$. 5′AMP (10 μM), adenosine (1–10 μM) and D-ribose 5-phosphate (10 μM) did not increase $[Ca^{2+}]_i$ in these cells (data not shown). OAADPr is a new metabolite of NAD^+ structurally related to ADPr (Borra et al., 2002). OAADPr (10 μM) also increased $[Ca^{2+}]_i$ in a biphasic manner (Fig. 3A). Similar pattern of $[Ca^{2+}]_i$ increase was observed also with the structurally related analogue ADP glucose (data not shown). Since ADPr is known to break down in minutes in aqueous solutions, we synthesized a stable phosphonate acetylene analogue of ADPr (PADPr) (Fig. 3E). This analogue of ADPr is resistant to non-enzymatic cleavage under aqueous conditions (Van derpoorten and Migaud, 2004). In contrast to ADPr, PADPr (up to 100 μM) did not increase $[Ca^{2+}]_i$. We then tested whether PADPr could be an inhibitor of the receptor for ADPr. Another reason for testing the effect of PADPr in this manner was that it is thought to be an inhibitor of ADPr pyrophosphatases. We found that PADPr did not alter the ADPr-induced $[Ca^{2+}]_i$ increase (Fig. 3B). In the absence of PADPr, the peak $[Ca^{2+}]_i$ increase by ADPr was 108 ± 43 nM and in the presence of PADPr, the peak $[Ca^{2+}]_i$ increase was 181 ± 73 nM ($p = 0.15$, $n = 3$). Brominated ADPr (8Br-ADPr) (30 μM) did not increase $[Ca^{2+}]_i$ (Fig. 3C).

3.4. ADPr released Ca^{2+} from the endoplasmic reticulum (ER) and induced Ca^{2+} entry through the plasma membrane

To test whether the increase of $[Ca^{2+}]_i$ was due to release of Ca^{2+} from the intracellular stores, the cells were stimulated with ADPr in nominally Ca^{2+} free medium. ADPr increased $[Ca^{2+}]_i$ even under these conditions. However, in Ca^{2+} free medium, the plateau phase of the $[Ca^{2+}]_i$ increase was absent (Fig. 4A cf. Fig. 1A), indicating that the plateau phase was due to Ca^{2+} entry from outside the cell. Nimodipine, a blocker of L-type voltage gated Ca^{2+} channels, did not alter the ADPr-induced $[Ca^{2+}]_i$ changes (data not shown). To examine whether ADPr released Ca^{2+} from the ER, the ER Ca^{2+} pool was depleted by thapsigargin (125 or 250 nM for 35 min). In thapsigargin-treated cells ADPr (100 μM) did not

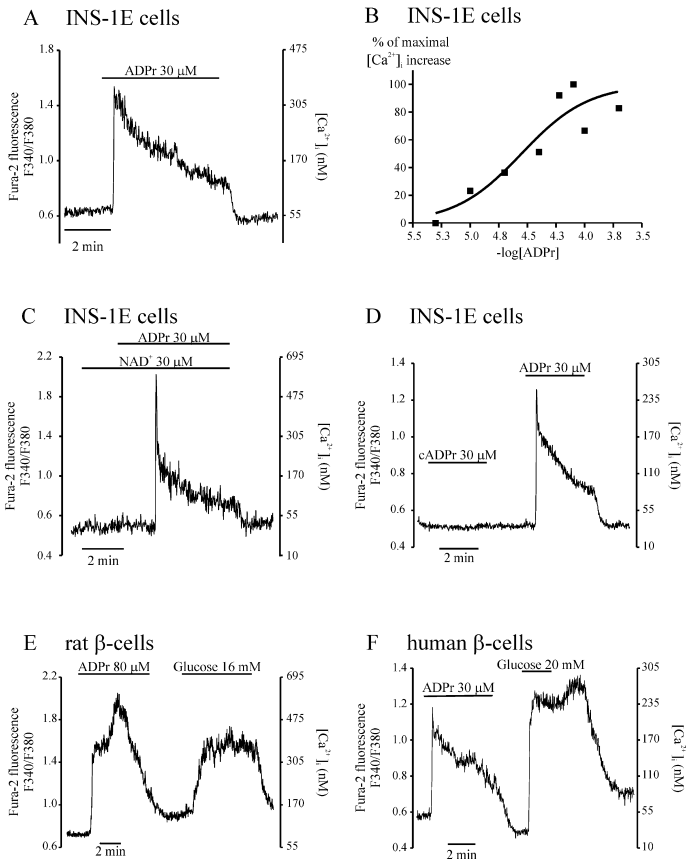

Fig. 1. Effect of extracellular ADPr, NAD+, and cADPr on $[Ca^{2+}]_i$ in INS-1E cells. $[Ca^{2+}]_i$ was measured by microfluorometry in cells loaded with fura-2. (A) ADPr (30 μM) increased $[Ca^{2+}]_i$ in INS-1E cells. The trace is representative of at least thirty experiments showing similar results. (B) Concentration–response curve of $[Ca^{2+}]_i$ increase by ADPr. The squares represent means of $[Ca^{2+}]_i$ increase obtained by different concentrations of ADPr, in percentage of maximal $[Ca^{2+}]_i$ increase. At least three experiments were done for each concentration of ADPr. (C) NAD^+ (10–30 μM) did not increase $[Ca^{2+}]_i$ or alter the amplitude of ADPr-induced $[Ca^{2+}]_i$ increase. The trace is representative of ten experiments. (D) Extracellular cyclic ADPr (30 μM) also did not increase $[Ca^{2+}]_i$. The trace is representative of five experiments. (E) ADPr (80 μM) increased $[Ca^{2+}]_i$ in primary β-cells from Wistar rat. Glucose (16 mM), which was used as a control, increased $[Ca^{2+}]_i$. The trace is representative of four experiments. (F) ADPr also induced $[Ca^{2+}]_i$ increase in human β-cells. Glucose (20 mM), which was used as a control, increased $[Ca^{2+}]_i$. The trace is representative of eight experiments.

increase $[Ca^{2+}]_i$ as it did in the untreated cells (Fig. 4B cf. Fig. 4C). Subsequent application of carbachol (Cch) (10 μM) to thapsigargin-treated cells also failed to increase $[Ca^{2+}]_i$, indicating that the ER Ca^{2+} pool was completely depleted of Ca^{2+} (Fig. 4B cf. Fig. 4C). However, as expected, depolarization of the membrane potential by KCl (25 mM) increased $[Ca^{2+}]_i$.

3.5. ADPr did not increase $[Ca^{2+}]_i$ through activation of TRPM2

The only known Ca^{2+}-permeable channel that is activated by ADPr is TRPM2 (Eisfeld and Luckhoff, 2007). We tested whether the $[Ca^{2+}]_i$ response to ADPr could be blocked by inhibitors of TRPM2 channels such as flufenamic acid and niflumic acid (Hill et al., 2004). These substances did not alter the Ca^{2+} response to ADPr (data not shown). Another more specific and more potent inhibitor of TRPM2 channels is ACA (Bari et al., 2009; Kraft et al., 2006). Even this inhibitor did not inhibit the ADPr-induced $[Ca^{2+}]_i$ increase (Fig. 5A cf. Fig. 5B). The peak $[Ca^{2+}]_i$ increase in the control group was 190 ± 20 nM and that in the presence of ACA was 312 ± 78 nM ($p = 0.21$, $n = 6$).

3.6. ADPr induced $[Ca^{2+}]_i$ increase by activation of P2Y1 receptors

2′ Deoxy-N^6-methyladenosine 3′,5′-bisphosphate (MRS 2179) and 2-chloro N^6-methyl-(N)-methanocarba-2′-deoxyadenosine-3′,5′-bisphosphate (MRS 2279) are two selective inhibitors of the purinergic receptor subtype Y1 (Boyer et al., 2002; Moro et al., 1998). To find out whether P2Y1 receptors could be involved in ADPr-induced $[Ca^{2+}]_i$ increase, MRS 2179 and MRS 2279 were tested. MRS 2179 (1 and 10 μM) completely blocked the ADPr-

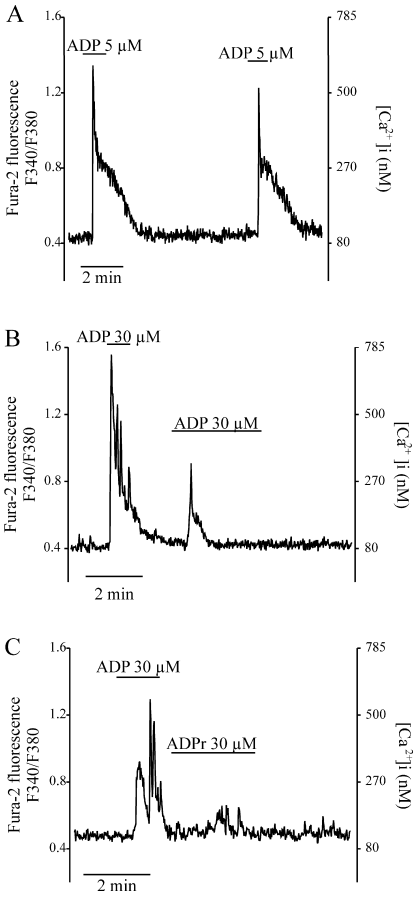

Fig. 2. Effect of repeated application of ADP and ADPr in INS-1E cells.Experiments were done as described in legend to Fig. 1. (A) $[Ca^{2+}]_i$ was increased by ADP (5 μM). After prolonged washout and new application of ADP, there was a second, almost similar $[Ca^{2+}]_i$ response. (B) Repeated application of ADP shortly after a first application of ADP elicited a much smaller $[Ca^{2+}]_i$ increase. (C) Prior application of ADP decreased the ADPr-induced $[Ca^{2+}]_i$ increase. The figures are representatives of at least three experiments each.

induced $[Ca^{2+}]_i$ increase. MRS 2279 (10 μM), which is an even more specific P2Y1 receptor inhibitor, also blocked the ADPr-induced $[Ca^{2+}]_i$ increase completely (Fig. 6A, B and D). In control experiments without the antagonists, ADPr induced $[Ca^{2+}]_i$ increase as usual (Fig. 6C and E).

3.7. Activation of phospholipase C is involved in ADPr-induced $[Ca^{2+}]_i$ increase

To examine whether activation of phospholipase C (PLC) was involved in ADPr-induced $[Ca^{2+}]_i$ increase, we used U73122, an inhibitor of PLC. Lower concentration of U73122 (4 μM) reduced the $[Ca^{2+}]_i$ response by 40%, but the difference was not statistically significant. Peak $[Ca^{2+}]_i$ increase in the control group was 200 ± 47 nM and that in the presence of U73122 (4 μM) was 94 ± 37 nM ($p < 0.1$, $n = 16$). When the cells were incubated with a higher concentration of U73122 (10 μM) for 10–45 min, U73122 inhibited the ADPr-induced $[Ca^{2+}]_i$ increase completely (Fig. 7).

3.8. Ca^{2+} released by ADPr was through the IP_3 receptor

We next investigated which intracellular Ca^{2+} channel was involved in ADPr-induced $[Ca^{2+}]_i$ release. To test whether the IP_3 receptor was involved, we used 2-aminoethoxydiphenyl borate (2-APB) (50 μM), which is a known blocker of IP_3 receptors (Maruyama et al., 1997; Peppiatt et al., 2003). On the average, 2-APB inhibited the ADPr-induced Ca^{2+} release by 82%. Peak $[Ca^{2+}]_i$ increase in the control group was 307 ± 46 nM (Fig. 8A) and that in the presence of 2-APB was 56 ± 27 nM ($p < 0.01$, $n = 6$) (Fig. 8B). 2-APB also reduced the $[Ca^{2+}]_i$ response induced by Cch (100 μM) by 34%, but the difference was not statistically significant. In the controls, the peak $[Ca^{2+}]_i$ increase obtained by Cch was 394 ± 144 nM and that in the presence of 2-APB was 262 ± 97 nM ($p = 0.49$, $n = 6$) (Fig. 8A cf. Fig. 8B).

3.9. ADPr increased $[Ca^{2+}]_i$ in human astrocytoma cells stably expressing P2Y1 receptors

To make sure that ADPr indeed could activate P2Y1 receptors, we performed experiments with 1321N1 human astrocytoma cells that stably overexpress recombinant human P2Y1 receptors, and used WT astrocytoma cells that do not express P2Y1 receptors as controls (Schachter et al., 1996). ADPr increased $[Ca^{2+}]_i$ in all the cells that expressed the recombinant human P2Y1 receptors. ADPr did not induce any $[Ca^{2+}]_i$ increase in WT astrocytoma cells (Fig. 9A cf. Fig. 9B).

3.10. Effect of extracellular ADPr on insulin secretion

We tested the effect of ADPr on insulin secretion from primary mouse β-cells. ADPr (80 μM) was added to cells in the presence of 3.3 mM or 16.7 mM glucose. The insulin secretion induced by ADPr in the presence of 3.3 mM glucose was 22.0 ± 0.9 ng/ml. In the control experiments with 3.3 mM glucose alone, the insulin secretion was 21.9 ± 0.6 ng/ml ($p = 0.94$, $n = 6$). In the presence of 16.7 mM glucose, ADPr-induced insulin secretion was 59.0 ± 1.8 ng/ml. In control experiments with 16.7 mM glucose alone, the insulin secretion was 70.6 ± 21.7 ng/ml. Thus, there was no significant increase of insulin secretion by ADPr ($p = 0.62$, $n = 6$).

3.11. Effect of ADPr on platelet activation

Since there was no alteration in insulin secretion by ADPr, we tested the biological function of ADPr in another cellular system, namely the platelets, where the role of P2Y1 in mediating platelet activation is well known. ADPr (100 μM) induced platelet shape change, by a maximum of 52.1 ± 10.9% (Fig. 10). In control experiments, ADP (10 μM) induced platelet shape changes in 46.2 ± 15.4% of cells. We have also measured other aspects of platelet activation, namely platelet fibrogen binding and P-selectin expression. ADPr dose-dependently enhanced platelet fibrinogen binding. The maximal effect was seen at 100 μM that increased platelet fibrinogen binding from 3.9 ± 1.7% in unstimulated cells to 18.1 ± 5.0%. ADP (10 μM), which activates both P2Y1 and P2Y12 receptors, induced more marked increase of platelet fibrogen binding (to 55.3 ± 15.4%). ADPr (100 μM) increased platelet P-selectin expression from 1.9 ± 0.3% in unstimulated samples to 10.9 ± 0.5%. In contrast, ADP (10 μM) markedly increased P-selectin expression to 59.2 ± 8.7% (data not shown).

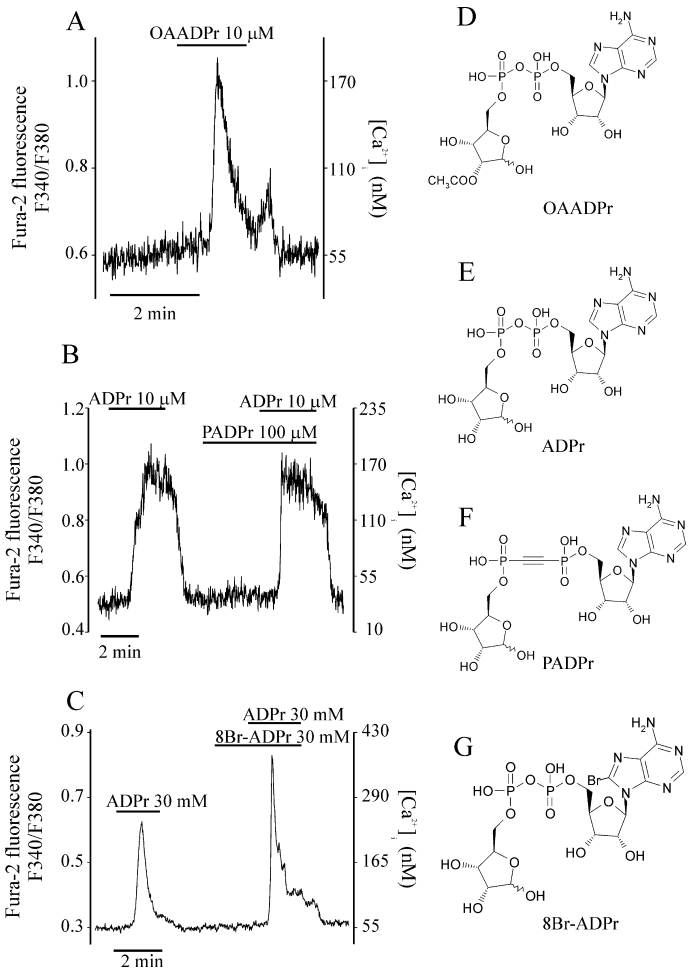

Fig. 3. Effects of OAADPr, PADPr and 8Br-ADPr on $[Ca^{2+}]_i$ in INS-1E cells. Experiments were done as described in the legend to Fig. 1. (A) OAADPr (10 μM) increased $[Ca^{2+}]_i$ in INS-1E cells. (B) PADPr (100 μM) did not increase $[Ca^{2+}]_i$ by itself and did not alter the ADPr-induced $[Ca^{2+}]_i$ increase. (C) 8Br-ADPr (30 μM) did not increase $[Ca^{2+}]_i$. Each trace is representative of at least three experiments. (D) Molecular structure of OAADPr. (E) Molecular structure of ADPr. (F) Molecular structure of PADPr. (G) Molecular structure of 8Br-ADPr.

4. Discussion

The present study was undertaken to find out the effect of extracellular ADPr on $[Ca^{2+}]_i$ in pancreatic β-cells and to identify the cell surface receptor that could be involved in mediating the $[Ca^{2+}]_i$ response. In our study, extracellular ADPr increased $[Ca^{2+}]_i$ in a concentration-dependent manner with an EC_{50} of ~30 μM. $[Ca^{2+}]_i$ increase was observed in INS-1E cells, as well as in primary rat and human β-cells. Initially, we suspected that commercially available ADPr that we used could contain ADP as contaminant, which could elicit the observed $[Ca^{2+}]_i$ increase. We, therefore, synthesized highly purified ADPr that was free from ADP and NAD^+. Still, we observed similar $[Ca^{2+}]_i$ increase by ADPr. The concentration of ADPr required for inducing $[Ca^{2+}]_i$ increase in our experiments is relatively high compared to the concentration of ADP that induces $[Ca^{2+}]_i$ increase. However, such concentrations of ADPr have been used in the past to demonstrate biological effects of ADPr in different tissues (Bortell et al., 2001; Broetto-Biazon et al., 2008; Hoyle and Edwards, 1992; Miller et al., 1999; Zhang et al., 2001). It is possible that the concentration of ADPr at its local sites of actions is in the micromolar range.

The $[Ca^{2+}]_i$ increase elicited by ADPr was biphasic and consisted of an initial transient peak followed by a plateau. The initial $[Ca^{2+}]_i$ rise was due to release of Ca^{2+} from the ER, as evidenced from

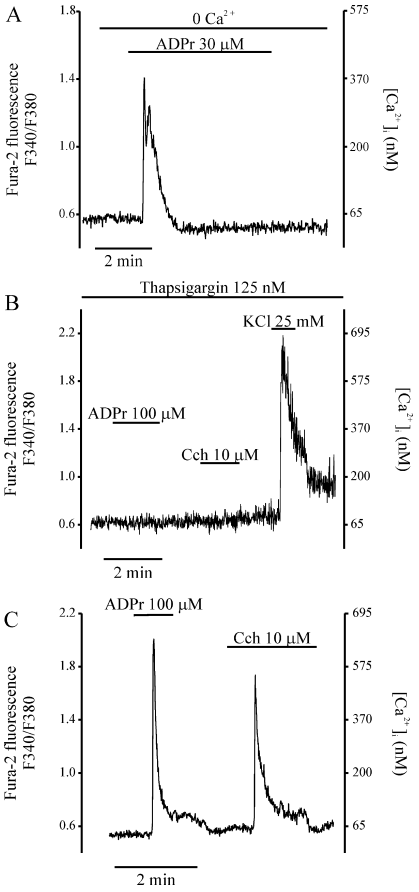

Fig. 4. ADPr-induced $[Ca^{2+}]_i$ increase was due to Ca^{2+}-release from the ER. (A) ADPr increased $[Ca^{2+}]_i$ in INS-1E cells even when Ca^{2+} was omitted from the extracellular medium. Under these conditions the plateau phase of $[Ca^{2+}]_i$ increase was absent (cf. Fig. 1A). The trace represents six experiments with similar results. (B) When β-cells were treated with thapsigargin (125 or 250 nM) for 35 min, there was no $[Ca^{2+}]_i$ increase by ADPr (100 μM) or Cch (10 μM). KCl (25 mM), which was used as a control, increased $[Ca^{2+}]_i$. The trace is representative for eight experiments with similar results. (C) Control experiments for Fig. 3B where the cell was not treated with thapsigargin. Both ADPr (100 μM) and Cch (10 μM) caused large $[Ca^{2+}]_i$ increase. The trace is representative of at least ten experiments.

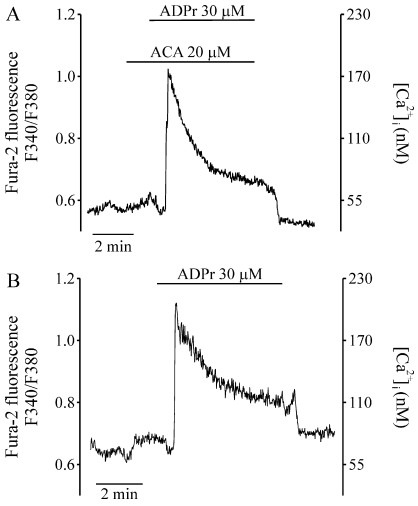

Fig. 5. ADPr did not increase Ca^{2+} by activating the TRPM2 channels. (A) N-(p-amylcinnamoyl) anthranilic acid, ACA (20 μM), a specific inhibitor of TRPM2 channels, did not alter the ADPr-induced $[Ca^{2+}]_i$ increase in INS-1E cells. (B) Control experiment with ADPr (30 μM). Each trace represents three experiments.

the fact that the $[Ca^{2+}]_i$ increase was abolished by thapsigargin, which depletes the ER Ca^{2+} pool. Furthermore, this $[Ca^{2+}]_i$ increase was abolished by U73122, which inhibits PLC, and by 2-APB, which inhibits the IP_3 receptor. The plateau phase of $[Ca^{2+}]_i$ induced by ADPr was abolished when Ca^{2+} was omitted from the extracellular medium, indicating that this phase was due to Ca^{2+} entry from outside the cell. Such biphasic $[Ca^{2+}]_i$ increase resembles the $[Ca^{2+}]_i$ changes upon activation of receptors coupled to PLC. The plateau phase was not inhibited by inhibitors of TRPM2 or of L-type voltage gated Ca^{2+} channels, indicating lack of involvement of these channels in mediating the Ca^{2+} entry. It is likely that the plateau phase is due to Ca^{2+} entry through store-operated channels in the plasma membrane.

It is known that intracellular application of ADPr in insulin-secreting cells, activates the TRPM2 channel (Inamura et al., 2003; Togashi et al., 2006; Bari et al., 2009). However, the $[Ca^{2+}]_i$ increase caused by extracellularly applied ADPr, as observed in our study, was not due to the activation of the TRPM2 channel. This is supported by several lines of evidence. TRPM2 is located on the plasma membrane and allows Ca^{2+}-entry into the cell. In our experiments, extracellularly applied ADPr increased $[Ca^{2+}]_i$ primarily by releasing Ca^{2+} from the ER. Moreover, gating of TRPM2 requires binding of ADPr to the cytosolic C-terminal Nudix motif of TRPM2. Extracellularly applied ADPr, which is a polar substance, cannot enter into the cytoplasm and thus is unlikely to activate the TRPM2 channel (Kuhn and Luckhoff, 2004). Furthermore, in our study, three well established inhibitors of TRPM2, failed to inhibit the $[Ca^{2+}]_i$ increase by ADPr, indicating lack of involvement of TRPM2 in this process.

The most interesting observation of our study was that the $[Ca^{2+}]_i$ increase by ADPr was completely blocked by two highly specific blockers of P2Y1 purinergic receptors. These two inhibitors of P2Y1 are MRS 2179 and MRS 2279 (Boyer et al., 2002; Moro et al., 1998). MRS 2279 inhibits only the P2Y1 receptor, in contrast to MRS 2179 that also blocks P2X1 and P2X3 receptors (Brown et al., 2000). The inhibition of ADPr-induced $[Ca^{2+}]_i$ increase by two structurally different selective antagonists of the P2Y1 receptor, is strong evidence for the involvement of the P2Y1 receptor in ADPr-induced $[Ca^{2+}]_i$ increase. We also demonstrated that ADPr did not increase $[Ca^{2+}]_i$ in undifferentiated PC12 cells, a cell type that lacks P2Y1 receptors, providing further evidence that ADPr increased $[Ca^{2+}]_i$ by activating the P2Y1 receptors (Arslan et al., 2000; Moskvina et al., 2003). From previous studies, it is established that in addition to P2Y1, several other purinergic receptors, namely P2Y2, P2Y4, P2Y6 and P2Y12 are expressed in pancreatic β-cells (Lugo-Garcia et al.,

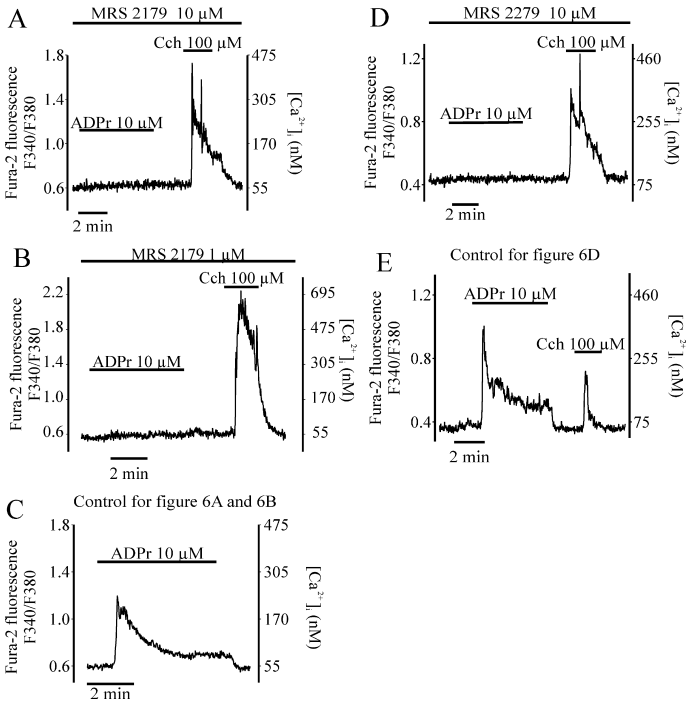

Fig. 6. ADPr-induced $[Ca^{2+}]_i$ increase was due to the activation of P2Y1 receptors. The INS-1E cells were incubated for 10 min with either MRS 2179 (1 and 10 μM) (Fig. 6A and B) or MRS 2279 (10 μM) (Fig. 6D). The inhibitors were also present in the perfusion during the experiment. Both MRS 2179 and MRS 2279 completely inhibited the $[Ca^{2+}]_i$ increase by ADPr (10 μM). Fig. 6C and E are control experiments that show ADPr-induced $[Ca^{2+}]_i$ increase in the absence of the inhibitors. MRS 2179 and MRS 2279 did not block the Cch-induced $[Ca^{2+}]_i$ increase (Fig. 6A, B and D). The traces are representatives of at least three experiments each.

2007; Verspohl et al., 2002). Of these P2Y1, P2Y2, P2Y4 and P2Y6 are linked to the PLC-mediated Ca^{2+} signaling system (Abbracchio et al., 2006). Inhibition of ADPr-induced $[Ca^{2+}]_i$ increase by the inhibitors of P2Y1 confirms that P2Y1 is the sole target for ADPr-induced $[Ca^{2+}]_i$ increase. It is generally known that ADP is the cognate agonist of the P2Y1 receptor and it desensitizes the receptor. However, we found that after a prolonged washout period after a first exposure to ADP, the receptor became sensitive to a second stimulation by ADP (Fig. 2A). On the other hand, when ADP was applied repeatedly without an intervening prolonged washout period, the $[Ca^{2+}]_i$ response was decreased because of receptor desensitization. Application of ADPr after ADP without an intervening prolonged washout period also elicited a reduced $[Ca^{2+}]_i$ increase. These results further establish that ADP and ADPr activate the same receptor, namely the P2Y1 receptor.

At first sight, it may appear that many adenine-containing nucleotides could activate P2Y1 receptors. We found that that is not at all the case. cADPr, NAD^+, and breakdown products of ADPr, namely 5′AMP, adenosine and D-ribose 5-phosphate, did not increase $[Ca^{2+}]_i$. A recent study (Lange et al., 2009) has shown that when ADPr is applied together with NAD^+ (1:1 ratio) to primary β-cells, there is no increase of $[Ca^{2+}]_i$. In our study, when we applied ADPr together with NAD (1:1 ratio) to INS-1E cells, there was normal $[Ca^{2+}]_i$ increase. Differences in cell types may possibly explain such differences.

PADPr, which is a phosphonate analogue of ADPr where an alkynyl moiety has replaced the bridging oxygen of the pyrophosphate linkage, did neither increase $[Ca^{2+}]_i$ by itself nor did it alter the ADPr-induced $[Ca^{2+}]_i$ increase. Thus, while ADP and ADPr both activate P2Y1 receptors, PADPr had no effect on P2Y1. This lack of activity of PADPr is likely due to the fact that the pyrophosphonate moiety linking the ribose ring to the adenosine moiety does not have the same chemical properties as the pyrophosphate found in ADP and ADPr. It is indeed possible that the ADP moiety of ADPr provides tight binding of the molecule to the P2Y1 receptor and the ribose ring brings specificity, thus requiring an unmodified pyrophosphate moiety. Brominated ADPr (8Br-ADPr) was not able to increase $[Ca^{2+}]_i$ either. Together, these results show that small changes in the structure of ADPr abolishes its ability to elicit $[Ca^{2+}]_i$ response.

To convince further that the effect of ADPr on $[Ca^{2+}]_i$ was due to activation of the P2Y1 receptors, we performed experiments with 1321N1 human astrocytoma cells that stably overexpress the recombinant human P2Y1 receptor. ADPr induced robust $[Ca^{2+}]_i$ increase in these transfected cells. In the WT astrocytoma cells that do not express P2Y1 receptors, ADPr did not induce $[Ca^{2+}]_i$ increase. This is a strong evidence that ADPr increased $[Ca^{2+}]_i$ by activation of the P2Y1 receptor.

After preliminary studies, we have realized that a radioligand assay for studying binding of ADPr to P2Y1 is not feasible at

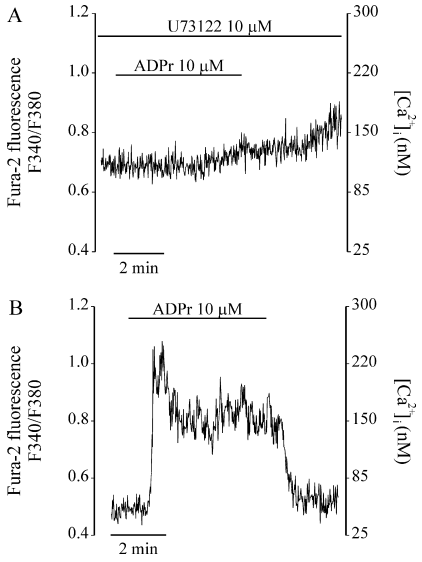

Fig. 7. $[Ca^{2+}]_i$ increase by ADPr requires activation of PLC. (A) INS-1E cells were incubated with U73122 (10 μM), an inhibitor of PLC, for 10–45 min. U73122 inhibited the ADPr induced $[Ca^{2+}]_i$ increase completely. (B) Control experiment where cells were not treated with U73122. The traces are representatives of experiments that have been repeated at least three times.

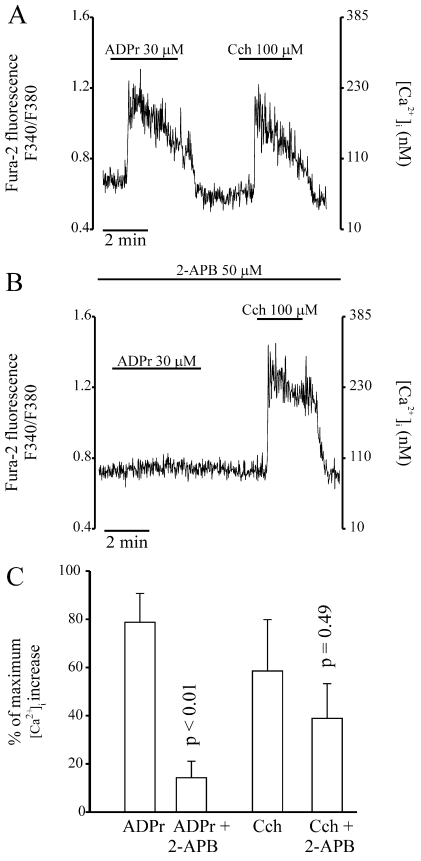

Fig. 8. Ca^{2+} released by ADPr was through the IP_3 receptor. (A) 2-APB (50 μM), a blocker of IP_3 receptors, inhibited the ADPr-induced $[Ca^{2+}]_i$ increase by 82% (C). 2-APB also decreased Cch-induced $[Ca^{2+}]_i$ increase by 34%, but the decrease was not statistically significant (C). (B) Control experiment that shows $[Ca^{2+}]_i$ increase by ADPr and Cch in the absence of 2-APB. Traces in A and B are representative of three experiments each.

this stage. ADPr is a low affinity ligand and thus requires long incubation in binding assays. But ADPr breaks down in aqueous solutions in minutes. For this reason, as mentioned before, we synthesized a stable analogue of ADPr, PADPr. But this analogue turned out to be inactive as an agonist or antagonist. Because of instability of ADPr we were not even able to use it in static fluorometric assays in multiwell plates, and instead chose to use a system of continuous perfusion of ADPr in single cell microfluorometry assay. We are at present trying different options to overcome the difficulties involved in establishing a radiotracer assay. It may be noted that fluorometric assays involving whole cells are being increasingly used as they provide more physiological alternatives compared to the radioligand assays that use membrane preparations.

The effect of P2Y1 activation on insulin secretion remains controversial. It has been shown that P2Y1 agonists are able to increase or inhibit the insulin secretion, depending on cell types used, choice for agonist for P2Y1, dosage and other experimental conditions (Fischer et al., 2000; Petit et al., 1998; Poulsen et al., 1999; Verspohl et al., 2002). In β-cells, the voltage gated Ca^{2+} channels are the major sources for the Ca^{2+} that is coupled to $[Ca^{2+}]_i$ increase leading to the exocytosis of insulin (Braun et al., 2008). Consistent with this, there was no effect of ADPr on basal or glucose-induced insulin secretion in our experiments.

We studied the role of P2Y1 activation in another cell type, namely the platelets, where the role of P2Y1 is well established. Activation of P2Y1 in platelets results in platelet shape change and initiates weak and transient platelet aggregation (Gachet, 2008; Jin et al., 1998). There are three purinergic receptors expressed in platelets: P2X1, P2Y1 and P2Y12. The P2Y1 receptor is expressed on platelets at a low density (≈150 receptors per platelet), and its expression density is only about 8% of P2Y12 and 25% of P2X1 (Wang et al., 2003). Alteration of platelet shape change is a phenomenon dependent on $[Ca^{2+}]_i$. In our experiments, activation of P2Y1 by ADPr induced platelet shape change, the magnitude of which was comparable to that obtained by ADP. In contrast, effect of P2Y1 receptor activation by ADPr on fibrinogen binding and P-selectin expression was only modest compared to those obtained by ADP, which activates the P2Y12, in addition to the P2Y1 receptors. Our findings are consistent with the known roles of P2Y1 receptors in platelet activation. Overall, the P2Y1 receptor mediates weak responses to ADP but is nevertheless a crucial factor in the initiation of the platelet activation (Gachet, 2008). ADP is unequivocally accepted to be the cognate agonist of the P2Y1 receptor (Jin et al., 1998). However, ADP lacks specificity in the sense that it increases $[Ca^{2+}]_i$ by activating other purinergic receptors too (Abbracchio et al., 2006). In this respect, ADPr is remarkable since it

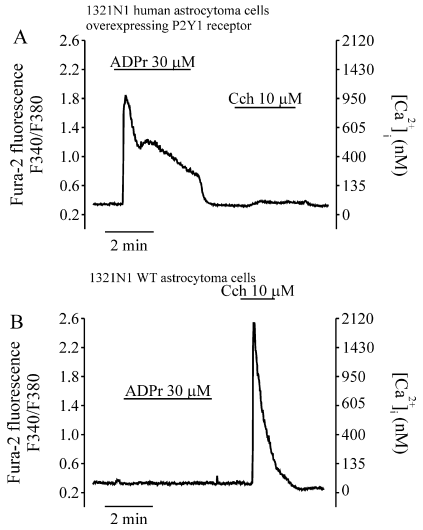

Fig. 9. ADPr induced $[Ca^{2+}]_i$ increase in astrocytoma cells that stably expressed P2Y1 receptors but not in WT astrocytoma cells. (A) ADPr (30 μM) induced a $[Ca^{2+}]_i$ increase in 1321N1 human astrocytoma cells stably overexpressing human P2Y1. Subsequent application of Cch (10 μM) induced little $[Ca^{2+}]_i$ increase. (B) In WT astrocytoma cells that did not express P2Y1 receptors, ADPr (30 μM) did not increase $[Ca^{2+}]_i$ at all. Subsequent application of Cch induced $[Ca^{2+}]_i$ increase. The traces are representatives of three experiments each.

increases $[Ca^{2+}]_i$ by activating only the P2Y1 receptor. ADPr might have a physiological or pathological relevance when it comes to platelet aggregation.

As mentioned earlier, ADPr is formed by the action of CD38 and is released into the extracellular space (Hotta et al., 2000).

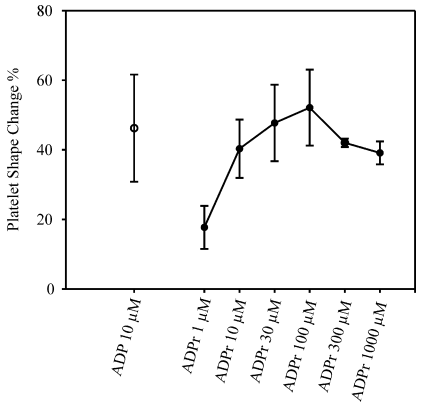

Fig. 10. ADPr induced platelet shape change. Hirudinized whole-blood was incubated in the presence of 10 μM ADP (open circle) or 1–1000 μM ADPr (filled circles). Platelet shape change was measured by flow cytometry. ≥10 μM ADPr gave similar increase in percent platelet shape change as seen with ADP (10 μM). Each circle represents the mean ± SEM from three experiments each.

It is also released from nerve terminals (Smyth et al., 2004). It is established from numerous reports that various insulin secreting cells express CD38 (Bruzzone et al., 2008; Kato et al., 1995). However, in vivo, ADPr could also be available from neighbouring cells and from nerve terminals. We speculate that extracellular ADPr exerts its biological actions by increasing $[Ca^{2+}]_i$ specifically by activating the P2Y1 receptors. Both P2Y1 receptors and CD38 are expressed in many cell types, giving rise to the possibility that ADPr-mediated activation of the P2Y1 receptor could be a widespread phenomenon. We conclude that ADPr is an endogenous and specific agonist of P2Y1 receptors and that it shows stringent structural requirements for activation of this receptor. The physiological impact of our observations at whole organism level needs, however, further studies.

Conflicts of interest

We confirm that there is no conflict of interest involved in this manuscript.

Acknowledgements

This work was supported in part by the Swedish Research Council Grant K2006-72X-10159-01-3, funds of Karolinska Institutet, Swedish Medical Society, the Swedish Research Council and the Swedish Heart-Lung Foundation. A.J.G. was funded by Karolinska Institutet's MD PhD program, Stiftelsen Irma och Arvid Larsson-Rösts minne, Stiftelsen Goljes minne and Svenska Diabetesstiftelsen. L.M. was supported by scholarship from the Leonardo da Vinci project Unipharma-Graduates coordinated by Sapienza University of Rome. We are grateful to J.M. Denu, Wisconsin, who synthesized OAADPr and T.F. Walseth, Minneapolis, who synthesized 8Br-ADPr.

Appendix A. Supplementary data

Supplementary data associated with this article can be found, in the online version, at doi:10.1016/j.mce.2010.11.004.

References

Abbracchio, M.P., Burnstock, G., Boeynaems, J.M., Barnard, E.A., Boyer, J.L., Kennedy, C., Knight, G.E., Fumagalli, M., Gachet, C., Jacobson, K.A., Weisman, G.A., 2006. International Union of Pharmacology LVIII: update on the P2Y G protein-coupled nucleotide receptors: from molecular mechanisms and pathophysiology to therapy. Pharmacol. Rev. 58, 281–341.

Arslan, G., Filipeanu, C.M., Irenius, E., Kull, B., Clementi, E., Allgaier, C., Erlinge, D., Fredholm, B.B., 2000. P2Y receptors contribute to ATP-induced increases in intracellular calcium in differentiated but not undifferentiated PC12 cells. Neuropharmacology 39, 482–496.

Bari, M.R., Akbar, S., Eweida, M., Kühn, F.J.P., Jabin Gustafsson, A., Lückhoff, A., Islam, M.S., 2009. H_2O_2-induced Ca^{2+} influx and its inhibition by N-(p-amylcinnamoyl)anthranilic acid in the beta cells: involvement of TRPM2 channels. J. Cell. Mol. Med. 13, 3260–3267.

Bernet, D., Pinto, R.M., Costas, M.J., Canales, J., Cameselle, J.C., 1994. Rat liver mitochondrial ADP-ribose pyrophosphatase in the matrix space with low Km for free ADP-ribose. Biochem. J. 299 (Pt 3), 679–682.

Berthelier, V., Tixier, J.M., Muller-Steffner, H., Schuber, F., Deterre, P., 1998. Human CD38 is an authentic NAD(P)+ glycohydrolase. Biochem. J. 330 (Pt 3), 1383–1390.

Bonicalzi, M.E., Haince, J.F., Droit, A., Poirier, G.G., 2005. Regulation of poly(ADP-ribose) metabolism by poly(ADP-ribose) glycohydrolase: where and when? Cell Mol. Life Sci. 62, 739–750.

Borra, M.T., O'Neill, F.J., Jackson, M.D., Marshall, B., Verdin, E., Foltz, K.R., Denu, J.M., 2002. Conserved enzymatic production and biological effect of O-acetyl-ADP-ribose by silent information regulator 2-like NAD+-dependent deacetylases. J. Biol. Chem. 277, 12632–12641.

Bortell, R., Moss, J., McKenna, R.C., Rigby, M.R., Niedzwiecki, D., Stevens, L.A., Patton, W.A., Mordes, J.P., Greiner, D.L., Rossini, A.A., 2001. Nicotinamide adenine dinucleotide (NAD) and its metabolites inhibit T lymphocyte proliferation: role of cell surface NAD glycohydrolase and pyrophosphatase activities. J. Immunol. 167, 2049–2059.

Boyer, J.L., Adams, M., Ravi, R.G., Jacobson, K.A., Harden, T.K., 2002. 2-Chloro N(6)-methyl-(N)-methanocarba-2′-deoxyadenosine-3′,5′-bisphosphate is a selective high affinity P2Y(1) receptor antagonist. Br. J. Pharmacol. 135, 2004–2010.
Braun, M., Ramracheya, R., Bengtsson, M., Zhang, Q., Karanauskaite, J., Partridge, C., Johnson, P.R., Rorsman, P., 2008. Voltage-gated ion channels in human pancreatic beta-cells: electrophysiological characterization and role in insulin secretion. Diabetes 57, 1618–1628.
Breen, L.T., Smyth, L.M., Yamboliev, I.A., Mutafova-Yambolieva, V.N., 2006. Beta-NAD is a novel nucleotide released on stimulation of nerve terminals in human urinary bladder detrusor muscle. Am. J. Physiol. Renal Physiol. 290, F486–F495.
Broetto-Biazon, A.C., Bracht, F., Sa-Nakanishi, A.B., Lopez, C.H., Constantin, J., Kelmer-Bracht, A.M., Bracht, A., 2008. Transformation products of extracellular NAD(+) in the rat liver: kinetics of formation and metabolic action. Mol. Cell Biochem. 307, 41–50.
Brown, S.G., King, B.F., Kim, Y.C., Jang, S.Y., Burnstock, G., Jacobson, K.A., 2000. Activity of novel adenine nucleotide derivatives as agonists and antagonists at recombinant rat P2X receptors. Drug Develop. Res. 49, 253–259.
Bruzzone, S., Bodrato, N., Usai, C., Guida, L., Moreschi, I., Nano, R., Antonioli, B., Fruscione, F., Magnone, M., Scarfì, S., De Flora, A., Zocchi, E., 2008. Abscisic acid is an endogenous stimulator of insulin release from human pancreatic islets with cyclic ADP ribose as second messenger. J. Biol. Chem. 283, 32188–32197.
Chevallier, O.P., Migaud, M.E., 2008. Synthesis of simple adenosine diphosphate ribose analogues. Nucleosides Nucleotides Nucleic Acids 27, 1127–1143.
De Flora, A., Zocchi, E., Guida, L., Franco, L., Bruzzone, S., 2004. Autocrine and paracrine calcium signaling by the CD38/NAD+/cyclic ADP-ribose system. Ann. N. Y. Acad. Sci. 1028, 176–191.
Dunn, C.A., O'Handley, S.F., Frick, D.N., Bessman, M.J., 1999. Studies on the ADP-ribose pyrophosphatase subfamily of the nudix hydrolases and tentative identification of trgB, a gene associated with tellurite resistance. J. Biol. Chem. 274, 32318–32324.
Eisfeld, J., Luckhoff, A., 2007. TRPM2. Handb. Exp. Pharmacol., 237–252.
Fischer, B., Shahar, L., Chulkin, A., Boyer, J.L., Harden, K.T., Gendron, F.P., Beaudoin, A.R., Chapal, J., Hillaire-Buys, D., Petit, P., 2000. 2-Thioether-5′-O-(1-thiotriphosphate)-adenosine derivatives: new insulin secretagogues acting through P2Y-receptors. Isr. Med. Assoc. J. 2 (Suppl.), 92–98.
Gachet, C., 2008. P2 receptors, platelet function and pharmacological implications. Thromb. Haemost. 99, 466–472.
Gerth, A., Nieber, K., Oppenheimer, N.J., Hauschildt, S., 2004. Extracellular NAD+ regulates intracellular free calcium concentration in human monocytes. Biochem. J. 382, 849–856.
Grynkiewicz, G., Poenie, M., Tsien, R.Y., 1985. A new generation of Ca^{2+} indicators with greatly improved fluorescence properties. J. Biol. Chem. 260, 3440–3450.
Hill, K., Benham, C.D., McNulty, S., Randall, A.D., 2004. Flufenamic acid is a pH-dependent antagonist of TRPM2 channels. Neuropharmacology 47, 450–460.
Hotta, T., Asai, K., Fujita, K., Kato, T., Higashida, H., 2000. Membrane-bound form of ADP-ribosyl cyclase in rat cortical astrocytes in culture. J. Neurochem. 74, 669–675.
Howard, M., Grimaldi, J.C., Bazan, J.F., Lund, F.E., Santos-Argumedo, L., Parkhouse, R.M., Walseth, T.F., Lee, H.C., 1993. Formation and hydrolysis of cyclic ADP-ribose catalyzed by lymphocyte antigen CD38. Science 262, 1056–1059.
Hoyle, C.H., Edwards, G.A., 1992. Activation of P1- and P2Y-purinoceptors by ADP-ribose in the guinea-pig taenia coli, but not of P2X-purinoceptors in the vas deferens. Br. J. Pharmacol. 107, 367–374.
Inamura, K., Sano, Y., Mochizuki, S., Yokoi, H., Miyake, A., Nozawa, K., Kitada, C., Matsushime, H., Furuichi, K., 2003. Response to ADP-ribose by activation of TRPM2 in the CRI-G1 insulinoma cell line. J. Membr. Biol. 191, 201–207.
Ishii, M., Shimizu, S., Hagiwara, T., Wajima, T., Miyazaki, A., Mori, Y., Kiuchi, Y., 2006. Extracellular-added ADP-ribose increases intracellular free Ca(2+) concentration through Ca(2+) release from stores, but not through TRPM2-mediated Ca(2+) entry, in rat beta-cell line RIN-5F. J. Pharmacol. Sci..
Jin, J., Daniel, J.L., Kunapuli, S.P., 1998. Molecular basis for ADP-induced platelet activation. II. The P2Y1 receptor mediates ADP-induced intracellular calcium mobilization and shape change in platelets. J. Biol. Chem. 273, 2030–2034.
Kato, I., Takasawa, S., Akabane, A., Tanaka, O., Abe, H., Takamura, T., Suzuki, Y., Nata, K., Yonekura, H., Yoshimoto, T., 1995. Regulatory role of CD38 (ADP-ribosyl cyclase/cyclic ADP-ribose hydrolase) in insulin secretion by glucose in pancreatic beta cells. Enhanced insulin secretion in CD38-expressing transgenic mice. J. Biol. Chem. 270, 30045–30050.
Kato, I., Yamamoto, Y., Fujimura, M., Noguchi, N., Takasawa, S., Okamoto, H., 1999. CD38 disruption impairs glucose-induced increases in cyclic ADP-ribose, $[Ca^{2+}]i$, and insulin secretion. J. Biol. Chem. 274, 1869–1872.
Kelly, C.B., Blair, L.A., Corbett, J.A., Scarim, A.L., 2003. Isolation of islets of Langerhans from rodent pancreas. Methods Mol. Med. 83, 3–14.
Kim, U.H., Han, M.K., Park, B.H., Kim, H.R., An, N.H., 1993. Function of NAD glycohydrolase in ADP-ribose uptake from NAD by human erythrocytes. Biochim. Biophys. Acta 1178, 121–126.
Kraft, R., Grimm, C., Frenzel, H., Harteneck, C., 2006. Inhibition of TRPM2 cation channels by N-(p-amylcinnamoyl)anthranilic acid. Br. J. Pharmacol. 148, 264–273.
Kühn, F.J., Lückhoff, A., 2004. Sites of the NUDT9-H domain critical for ADP-ribose activation of the cation channel TRPM2. J. Biol. Chem. 279, 46431–46437.
Lange, I., Yamamoto, S., Partida-Sanchez, S., Mori, Y., Fleig, A., Penner, R., 2009. TRPM2 functions as a lysosomal Ca^{2+}-release channel in beta cells. Sci. Signal. 2, ra23.
Lee, H.C., 1997. Mechanisms of calcium signaling by cyclic ADP-ribose and NAADP. Physiol. Rev. 77, 1133–1164.
Lee, H.C., 2006. Structure and enzymatic functions of human CD38. Mol. Med. 12, 317–323.
Lee, H.C., Munshi, C., Graeff, R., 1999. Structures and activities of cyclic ADP-ribose and NAADP and their metabolic enzymes. Mol. Cell Biochem. 193, 89–98.
Li, N., Wallen, N.H., Hjemdahl, P., 1999. Evidence for prothrombotic effects of exercise and limited protection by aspirin. Circulation 100, 1374–1379.
Lin, W., Ame, J.C., Aboul-Ela, N., Jacobson, E.L., Jacobson, M.K., 1997. Isolation and characterization of the cDNA encoding bovine poly(ADP-ribose) glycohydrolase. J. Biol. Chem. 272, 11895–11901.
Lugo-Garcia, L., Filhol, R., Lajoix, A.D., Gross, R., Petit, P., Vignon, J., 2007. Expression of purinergic P2Y receptor subtypes by INS-1 insulinoma beta-cells: a molecular and binding characterization. Eur. J. Pharmacol. 568, 54–60.
Lund, F.E., Muller-Steffner, H.M., Yu, N.X., Stout, C.D., Schuber, F., Howard, M.C., 1999. CD38 signaling in B lymphocytes is controlled by its ectodomain but occurs independently of enzymatically generated ADP-ribose or cyclic ADP-ribose. J. Immunol. 162, 2693–2702.
Maruyama, T., Kanaji, T., Nakade, S., Kanno, T., Mikoshiba, K., 1997. 2APB, 2-aminoethoxydiphenyl borate, a membrane-penetrable modulator of Ins(1,4,5)P3-induced Ca^{2+} release. J. Biochem. (Tokyo) 122, 498–505.
Merglen, A., Theander, S., Rubi, B., Chaffard, G., Wollheim, C.B., Maechler, P., 2004. Glucose sensitivity and metabolism-secretion coupling studied during two-year continuous culture in INS-1E insulinoma cells. Endocrinology 145, 667–678.
Miller, J.S., Cervenka, T., Lund, J., Okazaki, I.J., Moss, J., 1999. Purine metabolites suppress proliferation of human NK cells through a lineage-specific purine receptor. J. Immunol. 162, 7376–7382.
Moro, S., Guo, D., Camaioni, E., Boyer, J.L., Harden, T.K., Jacobson, K.A., 1998. Human P2Y1 receptor: molecular modeling and site-directed mutagenesis as tools to identify agonist and antagonist recognition sites. J. Med. Chem. 41, 1456–1466.
Moskvina, E., Unterberger, U., Boehm, S., 2003. Activity-dependent autocrine–paracrine activation of neuronal P2Y receptors. J. Neurosci. 23, 7479–7488.
Oppenheimer, N.J., 1994. NAD hydrolysis: chemical and enzymatic mechanisms. Mol. Cell Biochem. 138, 245–251.
Partida-Sanchez, S., Gasser, A., Fliegert, R., Siebrands, C.C., Dammermann, W., Shi, G., Mousseau, B.J., Sumoza-Toledo, A., Bhagat, H., Walseth, T.F., Guse, A.H., Lund, F.E., 2007. Chemotaxis of mouse bone marrow neutrophils and dendritic cells is controlled by adp-ribose, the major product generated by the CD38 enzyme reaction. J. Immunol. 179, 7827–7839.
Peppiatt, C.M., Collins, T.J., MacKenzie, L., Conway, S.J., Holmes, A.B., Bootman, M.D., Berridge, M.J., Seo, J.T., Roderick, H.L., 2003. 2-Aminoethoxydiphenyl borate (2-APB) antagonises inositol 1,4,5-trisphosphate-induced calcium release, inhibits calcium pumps and has a use-dependent and slowly reversible action on store-operated calcium entry channels. Cell Calcium 34, 97–108.
Perraud, A.L., Fleig, A., Dunn, C.A., Bagley, L.A., Launay, P., Schmitz, C., Stokes, A.J., Zhu, Q., Bessman, M.J., Penner, R., Kinet, J.P., Scharenberg, A.M., 2001. ADP-ribose gating of the calcium-permeable LTRPC2 channel revealed by Nudix motif homology. Nature 411, 595–599.
Petit, P., Hillaire-Buys, D., Manteghetti, M., Debrus, S., Chapal, J., Loubatieres-Mariani, M.M., 1998. Evidence for two different types of P2 receptors stimulating insulin secretion from pancreatic B cell. Br. J. Pharmacol. 125, 1368–1374.
Poenie, M., 1990. Alteration of intracellular Fura-2 fluorescence by viscosity: a simple correction. Cell Calcium 11, 85–91.
Polzonetti, V., Orsomando, G., Micossi, L., Vita, A., Egidi, D., Natalini, P., 2002. NAD+ catabolism in pheochromocytoma rat cells. J. Biol. Regul. Homeost. Agents 16, 196–201.
Poulsen, C.R., Bokvist, K., Olsen, H.L., Hoy, M., Capito, K., Gilon, P., Gromada, J., 1999. Multiple sites of purinergic control of insulin secretion in mouse pancreatic beta-cells. Diabetes 48, 2171–2181.
Schachter, J.B., Li, Q., Boyer, J.L., Nicholas, R.A., Harden, T.K., 1996. Second messenger cascade specificity and pharmacological selectivity of the human P2Y1-purinoceptor. Br. J. Pharmacol. 118, 167–173.
Smyth, L.M., Bobalova, J., Mendoza, M.G., Lew, C., Mutafova-Yambolieva, V.N., 2004. Release of beta-nicotinamide adenine dinucleotide upon stimulation of post-ganglionic nerve terminals in blood vessels and urinary bladder. J. Biol. Chem. 279, 48893–48903.
Snell, C.R., Snell, P.H., Richards, C.D., 1984. Degradation of NAD by synaptosomes and its inhibition by nicotinamide mononucleotide: implications for the role of NAD as a synaptic modulator. J. Neurochem. 43, 1610–1615.
Togashi, K., Hara, Y., Tominaga, T., Higashi, T., Konishi, Y., Mori, Y., Tominaga, M., 2006. TRPM2 activation by cyclic ADP-ribose at body temperature is involved in insulin secretion. EMBO J. 25, 1804–1815.
Trautmann, M.E., Wollheim, C.B., 1987. Characterization of glucose transport in an insulin-secreting cell line. Biochem. J. 242, 625–630.
Van derpoorten, K., Migaud, M.E., 2004. Isopolar phosphonate analogue of adenosine diphosphate ribose. Org. Lett. 6, 3461–3464.
Verspohl, E.J., Johannwille, B., Waheed, A., Neye, H., 2002. Effect of purinergic agonists and antagonists on insulin secretion from INS-1 cells (insulinoma cell line) and rat pancreatic islets. Can. J. Physiol. Pharmacol. 80, 562–568.
Wang, L., Ostberg, O., Wihlborg, A.K., Brogren, H., Jern, S., Erlinge, D., 2003. Quantification of ADP and ATP receptor expression in human platelets. J. Thromb. Haemost. 1, 330–336.
Zhang, D.X., Zou, A.P., Li, P.L., 2001. Adenosine diphosphate ribose dilates bovine coronary small arteries through apy. J. Vasc. Res. 38, 64–72.
Zimmermann, H., 1992. 5′-Nucleotidase: molecular structure and functional aspects. Biochem. J. 285 (Pt 2), 345–365.

Amanda Jabin Gustafsson pursued MD degree in 2007 from Uppsala University, Sweden. She has been a PhD student in Md Shahidul Islam's research group at the Department of Clinical Science and Education, Karolinska Institutet, Stockholm, Sweden since October 2004. Her subject for PhD is "The role of calcium signaling and ion channels in insulin-secreting beta cells".

Lucia Muraro has been a Post-Doct, Chiara Zurzolo group, Institut Pasteur Paris, France since September 2009. Her subject for Post-Doct is "Super-resolution analysis of GPI-anchored proteins membrane organization". She pursued her PhD on cellular biology in Cesare Montecucco group, Padua University, Italy from January 2006 to April 2009. Her subjects were "Study of the binding of the Botulinum Neurotoxin A to the plasma membrane" and "The possible role of the lectin like subdomain". She was offered a Leonardo international exchange fellowship, in Shahidul Islam group Karolinska Institute, Stockholm, Sweden from July 2005 to December 2005. Her subject was Study of the role of calcium signaling and ion channels in stimulate-secretion coupling in beta cells. She underwent research training at Cesare Montecucco group, Padua University, Italy from March 2004 to June 2005. Her subject for the training was Study of AB toxins translocation mechanism.

Carin Dahlberg was a research student in Md Shahidul Islam's Group at the Department of Clinical Science and education, Karolinska Institute, Stockholm, Sweden from 2005 to 2007. Her project involved Study of different ion channels in rat insulinoma cell line INS -1E. She obtained a degree in Biomedicine from Karolinska Institutet, Stockholm, Sweden.

Dr Marie E. Migaud obtained her BSc from Ecole Superieure de Chemie Organique et Minerale, Paris, France, in 1992 and her PhD from Michigan State University, Lansing, Michigan, USA in 1996. Her research area included "Understanding the biosynthesis and the roles of phopho-sugar nucleotides and dinucleotides in various biological processes by studying different enzymatic mechanisms".

Dr Olivier Chevallier obtained his MSc in Organic Chemistry from Université Monpellier II (France) in 2002. He then moved to The Queen's University of Belfast where he was awarded a PhD within the School of Chemistry and Chemical Engineering in 2008. His project involved the synthesis of new adenosine diphospho ribose analogues. He then worked as a R D synthetic chemist for Almac Sciences before joining The Institute of Agri-food and Land Use as a research fellow in January 2009 where he is investigating the synthesis of various hapten derivatives.

Hoa Nguyen Khahn has been a Post-Doct, Diabetes group, University of Manitoba, Winnipeg, Manitoba, Canada since July 2007. His subject for Post-Doct includes "Ethanol-Mechanism of failure of insulin secretion from isolated islets. IGFBP3- the role in islet development and insulin resistance". He worked as a Lecturer and as a Researcher in Hanoi Medical University, Hanoi, Vietnam from January 1998 to July 2007. His subjects included Drug discovery from Vietnamese Traditional Medicine. He was a PhD candidate at Department of Molecular Medicine and Surgery, The Endocrinology and Diabetes Unit, Karolinska Institute, Stockholm, Sweden from May 2000 to December 2005. His subject for PhD was "Study the anti-diabetic effect of Vietnamese herbal drugs". He was a Medical student of Hanoi Medical University, Hanoi, Vietnam from September 1991 to September 1997.

Kalaiselvan Krishnan is a research student working on Transient Receptor Potential Channels in insulin secreting channels, in the Department of Clinical Sciences and Education, Södersjukhuset, Karolinska Institutet, Stockholm, Sweden. He has a Masters of Science degree in molecular genetics and physiology. He also has a Batchelor of technology in biotechnology from Anna University, Chennai, Tamil Nadu, India.

Nailin Li obtained his M.D. in 1986 and Master of Medical Science in 1989 from Southern Medical University, Guangzhou, China. He completed his PhD in Clinical Pharmacology in 1999 from Department of Medicine Division of Clinical Pharmacology, Karolinska Institute and Hospital Stockholm, Sweden. He worked as an assistant professor from 1989 to 1991 and as a lecturer from 1991 to 1995 in the Department of Histology & Embryology Southern Medical University, Guangzhou, China

Md. Shahidul Islam pursued his PhD in Karolinska Institutet, Stockholm, Sweden in 1994 and his MD, in University of Chittagong; Certified by ECFMG (USA). Present positions: He is currently working as a associate professor and group leader in Karolinska Institutet, Department of Clinical Science and Education, Södersjukhuset, Stockholm, Sweden. He is a consultant physician in Uppsala University Hospital, Uppsala, Sweden. Also he is the editor-in-chief of Islets and editor of Advances in Experimental Medicine and Biology. He is the president of Islet Society.

G Model
MCE 7771 1–2
ARTICLE IN PRESS

Molecular and Cellular Endocrinology xxx (2011) xxx–xxx

Contents lists available at ScienceDirect

Molecular and Cellular Endocrinology

journal homepage: www.elsevier.com/locate/mce

Erratum

Erratum to "ADP ribose is an endogenous ligand for the purinergic P2Y1 receptor" [Mol. Cell. Endocrinol. 333 (2011) 8–19]

Amanda Jabin Gustafsson[a,*], Lucia Muraro[a], Carin Dahlberg[a], Marie Migaud[b], Olivier Chevallier[b], Hoa Nguyen Khanh[c], Kalaiselvan Krishnan[a], Nailin Li[d], Md. Shahidul Islam[a,e]

[a] Department of Clinical Science and Education, Karolinska Institutet, Research Centre, Stockholm South Hospital, 118 83 Stockholm, Sweden
[b] School of Chemistry and Chemical Engineering, Queen's University Belfast, BT9 5AG, Northern Ireland, United Kingdom
[c] Department of Molecular Medicine and Surgery, Karolinska Institutet, 171 76 Stockholm, Sweden
[d] Department of Medicine Solna, Clinical Pharmacology Unit, Karolinska University Hospital Institutet, 171 76 Stockholm, Sweden
[e] Uppsala University Hospital, AR division, Uppsala, Sweden

The authors regret that an error appeared in Fig. 3C, where the concentrations of ADPr and 8Br-ADPr are in μM (micromolar) and not in mM.

The corrected figure is now reproduced below.

DOI of original article: 10.1016/j.mce.2010.11.004.
* Corresponding author. Tel.: +46 709 961 962; fax: +46 8 616 2933.
E-mail address: amajab@ki.se (A.J. Gustafsson).

0303-7207/$ – see front matter
doi:10.1016/j.mce.2011.02.008

Please cite this article in press as: Gustafsson, A.J., et al., Erratum to "ADP ribose is an endogenous ligand for the purinergic P2Y1 receptor" [Mol. Cell. Endocrinol. 333 (2011) 8–19]. Mol. Cell. Endocrinol. (2011), doi:10.1016/j.mce.2011.02.008

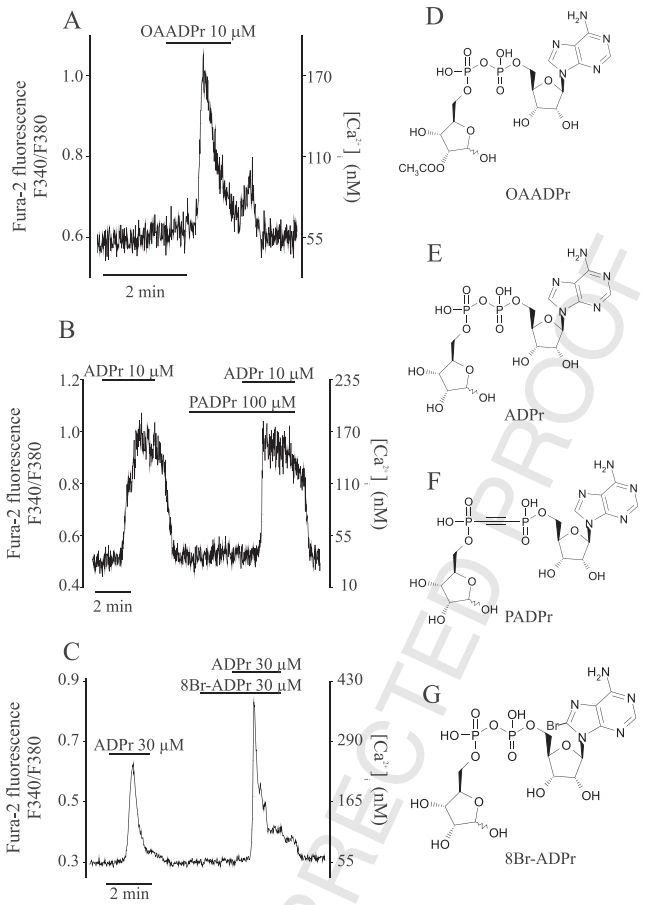

Fig. 3. Effects of OAADPr, PADPr and 8Br-ADPr on $[Ca^{2+}]_i$ in INS-1E cells. Experiments were done as described in the legend to Fig. 1. (A) OAADPr (10 μM) increased $[Ca^{2+}]_i$ in INS-1E cells. (B) PADPr (100 μM) did not increase $[Ca^{2+}]_i$ by itself and did not alter the ADPr-induced $[Ca^{2+}]_i$ increase. (C) 8Br-ADPr (30 μM) did not increase $[Ca^{2+}]_i$. Each trace is representative of at least three experiments. (D) Molecular structure of OAADPr. (E) Molecular structure of ADPr. (F) Molecular structure of PADPr. (G) Molecular structure of 8Br-ADPr.

Please cite this article in press as: Gustafsson, A.J., et al., Erratum to "ADP ribose is an endogenous ligand for the purinergic P2Y1 receptor" [Mol. Cell. Endocrinol. 333 (2011) 8–19]. Mol. Cell. Endocrinol. (2011), doi:10.1016/j.mce.2011.02.008

III

Insulin-secreting INS-1E cells express functional TRPV1 channels

Amanda Jabin Fågelskiöld*[,a], Kristina Kannisto[a,e], Anna Boström[a], Banina Hadrovic[a], Cecilia Farre[b], Mohamed Eweida[a], Kenneth Wester[c] and Md Shahidul Islam[a,d]

[a]Department of Clinical Science and Education, Södersjukhuset, Karolinska Institutet, Research Centre, Stockholm, Sweden;
[b]Nanion Technologies GmbH, Munich, Germany;
[c]Department of Genetics & Pathology, Uppsala University, The Rudbeck laboratory, Uppsala, Sweden;
[d]Uppsala University Hospital, AR division, Uppsala, Sweden;
[e]Present address: Department of Laboratory Medicine, Clinical chemistry, Karolinska Institutet, Karolinska University Hospital, Huddinge, Sweden.

*Correspondence to: Amanda Jabin Fågelskiöld, Department of Clinical Science and Education, Södersjukhuset, Karolinska Institutet, Research Centre, S-118 83 Stockholm, Sweden. Tel: +46 709 961962, Fax: +46 8 616 2933, E-mail: amajab@ki.se.

Abstract

We have studied whether functional TRPV1 channels exist in the INS-1E cells, a cell type used as a model for β-cells, and in primary β-cells from rat and human. The effects of the TRPV1 agonists capsaicin and AM404 on the intracellular free Ca^{2+} concentration ($[Ca^{2+}]_i$) in the INS-1E cells were studied by fura-2 based microfluorometry. Capsaicin increased $[Ca^{2+}]_i$ in a concentration-dependent manner, and the $[Ca^{2+}]_i$ increase was dependent on extracellular Ca^{2+}. AM404 also increased $[Ca^{2+}]_i$ in the INS-1E cells. Capsazepine, a specific antagonist of TRPV1, completely blocked the capsaicin- and AM404-induced $[Ca^{2+}]_i$ increases. Capsaicin did not increase $[Ca^{2+}]_i$ in primary β-cells from rat and human. Whole cell patch clamp configuration was used to record currents across the plasma membrane in the INS-1E cells. Capsaicin elicited inward currents that were inhibited by capsazepine. Western blot analysis detected TRPV1 proteins in the INS-1E cells and the human islets. Immunohistochemistry was used to study the expression of TRPV1, but no TRPV1 protein immunoreactivity was detected in the human islets and the human insulinoma cells. We conclude that the INS-1E cells, but not the primary β-cells, express functional TRPV1 channels.

Keywords: cell signaling, Ca^{2+}, INS-1E cells, TRPV1, capsaicin, and AM404.

Abbreviations: AM404, N-(4-hydroxyphenyl)-5,8,11,14-eicosatetraenamide; $[Ca^{2+}]_i$, intracellular free Ca^{2+} concentration; BSA, bovine serum albumin; ER, endoplasmic reticulum; ECL, enhanced chemiluminescence; FBS, fetal bovine serum; HBSS, Hanks' Balanced Salt Solution; INS-1E, rat insulinoma cell line INS-1E; PBS, Phosphate Buffered Saline; RT, room temperature; TRPV1, transient receptor potential vanilloid type 1.

1. Introduction

Insulin-secreting rat insulinoma INS-1E cells are widely used as a model for studying the basic mechanism of stimulus-secretion coupling, and Ca^{2+} signaling in pancreatic β-cells. Many studies have so far been done with INS-1E cells, and it is likely that their use in β-cell research will continue. For this reason, it is important to identify the ion channel repertoire of these cells. So far, electrical activity and stimulus-secretion coupling in these cells have been explained by a handful of ion channels, namely the voltage-gated Ca^{2+} channels, ATP-sensitive K^+ channels and Ca^{2+}-activated K^+ channels. The most well known Ca^{2+} channels in the INS-1E cells are the L-type voltage gated Ca^{2+} channels in the plasma membrane. However, recently, a group of ion channels belonging to the transient receptor potential (TRP) family has emerged. We have reported that INS-1E cells express TRP-like channels (Gustafsson et al. 2004). We have also shown that a member of the TRP subfamily related to melastatin, namely TRPM2, is present in both the INS-1E cells and the human β-cells (Bari et al. 2009). TRP channels of insulin-secreting cells have recently been reviewed (Islam 2011). However, the identity of the TRP channels in insulin-secreting cells has not yet been fully elucidated.

Mammalian TRP channels form a big family of cation channels with 28 members. TRP channels are activated by a variety of stimuli including intra- or extracellular messengers, heat, cold, tastants, chemicals, osmotic stress and by the filling state of the endoplasmic reticulum (ER) (Islam 2011). The TRP family consists of seven subfamilies. The transient receptor potential vanilloid type 1 (TRPV1) is a non-selective cation channel that mediates peripheral nociception and pain sensation. Capsaicin, resiniferatoxin, elevated temperature and low pH are some of the activators of TRPV1 (Planells-Cases et al. 2011). The active metabolite of paracetamol, AM404, has also been shown to activate TRPV1 at analgesic doses of paracetamol (Bertolini et al. 2006; Zygmunt et al. 2000). After ingestion, paracetamol is metabolized into, among others, *p*-aminophenol. AM404 is formed by conjugation of *p*-aminophenol and arachidonic acid. AM404 is formed in the brain by the action of fatty acid amide hydrolase (FAAH) (Högestätt et al. 2005).

TRPV1 is mainly expressed in the trigeminal and the dorsal root ganglia. One group has reported that TRPV1 protein is expressed in the rat insulinoma cell lines RIN and INS-1, and that capsaicin increases insulin secretion in the RIN cells (Akiba et al. 2004). It is not known whether TRPV1 activation increases $[Ca^{2+}]_i$ or induces currents in such cells. We studied the effects of two different agonists of TRPV1, namely capsaicin and AM404, on $[Ca^{2+}]_i$ in the INS-1E cells to elucidate whether functional TRPV1 channels are expressed in these cells.

Whether TRPV1 exists in the primary β-cells is even more controversial. TRPV1 immunoreactivity has been described in primary β-cells of Sprague-Dawley rats by one group (Akiba et al 2004), but not in those of Zucker diabetic rats (Gram et al. 2007) or NOD mice (Razavi et al. 2006). It has been shown that TRPV1 is expressed in nerve fibres in the islets of Langerhans in rats and mice (Gram et al 2007; Razavi et al 2006). It is not known whether TRPV1 is present in the human β-cells. Therefore, we investigated the effect of capsaicin on $[Ca^{2+}]_i$ in rat and human primary β-cells, and used immunohistochemistry to look for the expression of TRPV1 protein in the human islet cells and the human insulinoma cells.

2. Materials and methods

2.1. Chemicals

Fura-2 acetoxymethyl ester (AM), RPMI 1640, fetal bovine serum (FBS), penicillin, and streptomycin were from Invitrogen, Stockholm, Sweden. Capsaicin, capsazepine and Tween-20 were from Sigma-Aldrich, Stockholm, Sweden. AM404 was from Cayman, Stockholm, Sweden. Cell culture materials were from Gibco/Life Technologies, Stockholm, Sweden.

2.2. Cell culture

INS-1E cells were provided by C. B. Wollheim and P. Maechler, Geneva (Merglen et al. 2004). A highly differentiated rat insulinoma cell line (S5) was subcloned from these INS-1E cells. The cells were cultured in RPMI-1640 medium supplemented with FBS (2.5%, v/v), penicillin (50 IU/ml), streptomycin (50 µg/ml), 2-mercaptoethanol (500 µM), HEPES (10 mM) and sodium pyruvate (1 mM). The cells were cultured in a humidified incubator with 5% CO_2 at 37 ºC. The medium was changed every other day and the cells were trypsinized and passaged once weekly.

2.3. Preparation of primary β-cells from rat

The local ethics committee approved the use of the rat islets. Male Wistar rats were anaesthetized with CO_2, and then killed by cervical dislocation. Collagenase A in Hanks' solution (9mg/10ml) was injected through the pancreatic duct into the pancreas. After removal, the pancreatic gland was incubated for 24 min at 37 ºC, washed with Hanks' solution and islets were collected after separation on Histopaque gradient. The islets were dispersed by trypsin digestion and plated on glass coverslips. Only large cells, which were likely to be β-cells and not α- or δ-cells, were used for $[Ca^{2+}]_i$ measurements.

2.4. Preparation of human islets

The local ethics committee approved the use of human islets obtained from islet transplantation programmes. Islets were isolated, cultured for 1-3 days and shipped overnight. The islets were controlled for sterility and structural integrity. About 2500 islets were placed in each centrifuge tube, centrifuged at 190 *g* for 2 min at 18-20 °C, and washed with Hanks´ Buffered Salt Solution (HBSS). The centrifugation and washing procedure were repeated two times. The islets were then mildly trypsinized (0.025% trypsin-EDTA, diluted with HBSS without Ca^{2+} and Mg^{2+}) and triturated with a sterile transfer pipette. We added RPMI 1640 medium supplemented as described above, and 10% FBS to the cells. Cells were centrifuged at 250 *g* for 5 min at 4 ºC. Cells were resuspended in the new medium, plated on glass coverslips and incubated for 1 hour to allow cell attachment. Finally, we added 2 ml of medium to each petridish, and incubated the cells overnight before use.

2.5. Measurement of $[Ca^{2+}]_i$ by microfluorometry

The cells were incubated for 35 min at 37 ºC in RPMI 1640 medium supplemented with bovine serum albumin (0.1%) and fura-2 AM (1 µM). To allow de-esterification of the loaded dye, the cells were incubated for another 10 min in modified Krebs-Ringer bicarbonate-HEPES buffer (KRBH) containing (in mM): 140 NaCl, 3.6 KCl, 0.5 NaH_2PO_4, 0.5 $MgSO_4$, 1.5 $CaCl_2$, 10 HEPES, 3 glucose and 0.1% BSA (pH 7.4). Nominally Ca^{2+} free medium was made by omission of Ca^{2+} and addition of EGTA (0.5 mM). A coverslip was mounted as the exchangeable bottom of an open perfusion chamber on the stage of an inverted epifluorescence microscope (Olympus CK 40). A peristaltic pump allowed fluids to perfuse through the chamber and the temperature in the chamber was maintained stable by a temperature controller (Warner TC-344B). The microscope was connected with a system (PhotoMed M-39/2000 RatioMaster) for dual wavelength excitation fluorometry. A monochromator (PhotoMed DeltaRam) generated the excitation wavelengths that were directed to the cell by a dichroic mirror. Emitted light selected by a 510 nm filter was monitored by a photomultiplier tube detector. The excitation wavelengths were alternated at a specified rate to obtain one ratio data point per second. The fluorescence ratio (*F*340/*F*380) was calculated by using the emissions at the excitation wavelength of 340 nm (*F*340) and that of 380 nm (*F*380). Single cells were optically isolated and studied through a 40x1.3 NA oil immersion objective (40X UV, APO). The background fluorescence was subtracted from the traces before calculation of $[Ca^{2+}]_i$. $[Ca^{2+}]_i$ was calculated from *F*340/*F*380 as described before (Grynkiewicz et al. 1985). External standards containing fura-2 free acid and sucrose (2 M) were used for determination of R_{max} and R_{min} (Poenie 1990). The K_d for Ca^{2+}-fura-2 was taken as 225 nM.

2.6. Electrophysiology

INS-1E cells were patch clamped in the whole cell voltage clamp configuration, using a fully automated patch clamp workstation (Port-a-patch, Nanion, Munich, Germany) equipped with an HEKA EPC 10 amplifier (HEKA, Lambrecht/Pfalz, Germany). Before the experiments, cells were detached using a mild trypsination protocol where the cells were washed one time with a Phosphate Buffered Saline, PBS (without Ca^{2+} and Mg^{2+}), and then trypsinized for 3 min at 37 °C, using 0.5% trypsin in HBSS. Cells were spun at 100 *g*, and resuspended in 0.5 ml of the external recording solution. The external recording solution contained (in mM): 140 NaCl, 4 KCl**,** 1 $MgCl_2$, 2 $CaCl_2$, 5 D-glucose monohydrate, 10 Hepes, NaOH, pH 7.4. The internal recording solution contained (in mM): 50 CsCl, 10 NaCl, 60 CsF, 20 EGTA, 10 Hepes/CsOH, pH 7.2.

The planar patch clamp glass chip containing a micron sized aperture was primed by adding 5 µl of internal and external solution to the respective sides of the chip. 5 µl of the cell suspension (~10^6 cells/ml) were added to the external side of the patch clamp chip. The PatchControl software (Nanion Technologies, Munich, Germany) applied a suction protocol to automatically capture a cell, and to obtain a G-Ohm seal between the glass substrate and the cellular membrane. Eventually a whole cell configuration was obtained. The compounds dissolved at the appropriate final concentration in external solution, were directly pipetted onto the chip after removing excess control solution. To prevent drug dilution over the chip surface, the drug containing solution was changed three times during each experiment.

Currents were recorded using an EPC-10 patch clamp amplifier and the Patchmaster software (HEKA Elektronik GmbH, Lambrecht/Pfalz, Germany). The signal was collected at a sample rate of 10 kHz, filtered at 3 kHz (built in Bessel filter) and stored in a computer hard disc. Currents were analyzed off line using the Igor Pro software (Wavemetrics Inc., USA).

2.7. Western Blot analysis of INS-1E cells and human islets

The cells were centrifuged and sonicated for 2 min in a modified RIPA lysis buffer, an ice-cold buffer consisting of 150 mM NaCl, 20 mM Tris pH 7.4, 0.25 % Na-Deoxycholate, 0.1 % SDS, 1% Triton X-100, 1 mM EDTA and complete protease inhibitor cocktail (Roche, Bromma, Sweden). The homogenate was centrifuged at 450 *g* for 30 min at 4 °C. The supernatant containing the membrane proteins was collected, and protein concentration was measured using Bio-Rad Protein Assay kit. The concentration of total protein was 40 mg/ml.

The protein was fractionated in a 10% SDS-polyacrylamid/4% stacking gel, using Mini-Protean-3 Cell Electrophoresis System (BioRad). 80 µg of the total protein of the cells was loaded after adding loading buffer and after boiling at 98 ºC for 10 min. Precision Plus Protein Standards (BioRad) were used to estimate the molecular weight of the proteins. After the electrophoresis the proteins were transferred to PVDF membrane using Mini Trans-Blot cell (BioRad). Then the membrane was washed in TBS-T buffer (5 mM Tris, 138 mM NaCl, 2.7 mM KCl and 0.1% Tween-20) for 10 min at room temperature (RT) under constant shaking. The membrane was blocked either in TBS-T + 5% BSA + sodium azide 0.02% or TBS-T with 5% nonfat milk overnight at 4 °C.

The following step was overnight incubation at 4 ºC with the rat anti-TRPV1 as primary antibody (BIOMOL international, U.K., BML-SA564-0050, Lot # P9604a, cat. no. SA-6564). The primary antibody was an affinity-purified rabbit polyclonal antibody IgG directed against the peptide sequence DASTRDRHATQQEEV, which represents the amino acid residues 824-838 in the C-terminal region of the rat TRPV1. The antibodies were diluted 1:300 in TBS-T with 5% BSA and 0.02% sodium azide. The PVDF membrane was then washed 4-5 times with TBS-T buffer at RT, each time for 10 min under constant shaking. After that, the membrane was incubated with goat anti-rabbit IgG conjugated to horseradish-peroxidase (1:5000) for 1 hour at RT with shaking. The membrane was finally washed, the immunoreactive bands were detected by enhanced chemiluminescence (ECL) (Amersham, Stockholm, Sweden) and exposed to x-ray film.

2.8. Specific Blocking Peptide test

Antibody-specificity was tested by using the amino acid sequence DASTRDRHATQQEEV as specific peptide (TRPV1 blocking peptide, BIOMOL international, U.K. BML-SA564-0050, Lot #P9604a, SA-564, UK). After visualizing the TRPV1 band with the anti-TRPV1, the PVDF membrane was stripped for 20 min at RT. The stripping buffer consisted of 200 mM glycine, 3mM SDS, 1% Tween-20, pH 2.2. After the stripping, the membrane was washed 4-5 times, 10 min each with TBS-T buffer at RT with shaking. The anti-TRPV1 antibody was incubated with the blocking peptide at 4 ºC overnight. The ratio between the anti-TRPV1 and its blocking peptide was 1:5. The mix was incubated with the stripped membrane overnight at 4 ºC with constant shaking. Next day, the membrane was washed and incubated with the conjugate under the same conditions as above. The membrane was washed and ECL was used to expose any possible band.

2.9. Immunohistochemistry

Human pancreas resection specimens were collected and stored in a biobank at the Rudbeck Laboratory in Uppsala, Sweden, after approval from the local ethics committee. Sections from the tissue microarray blocks were cut at 4 µm thickness and immunostained. Briefly, slides were baked for overnight in 50 ºC, deparaffinized in xylene, hydrated in graded alcohols and blocked for endogenous peroxidase in 0.3% hydrogen peroxide diluted in 95% ethanol. For antigen retrieval, a decloaking chamber® (Biocare Medical, Walnut Creek, CA) was used. Slides were immersed and boiled in Citrate buffer®, pH 6 (Lab Vision, Freemont, CA, USA) for 4 min at 125 ºC, and then allowed to cool to 90 ºC. Automated immunohistochemistry was done using an Autostainer 480 instrument® (Lab Vision). Primary antibodies and a dextran polymer visualization system (UltraVision LP HRP polymer®, Lab Vision) were incubated for 30 min each at RT and slides were developed for 10 min using Diaminobenzidine (Lab Vision) as chromogen. All incubations were followed by rinse in wash buffer® (Lab Vision). Slides were counterstained in Mayers hematoxylin (Histolab, Gothenburg, Sweden) and coversliped using Pertex® (Histolab) as mounting medium.

The antibodies used were eight different affinity purified rabbit polyclonal IgG antibodies raised against synthetic peptides corresponding to either the C-terminus or the N-terminus of TRPV1. The antibodies were from: 1. Biosensis (cat. no. R-076-100), 2. Alomone (cat. no. ACC-03), 3. Sigma (cat. no. V2764), 4. and 5. Santa Cruz Biotechnologies (cat. no. Sc-20813 and Sc-28759), 6. And 7. Chemicon (cat. no. AB5889 and AB5370P) and 8. The human protein atlas project (HRPK2180179, not published in the Protein Atlas, yet).

2.10. Statistical analysis

Data was expressed as mean ± SEM. Graph Pad software was used for making the concentration-response curve.

3. Results

3.1. Capsaicin increased $[Ca^{2+}]_i$ in INS-1E cells

Capsaicin induced $[Ca^{2+}]_i$ increase in INS-1E cells in a concentration-dependent manner. The $[Ca^{2+}]_i$ increase was immediate after addition of capsaicin without any latency. The $[Ca^{2+}]_i$ response consisted of an initial rapid increase to a peak followed either by a plateau phase or return to the baseline. After washout of capsaicin, $[Ca^{2+}]_i$ returned to the baseline, suggesting that the cells were not damaged by short period of exposure to 300 nM capsaicin (Fig. 1A). 10 nM capsaicin did not increase $[Ca^{2+}]_i$. The maximum $[Ca^{2+}]_i$ increase was obtained by 300 nM and the EC_{50} was 100 nM (Fig. 1C).

3.2. Capsazepine blocked the capsaicin-induced $[Ca^{2+}]_i$ increase

Capsazepine is a synthetic analogue made to competitively inhibit capsaicin binding (Bevan et al. 1992). We investigated whether capsazepine could inhibit the effect of capsaicin in the INS-1E cells. Capsazepine (10 µM) did not increase $[Ca^{2+}]_i$ by itself, but inhibited the capsaicin-induced $[Ca^{2+}]_i$ increase completely (Fig. 1B).

3.3. Capsaicin did not increase $[Ca^{2+}]_i$ in primary β-cells from rat or human

Primary β-cells from rat were stimulated by capsaicin (300 nM and 3 µM), but it did not increase $[Ca^{2+}]_i$ (Fig. 1D). The effect of capsaicin was also studied in human β-cells, but none of the 20 cells examined responded to capsaicin (300 nM) (data not shown).

3.4. Capsaicin-induced $[Ca^{2+}]_i$ increase was due to Ca^{2+} entry across the plasma membrane

Nominally Ca^{2+}-free extracellular solution was used to test whether the $[Ca^{2+}]_i$ increase was due to Ca^{2+} entry through the plasma membrane or due to Ca^{2+} release from the ER. Capsaicin did not elicit any $[Ca^{2+}]_i$ increase in the Ca^{2+} free solution (Fig. 2B). This showed that extracellular Ca^{2+} was essential for the capsaicin-induced $[Ca^{2+}]_i$ increase. As expected, carbachol increased $[Ca^{2+}]_i$ under Ca^{2+}-free condition, indicating that the ER Ca^{2+} stores were not depleted under such condition. KCl (25 mM) did not increase $[Ca^{2+}]_i$, confirming that there was no Ca^{2+} in the extracellular medium. These result indicated that the $[Ca^{2+}]_i$ increase by capsaicin was due to Ca^{2+} entry through channels located in the plasma membrane.

3.5. AM404 increased $[Ca^{2+}]_i$ in INS-1E cells

As mentioned earlier, AM404 is an agonist of TRPV1 (Bertolini et al 2006; Zygmunt et al 2000). AM404 (5 µM), but not its precursors *p*-aminophenol (5 µM) and arachidonic acid (5 µM), increased $[Ca^{2+}]_i$ in the INS-1E cells Fig. 3A, C and D). AM404 increased $[Ca^{2+}]_i$ within 60 seconds to an initial peak, followed by a plateau phase. After washout of AM404, $[Ca^{2+}]_i$ returned to the baseline. Capsazepine (10 µM) inhibited the AM404-induced $[Ca^{2+}]_i$ increase completely (Fig. 3B).

3.9. Capsaicin induced inward currents in INS-1E cells

In patch-clamp recordings in the whole-cell voltage clamp configuration, capsaicin (1 µM) immediately induced large inward currents in INS-1E cells. The amplitude of the inward current was -122 ± 30 pA (at a holding potential of -80 mV) (Fig. 4). Currents returned to the baseline after the addition of the TRPV1 antagonist capsazepine (10 µM) in the continued presence of capsaicin.

3.10. TRPV1 proteins in INS-1E cells

We performed western blot analysis with total protein prepared from INS-1E cells and isolated human islets. The blot was probed with a C-terminal rat anti-TRPV1 antibody. An immunoreactive band was detected at an apparent molecular weight of ~ 94 kDa in the INS-1E cells (Fig. 5A). In the human islets an immunoreactive band was detected at ~ 96 kDa (Fig. 5C). The membrane was stripped and incubated with the anti-TRPV1 antibody that was treated with the blocking peptide as described in the methods section. No immunoreactive band was detected (Fig. 5B and 5D).

3.11. Lack of TRPV1 immunoreactivity in human islets and human insulinomas

In immunohistochemistry experiments, we used eight different primary antibodies directed against human TRPV1. All of them detected immunoreactivity in the dorsal root ganglion cells that were used as control cells. Two of the antibodies stained well in dorsal root ganglion, but faintly in other tissues. These antibodies were from Chemicon and Sigma. The antibody from Chemicon was raised against a 21 amino acid sequence in the C-terminus of the rat TRPV1. The antibody from Sigma corresponded to the amino acids 817-838 of the C-terminus of the rat TRPV1. As shown in Fig. 6.1A and 6.2A, these two antibodies detected strong immunoreactivity in the dorsal root ganglion cells. However, these antibodies did not detect any TRPV1 immunoreactivity in the human islet cells (Fig. 6.1B and 6.2B) or the human insulinoma cells (Fig. 6.1C and 6.2C).

4. Discussion

Several members of the TRP superfamily of ion channels are present in the pancreatic β-cells. These are TRPC1-6 (Li and Zhang 2009; Roe et al. 1998; Sakura and Ashcroft 1997), TRPM2-5 (Bari et al. 2009; Cheng et al. 2007; Prawitt et al. 2003; Togashi et al. 2006; Wagner et al. 2008), and TRPV1, 2 and 4 (Akiba et al 2004; Casas et al. 2008; Hisanaga et al. 2009). We have investigated whether TRPV1 channels are expressed in the INS-1E cells and the primary β-cells of rat and human, and whether activation of TRPV1 leads to $[Ca^{2+}]_i$ increase and induce inward currents across the plasma membrane. The classical TRPV1 agonist capsaicin increased $[Ca^{2+}]_i$ in a concentration-dependent manner in INS-1E cells. Likewise, capsazepine, a specific antagonist of TRPV1, inhibited the capsaicin-induced $[Ca^{2+}]_i$ increase completely, further indicating that the $[Ca^{2+}]_i$ increase was due to TRPV1 activation. In some cell types such as dorsal root ganglion cells and bronchial epithelial and alveolar cells, TRPV1 is also present in the ER (Gallego-Sandin et al. 2009; Olah et al. 2001; Thomas et al. 2007). It is claimed that the ER TRPV1 channels can be transported to the plasma membrane when needed (Morenilla-Palao et al. 2004). In our study, the $[Ca^{2+}]_i$ increase by capsaicin was abolished when Ca^{2+} was omitted from the extracellular medium, indicating that the TRPV1 channels in the INS-1E cells responsible for the capsaicin-induced $[Ca^{2+}]_i$ increase were located in the plasma membrane and not in the ER.

AM404 is a TRPV1 agonist that mediates the antinociceptive action of paracetamol in the brain (Mallet et al. 2010). In our study, AM404 evoked $[Ca^{2+}]_i$ increase in the INS-1E cells. To rule out that the $[Ca^{2+}]_i$ increase was not due to any of the precursors of AM404, we tested the effects of *p*-aminophenol and arachidonic acid, which did not increase $[Ca^{2+}]_i$. These results indicate that the $[Ca^{2+}]_i$ increase was due to AM404 itself, and not due to its

precursors. Moreover, capsazepine inhibited the AM404-induced $[Ca^{2+}]_i$ increase completely, indicating that AM404-induced $[Ca^{2+}]_i$ increase was due to activation of the TRPV1 channel. Thus, two structurally unrelated specific agonists of TRPV1, namely capsaicin and AM404 increased $[Ca^{2+}]_i$ in the INS-1E cells, supporting the view that these cells have functional TRPV1 channels.

In agreement with $[Ca^{2+}]_i$ increase by capsaicin and AM404 and its inhibition by capsazepine, we found that capsaicin induced inward currents across the plasma membrane in INS-1E cells and that the current was inhibited by capsazepine. TRPV1 is more permeable to Ca^{2+} than Na^+ (PNa^+/PCa^{2+} = 1:9) (Clapham et al. 2005). Thus, it is likely that Ca^{2+} was the main carrier of the current. This view is consistent with the observation that capsaicin and AM404 readily induced conspicuous $[Ca^{2+}]_i$ increase in all of the cells examined.

By western blot, we detected TRPV1 proteins in the INS-1E cells and the human islets. Comparison of the expected size estimated from the mRNA, indicates that the bands seen at ~ 96 kDa and ~ 94 kDa represent TRPV1. Earlier studies of TRPV1 in different cells have also detected immunoreactive bands with apparent molecular weights of 90-100 kDa (Andaloussi-Lilja et al. 2009; Lazzeri et al. 2005; Tominaga et al. 1998; Vos et al. 2006; Wang et al. 2008). These results, together with the electrophysiological and pharmacological data described above, establish that TRPV1 protein and functional TRPV1 channels are present in these insulinoma cells.

As mentioned, an earlier study demonstrated TRPV1 immunoreactivity in primary β-cells from Sprague-Dawley rats (Akiba et al 2004). The authors did not report the effect of capsaicin on $[Ca^{2+}]_i$ in these cells. Other studies have reported TRPV1 immunoreactivity in the nerve fibres in the islets but not in the β-cells (Gram et al 2007). However, we did not see any capsaicin-induced $[Ca^{2+}]_i$ increase in primary β-cells cells from Wistar rat. There is no information in the literature on whether TRPV1 is expressed in human β-cells or not. In our study, capsaicin did not increase $[Ca^{2+}]_i$ in human β-cells, and no TRPV1 immunoreactivity was detected in the human islets or human insulinomas. These results suggest that TRPV1 is probably not expressed in human β-cells, at least not at as high level as in the dorsal root ganglion cells. In immunohistochemistry, we used eight antibodies, all of which demonstrated TRPV1 immunoreactivity in the dorsal root ganglion cells, which were used as a control, but none of these antibodies detected TRPV1 immunoreactivity in the human islets or human insulinomas. However, in western blot of proteins obtained from whole human islets, a ~ 96 kDa band that represents TRPV1 was observed. The purity of the islets used in these experiments was about 80%, and a logical explanation could be that the source of TRPV1 detected in the western blot of human islets could be the acinar cells, nerve cells or other non-β-cells that express TRPV1 (Gram et al 2007; Hartel et al. 2006). Another possibility is that the human β-cells express a capsaicin-insensitive isoform of TRPV1, namely the TRPV1b isoform (Lu et al. 2005) at low level, which can not be detected by immunohistochemistry but can be detected by western blot.

In summary, we have shown that TRPV1 protein and functional TRPV1 channels exist in the INS-1E cells. These cells may prove suitable for studying the regulation of native TRPV1 channels. However, functional TRPV1 channels are not expressed in primary rat or human β-cells.

5. Aknowledgements

This work was supported by funds of Karolinska Institutet, Swedish Medical Society and the Swedish Research Council, Landes Bioscience, Engelbrektskliniken and Landstinget i Uppsala Län. A.J.F. is funded by Karolinska Institutet´s MD PhD program, Karolinska Research Internship, Stiftelsen Irma och Arvid Larsson-Rösts minne, Stiftelsen Goljes minne and Svenska Diabetesstiftelsen. K.K. and A.B. were funded by Linköping University. B.H. was funded by Mälardalens högskola. The Human Protein Atlas (HPA) project is accessible at www.proteinatlas.org and is funded by the Knut & Alice Wallenberg Foundation (Stockholm, Sweden). The Atlas is part of the HUPO Human Antibody Initiative (Montreal Quebec, Canada).

6. References

Akiba, Y., Kato, S., Katsube, K. I., Nakamura, M., Takeuchi, K., Ishii, H., & Hibi, T., 2004. Transient receptor potential vanilloid subfamily 1 expressed in pancreatic islet beta cells modulates insulin secretion in rats. Biochem.Biophys.Res.Commun. 321, 219-225.

Andaloussi-Lilja, J., Lundqvist, J., & Forsby, A., 2009. TRPV1 expression and activity during retinoic acid-induced neuronal differentiation. Neurochem.Int. 55, 768-774.

Bari, M. R., Akbar, S., Eweida, M., Kühn, F. J.P., Gustafsson, A. J., Lückhoff, A., & Islam, M. S., 2009. H_2O_2-induced Ca^{2+} influx and its inhibition by N-(p-amylcinnamoyl) anthranilic acid in the beta-cells: involvement of TRPM2 channels. J Cell Mol Med 13, 3260-3267.

Bertolini, A., Ferrari, A., Ottani, A., Guerzoni, S., Tacchi, R., & Leone, S., 2006. Paracetamol: new vistas of an old drug. CNS.Drug Rev. 12, 250-275.

Bevan, S., Hothi, S., Hughes, G., James, I. F., Rang, H. P., Shah, K., Walpole, C. S., & Yeats, J. C., 1992. Capsazepine: a competitive antagonist of the sensory neurone excitant capsaicin. Br.J.Pharmacol. 107, 544-552.

Casas, S., Novials, A., Reimann, F., Gomis, R., & Gribble, F. M., 2008. Calcium elevation in mouse pancreatic beta cells evoked by extracellular human islet amyloid polypeptide involves activation of the mechanosensitive ion channel TRPV4. Diabetologia 51, 2252-2262.

Cheng, H., Beck, A., Launay, P., Gross, S. A., Stokes, A. J., Kinet, J. P., Fleig, A., & Penner, R., 2007. TRPM4 controls insulin secretion in pancreatic beta-cells. Cell Calcium 41, 51-61.

Clapham, D. E., Julius, D., Montell, C., & Schultz, G., 2005. International Union of Pharmacology. XLIX. Nomenclature and structure-function relationships of transient receptor potential channels. Pharmacol.Rev. 57, 427-450.

Gallego-Sandin, S., Rodriguez-Garcia, A., Alonso, M. T., & Garcia-Sancho, J., 2009. The endoplasmic reticulum of dorsal root ganglion neurons contains functional TRPV1 channels. J Biol.Chem. 284, 32591-32601.

Gram, D. X., Ahren, B., Nagy, I., Olsen, U. B., Brand, C. L., Sundler, F., Tabanera, R., Svendsen, O., Carr, R. D., Santha, P., Wierup, N., & Hansen, A. J., 2007. Capsaicin-sensitive sensory fibers in the islets of Langerhans contribute to defective insulin secretion in Zucker diabetic rat, an animal model for some aspects of human type 2 diabetes. Eur.J Neurosci. 25, 213-223.

Grynkiewicz, G., Poenie, M., & Tsien, R. Y., 1985. A new generation of Ca^{2+} indicators with greatly improved fluorescence properties. J Biol.Chem. 260, 3440-3450.

Gustafsson, A. J., Ingelman-Sundberg, H., Dzabic, M., Awasum, J., Hoa, N. K., Östenson, C. G., Pierro, C., Tedeschi, P., Woolcott, O., Chiounan, S., Lund, P. E., Larsson, O., & Islam, M. S., 2004. Ryanodine receptor-operated activation of TRP-like channels can trigger critical Ca^{2+} signaling events in pancreatic beta-cells. FASEB J 10.1096/fj.04-2621fje.

Hartel, M., di Mola, F. F., Selvaggi, F., Mascetta, G., Wente, M. N., Felix, K., Giese, N. A., Hinz, U., Di Sebastiano, P., Buchler, M. W., & Friess, H., 2006. Vanilloids in pancreatic cancer: potential for chemotherapy and pain management. Gut 55, 519-528.

Hisanaga, E., Nagasawa, M., Ueki, K., Kulkarni, R. N., Mori, M., & Kojima, I., 2009. Regulation of Calcium-Permeable TRPV2 Channel by Insulin in Pancreatic beta-Cells. Diabetes 58, 174-184.

Högestätt, E. D., Jönsson, B. A., Ermund, A., Andersson, D. A., Björk, H., Alexander, J. P., Cravatt, B. F., Basbaum, A. I., & Zygmunt, P. M., 2005. Conversion of acetaminophen to the bioactive N-acylphenolamine AM404 via fatty acid amide hydrolase-dependent arachidonic acid conjugation in the nervous system. J Biol.Chem. 280, 31405-31412.

Islam, M. S. 2011. TRP channels of islets. Adv.Exp.Med.Biol. 704, 811-830.

Lazzeri, M., Vannucchi, M. G., Spinelli, M., Bizzoco, E., Beneforti, P., Turini, D., & Faussone-Pellegrini, M. S., 2005. Transient receptor potential vanilloid type 1 (TRPV1) expression changes from normal urothelium to transitional cell carcinoma of human bladder. Eur.Urol. 48, 691-698.

Li, F. & Zhang, Z. M., 2009. Comparative identification of Ca^{2+} channel expression in INS-1 and rat pancreatic beta cells. World J Gastroenterol. 15, 3046-3050.

Lu, G., Henderson, D., Liu, L. J., Reinhart, P. H., & Simon, S. A., 2005. TRPV1b, a functional human vanilloid receptor splice variant. Molecular Pharmacology 67, 1119-1127.

Mallet, C., Barriere, D. A., Ermund, A., Jönsson, B. A., Eschalier, A., Zygmunt, P. M., & Högestätt, E. D., 2010. TRPV1 in brain is involved in acetaminophen-induced antinociception. PLoS One. 5.

Merglen, A., Theander, S., Rubi, B., Chaffard, G., Wollheim, C. B., & Maechler, P., 2004. Glucose sensitivity and metabolism-secretion coupling studied during two-year continuous culture in INS-1E insulinoma cells. Endocrinology 145, 667-678.

Morenilla-Palao, C., Planells-Cases, R., Garcia-Sanz, N., & Ferrer-Montiel, A., 2004. Regulated exocytosis contributes to protein kinase C potentiation of vanilloid receptor activity. J Biol.Chem. 279, 25665-25672.

Olah, Z., Szabo, T., Karai, L., Hough, C., Fields, R. D., Caudle, R. M., Blumberg, P. M., & Iadarola, M. J., 2001. Ligand-induced dynamic membrane changes and cell deletion conferred by vanilloid receptor 1. J Biol.Chem. 276, 11021-11030.

Planells-Cases, R., Valente, P., Ferrer-Montiel, A., Quin, F., & Szallasi, A., 2011. Complex Regulation of TRPV1 and Related ThermoTRPS: Implications for Therapeutic Intervention Adv Exp Med Biol. 704, 491-515

Poenie, M., 1990. Alteration of intracellular Fura-2 fluorescence by viscosity: a simple correction. Cell Calcium 11, 85-91.

Prawitt, D., Monteilh-Zoller, M. K., Brixel, L., Spangenberg, C., Zabel, B., Fleig, A., & Penner, R., 2003. TRPM5 is a transient Ca^{2+}-activated cation channel responding to rapid changes in [Ca2+]i. Proc.Natl.Acad.Sci.U S A 100, 15166-15171.

Razavi, R., Chan, Y., Afifiyan, F. N., Liu, X. J., Wan, X., Yantha, J., Tsui, H., Tang, L., Tsai, S., Santamaria, P., Driver, J. P., Serreze, D., Salter, M. W., & Dosch, H. M., 2006. TRPV1+ sensory neurons control beta cell stress and islet inflammation in autoimmune diabetes. Cell 127, 1123-1135.

Roe, M. W., Worley, J. F., III, Qian, F., Tamarina, N., Mittal, A. A., Dralyuk, F., Blair, N. T., Mertz, R. J., Philipson, L. H., & Dukes, I. D., 1998. Characterization of a Ca^{2+} release-activated nonselective cation current regulating membrane potential and $[Ca^{2+}]_i$ oscillations in transgenically derived beta-cells. J Biol.Chem. 273, 10402-10410.

Sakura, H. & Ashcroft, F. M., 1997. Identification of four trp1 gene variants murine pancreatic beta-cells. Diabetologia 40, 528-532.

Thomas, K. C., Sabnis, A. S., Johansen, M. E., Lanza, D. L., Moos, P. J., Yost, G. S., & Reilly, C. A., 2007. Transient receptor potential vanilloid 1 agonists cause endoplasmic reticulum stress and cell death in human lung cells. J Pharmacol.Exp.Ther. 321, 830-838.

Togashi, K., Hara, Y., Tominaga, T., Higashi, T., Konishi, Y., Mori, Y., & Tominaga, M., 2006. TRPM2 activation by cyclic ADP-ribose at body temperature is involved in insulin secretion. EMBO J. 25, 1804-1815.

Tominaga, M., Caterina, M. J., Malmberg, A. B., Rosen, T. A., Gilbert, H., Skinner, K., Raumann, B. E., Basbaum, A. I., & Julius, D., 1998. The cloned capsaicin receptor integrates multiple pain-producing stimuli. Neuron 21, 531-543.

Vos, M. H., Neelands, T. R., McDonald, H. A., Choi, W., Kroeger, P. E., Puttfarcken, P. S., Faltynek, C. R., Moreland, R. B., & Han, P., 2006. TRPV1b overexpression negatively regulates TRPV1 responsiveness to capsaicin, heat and low pH in HEK293 cells. J Neurochem. 99, 1088-1102.

Wagner, T. F., Loch, S., Lambert, S., Straub, I., Mannebach, S., Mathar, I., Dufer, M., Lis, A., Flockerzi, V., Philipp, S. E., & Oberwinkler, J., 2008. Transient receptor potential M3 channels are ionotropic steroid receptors in pancreatic beta cells. Nat.Cell Biol. 10, 1421-1430.

Wang, Y. X., Wang, J., Wang, C., Liu, J., Shi, L. P., Xu, M., & Wang, C., 2008. Functional expression of transient receptor potential vanilloid-related channels in chronically hypoxic human pulmonary arterial smooth muscle cells. J Membr.Biol. 223, 151-159.

Zygmunt, P. M., Chuang, H., Movahed, P., Julius, D., & Högestätt, E. D., 2000. The anandamide transport inhibitor AM404 activates vanilloid receptors. Eur.J.Pharmacol. 396, 39-42.

Figure legends

Fig. 1. Effect of capsaicin and capsazepine on $[Ca^{2+}]_i$ in insulin-secreting cells. $[Ca^{2+}]_i$ was measured by microfluorometry in cells loaded with fura-2. A. Capsaicin (300 nM) increased $[Ca^{2+}]_i$ in INS-1E cells. The trace is representative for 11 experiments. B. Capsazepine (10 µM) inhibited the $[Ca^{2+}]_i$ increase induced by capsaicin (300 nM) in INS-1E cells. The trace is representative of three experiments. C. Concentration-response curve for capsaicin-induced $[Ca^{2+}]_i$ increase in INS-1E cells. The squares represent means of $[Ca^{2+}]_i$ increase induced by the different concentrations of capsaicin, expressed as percentage of maximal $[Ca^{2+}]_i$ increase. The $[Ca^{2+}]_i$ response of 300 nM capsaicin was used as 100% of the maximal response. The estimated EC_{50} was 100 nM. D. Primary β-cells from Wistar rat were stimulated with capsaicin (300 nM and 3 µM) but it did not increase $[Ca^{2+}]_i$. Glucose (12 mM), carbachol (cch) (10 µM) and KCl (25 mM) increased $[Ca^{2+}]_i$. The trace is representative of at least three experiments.

Fig. 2. Capsaicin-induced $[Ca^{2+}]_i$ increase was due to Ca^{2+} entry through the plasma membrane. A. Capsaicin (300 nM) did not increase $[Ca^{2+}]_i$ when extracellular Ca^{2+} was omitted. Carbachol (100 µM) increased $[Ca^{2+}]_i$ in the absence of extracellular Ca^{2+}, indicating Ca^{2+} release from the intracellular stores. KCl (25 mM) did not increase $[Ca^{2+}]_i$, which confirmed that the extracellular medium did not contain Ca^{2+}. B. In control experiments where the extracellular medium contained 1.5 mM Ca^{2+}, capsaicin, carbachol and KCl increased $[Ca^{2+}]_i$. The traces are representatives of 11 experiments.

Fig. 3. AM404, an agonist of TRPV1, increased $[Ca^{2+}]_i$. A. AM404 (5 µM) increased $[Ca^{2+}]_i$ in INS-1E cells. B. Capsazepine (10 µM) inhibited the AM404-induced $[Ca^{2+}]_i$ increase. The two components of AM404, namely *p*-aminophenol (5 µM) and arachidonic acid (5 µM) did not increase $[Ca^{2+}]_i$ (C. and D. respectively). The traces are representatives of at least three experiments.

Fig. 4. Capsaicin evoked whole-cell current responses that were blocked by capsazepine. Whole-cell current responses were evoked by capsaicin (1 µM). Addition of the TRPV1 antagonist capsazepine (10 µM) inhibited the capsaicin-evoked currents. Currents were recorded from INS-1E cells in the whole cell configuration holding the membrane potential at -80 mV. The solid horizontal line indicates the time for capsaicin and the dotted line indicates the time for capsaicin plus capsazepine. The trace is representative of six experiments.

Fig. 5. Western blot analysis of TRPV1 proteins in INS-1E cells and human islets. 80 µg of membrane proteins from INS-1E and human islets were separated by 10% SDS-PAGE electrophoresis. The blots were probed with an anti-TRPV1 antibody (1:300). A. An immunoreactive band was detected at ~ 94 kDa for INS-1E cells and C. at ~ 96 kDa for human islets. No bands were detected after blocking the anti-TRPV1 antibody with the corresponding peptide (B. and D.). The experiments have been repeated at least three times with similar results.

Fig. 6. Lack of TRPV1 in human insulinoma and pancreatic islets. Eight different primary antibodies against TRPV1 were used in immunohistochemistry. Results obtained with two of the antibodies are shown. Panel 1 and 2 show results obtained with antibodies from Chemicon (cat. no. AB5370P) and Sigma (cat. no. V2764), respectively. Both of these antibodies detected TRPV1 immunoreactivity in the dorsal root ganglion cells, which were used as control cells (Fig. 6:1A and 6:2A). There was no TRPV1 immunoreactivity in human pancreatic islet cells (Fig. 6:1B and 6:2B) or in human insulinoma cells (Fig. 6:1C and 6:2C).

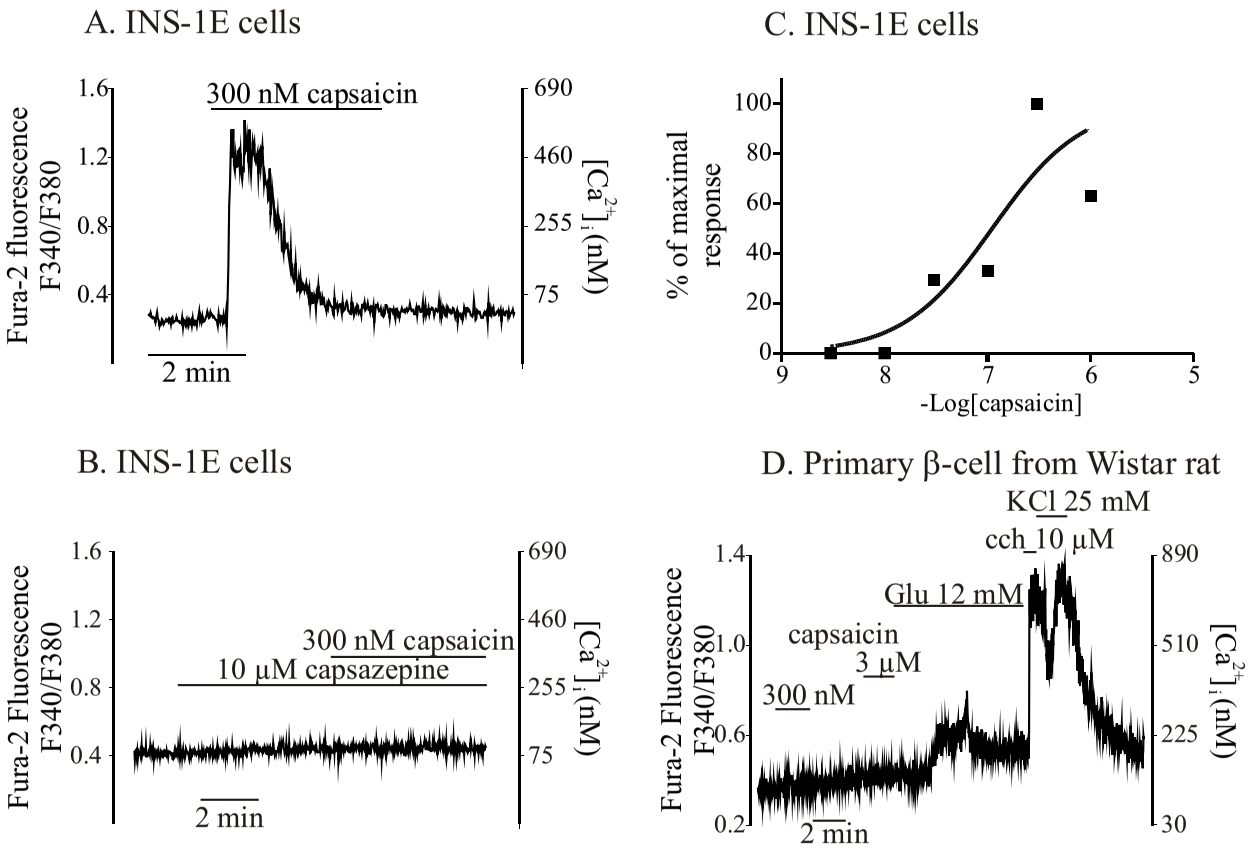
A. INS-1E cells
300 nM capsaicin
Fura-2 fluorescence
F340/F380
[Ca2+]i (nM)
2 min
C. INS-1E cells
% of maximal
response
-Log[capsaicin]
B. INS-1E cells
300 nM capsaicin
10 µM capsazepine
Fura-2 Fluorescence
F340/F380
2 min
D. Primary β-cell from Wistar rat
KCl 25 mM
cch 10 µM
Glu 12 mM
capsaicin
3 µM
300 nM
Fura-2 Fluorescence
F340/F380
2 min

Figure 1

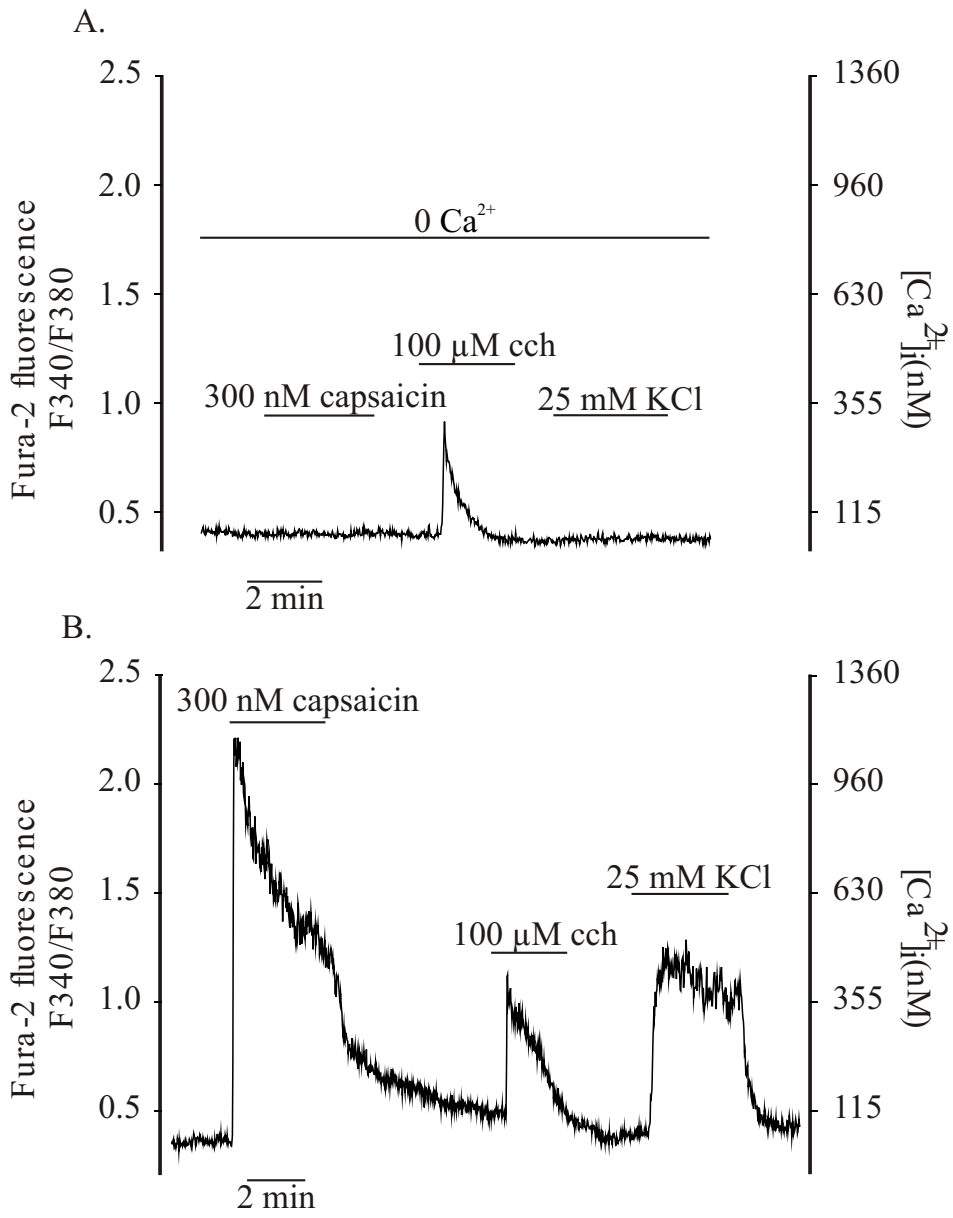
A.
2.5
2.0
1.5
1.0
0.5
1360
960
630
355
115
0 Ca2+
100 µM cch
300 nM capsaicin
25 mM KCl
Fura-2 fluorescence
F340/F380
[Ca 2+]i(nM)
2 min
B.
300 nM capsaicin
25 mM KCl
100 µM cch
2 min

Figure 2

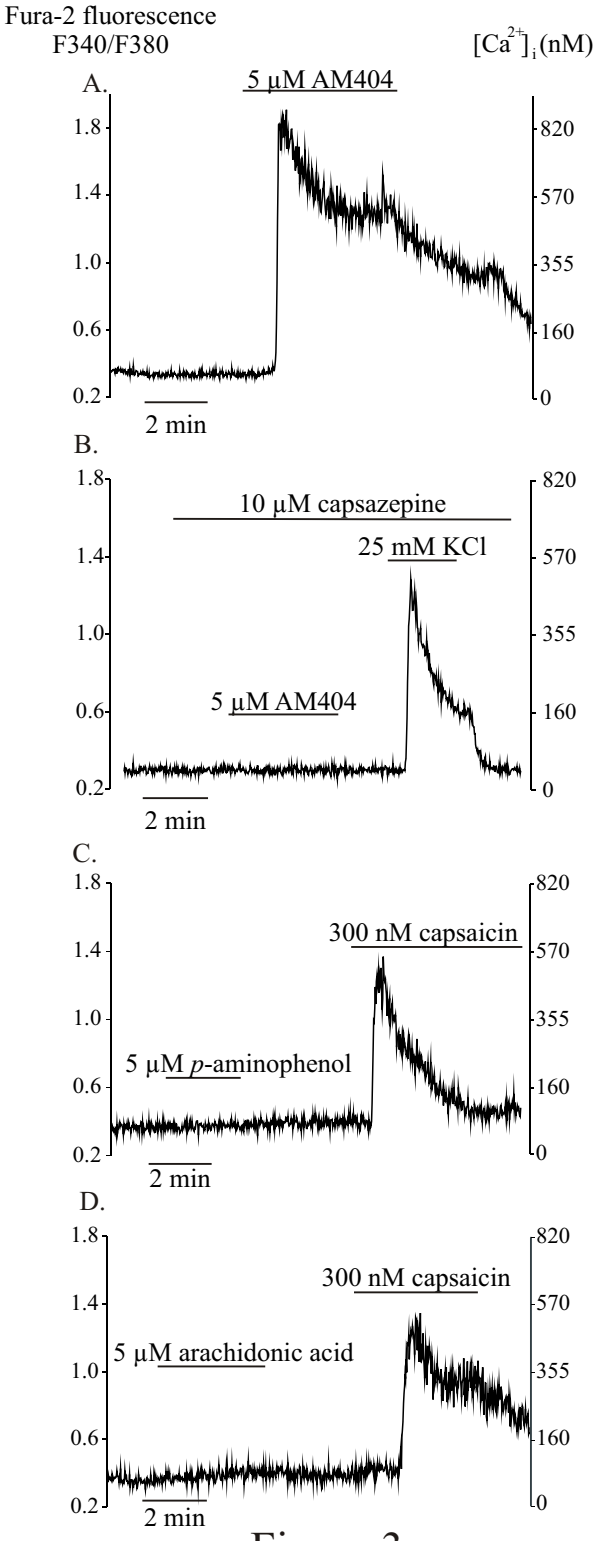
Fura-2 fluorescence
F340/F380
[Ca2+]i (nM)
A.
5 μM AM404
1.8
1.4
1.0
0.6
0.2
820
570
355
160
0
2 min
B.
10 μM capsazepine
25 mM KCl
5 μM AM404
2 min
C.
300 nM capsaicin
5 μM p-aminophenol
2 min
D.
300 nM capsaicin
5 μM arachidonic acid
2 min

Figure 3

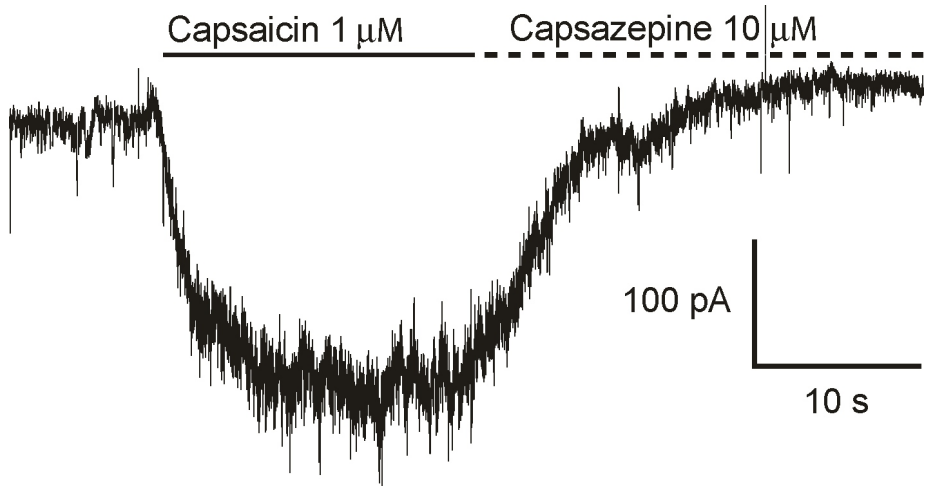

Figure 4

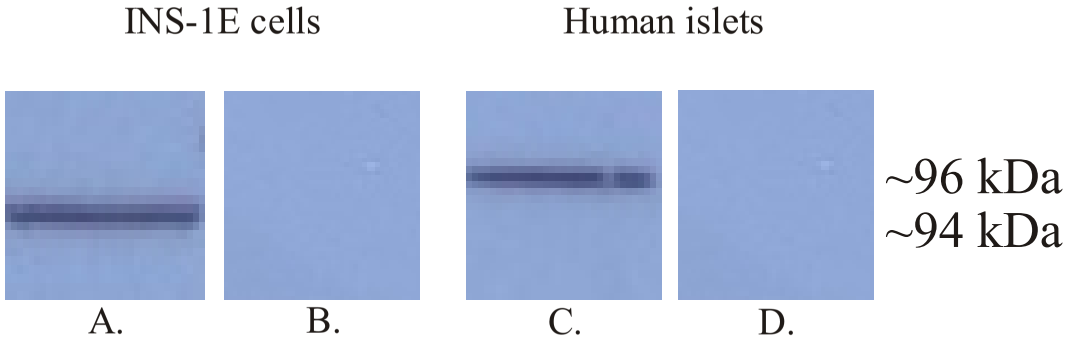

Figure 5

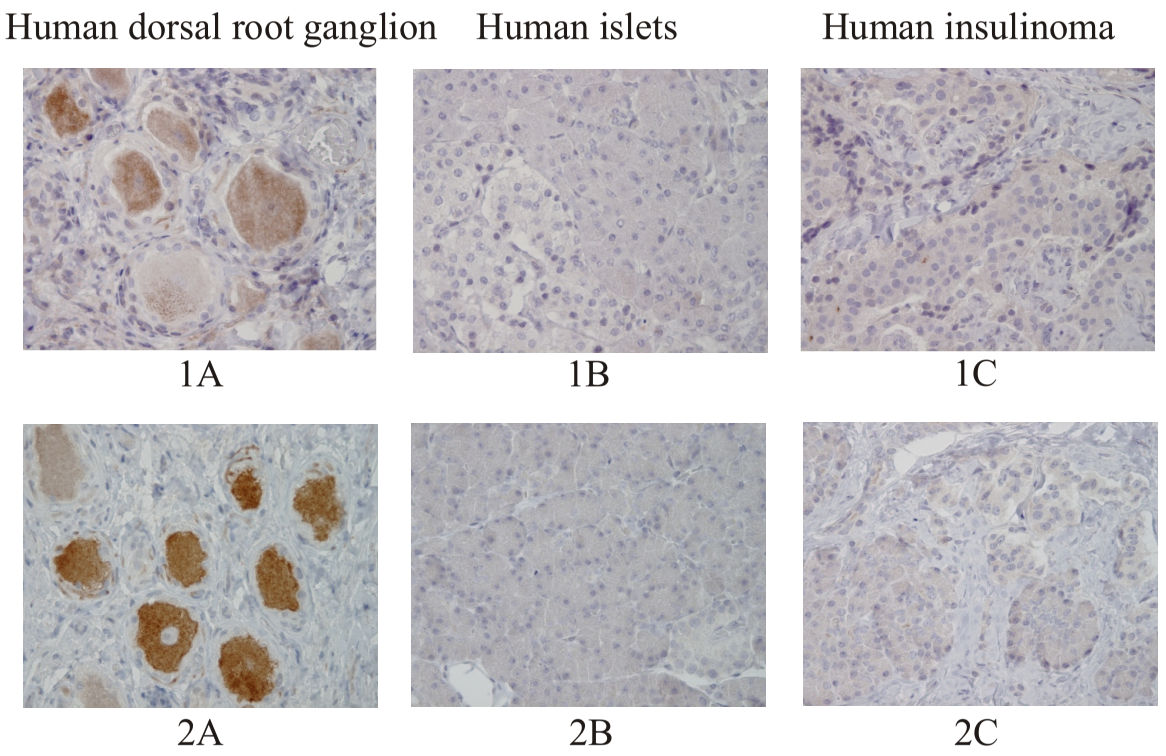
Human dorsal root ganglion
Human islets
Human insulinoma
1A
1B
1C
2A
2B
2C

Figure 6

US-AB universitetsservice digitaltryck
Printed in Sweden 2011, www.us-ab.com